

UNIVERSITY OF SOUTHAMPTON

ELECTROSTATIC CHARGING AND NOVEL APPLICATIONS  
OF ATOMISED LIQUIDS

by

LINDSEY FAYE WHITMORE, B.Sc

A thesis presented for the degree of

DOCTOR OF PHILOSOPHY

in the

FACULTY OF ENGINEERING AND APPLIED SCIENCE  
DEPARTMENT OF ELECTRICAL ENGINEERING

January 2000

ABSTRACT

FACULTY OF ENGINEERING AND APPLIED SCIENCE  
ELECTRICAL ENGINEERING

Doctor of Philosophy  
ELECTROSTATIC CHARGING AND NOVEL APPLICATIONS OF  
ATOMISED LIQUIDS  
By Lindsey Faye Whitmore

During the atomisation of liquids from pressure-pack dispensers, an electrostatic charge is imparted to the droplets. This is usually small, in the region of  $10^{-5}$  to  $10^{-8}$  C.kg<sup>-1</sup>, and therefore insufficient to affect the behaviour of the droplets. When the charge generated naturally is enhanced to a value in excess of  $1 \times 10^{-4}$  C.kg<sup>-1</sup> using the techniques presented in this thesis, the characteristics of the aerosol spray are beneficially modified. Highly charged aerosols have been generated by making modifications to the formulation, valve and actuator of pressure-pack dispensers. This has been shown to augment the current function of some pressure-pack products.

Charge separation is believed to result from the formation and shearing of electrical double layers at liquid-solid interfaces, as during flow electrification in pipes (Klinkenberg and van der Minne, 1958). In keeping with this theory, modifications that increase the flow turbulence, velocity and the contact area between liquid and solid results in a high level of electrostatic charge separation occurring during atomisation.

Two applications for this technology are investigated: removal of airborne particles by liquid sprays, and improved bioefficacy of insecticide sprays. It has been established that conventional liquid sprays rapidly reduce the concentration of airborne particles, and that this is significantly enhanced when the aerosol is highly charged, particularly for small particles. Particle depletion is believed to result from contact with the liquid droplets, which quickly precipitate onto surfaces. Increased contact between particles and highly charged droplets by electrostatic attraction and space charge effects would enhance depletion. Application of this novel technology to domestic sprays will be of particular benefit in achieving local depletion of particles that become airborne during domestic activities.

Highly charged aerosol insecticides demonstrated faster rates of knockdown and higher levels of mortality in houseflies and mosquitoes than conventional sprays. This improved performance is attributed to enhanced dispersion of the aerosol through the test chamber due to space charge effects, and to electrostatic attraction of the droplets to the insects during flight. Use of highly charged domestic insecticide sprays has not previously been considered, and would increase spray efficiency, or lead to equivalent bioefficacy with reduced concentrations of active ingredients.

The use of natural charge separation in liquids has not previously been considered with respect to improving spray performance. To obtain optimum performance, both the liquid formulation and the dispenser components must be carefully considered. However, the novel technology presented here could easily be applied to enhance the performance of a wide variety of domestic pressure-pack products.

# Contents

---

Abstract	i	
Contents	ii	
List of Figures	v	
List of Tables	ix	
Preface	x	
Acknowledgements	xii	
Chapter 1		
1.1	Introduction	1
1.2	Domestic Pressure-pack Dispensers	2
1.3	Electrostatic Principles	6
Chapter 2	Charge-to-Mass Ratio of Liquid Droplets Produced by Pressure-Pack Dispensers, and Enhancement of this Charge to an Electrostatically Useful Level	10
2.1	Introduction	10
2.1.1	Generation of Charged Droplets through the Spray Electrification Phenomenon	11
2.1.2	Separation of Charged Liquids Through the Flow Electrification Phenomenon	13
2.1.3	Characteristics of Flow Electrification	16
2.1.4	Charged Liquid Droplets	18
2.1.5	Objectives	18
2.2	Materials and Methods	20
2.2.1	Specifications of Pressure-Pack Formulations	20
2.2.2	Effect of Valve Modifications on Charge-to-Mass Ratio - Specifications of the Pressure-Pack Dispensers	21
2.2.3	Effect of Actuator Modifications on Charge-to-Mass Ratio - Specifications of the Pressure-Pack Dispensers	24
2.2.4	Effect of Combining Valve and Actuator Modifications on Charge-to-Mass Ratio - Specifications of the Pressure-Pack Dispensers for Formulation III	25
2.2.5	Effect of Novel Actuator Orifice Designs on the Charge-to-Mass Ratio of Formulation III - Specifications of the Pressure-Pack Dispensers	26
2.2.6	Measurement of Charge-to-Mass Ratio of Liquid Aerosols Generated by Pressure-Pack Dispensers	28
2.2.7	Measurement of Spray Rate	30
2.3	Results	
2.3.1	Effect of Valve Modifications on Charge-to-Mass Ratio	31
2.3.2	Effect of Actuator Modifications on Charge-to-Mass Ratio	39
2.3.3	Effect of Combining Valve and Actuator Modifications on Charge-to-Mass Ratio	45
2.3.4	Effect of Novel Actuator Orifice Designs on Charge-to-Mass Ratio	52
2.4	Discussion	54

2.4.1	Modifications to Components of the Valve Assembly of Pressure-Pack Sprays	55
2.4.2	Modifications to Actuator Components of Pressure-Pack Sprays	57
2.4.3	Differences Between Formulations	58
2.4.4	Combinations of Modifications to the Valve and Actuator Parameters of Pressure-Pack Dispensers	59
2.4.5	Novel Actuator Orifice Designs	61
2.4.6	Other Observations	61
2.4.7	Areas for Further Investigation	62
Chapter 3	Precipitation of Airborne Particles by Electrically Charged Aerosols Generated by Pressure-pack Dispensers	63
3.1	Introduction	63
3.1.1	Composition and Origin of Domestic Airborne Particles	64
3.1.2	Health Implications of Domestic Particulates	66
3.1.3	Natural Mechanisms of Particle Settling	66
3.1.4	Domestic Particle Reduction Strategies	70
3.1.5	Objectives	71
3.2	Materials and Methods	72
3.2.1	Preparation of Standard House Dust	72
3.2.2	Quantification of the Precipitation Rate of Airborne Particulates by Liquid Aerosols	72
3.2.3	Measurement of Droplet Size Distribution of Liquid Aerosols	77
3.2.4	Airborne Dust Precipitation by Uncharged and Artificially Charged Liquid Sprays	79
3.2.5	Airborne Dust Precipitation by Three Formulation Types, when Artificially Charged	81
3.2.6	Airborne Dust Precipitation by Uncharged and Naturally Charged Liquid Droplets	81
3.3	Results	83
3.3.1	Airborne Dust Precipitation by Artificially Charged Liquid Sprays of Formulation I	83
3.3.2	Airborne Dust Precipitation by Artificially Charged Aerosols of Three Formulation Types	87
3.3.3	Airborne Dust Precipitation by Naturally Charged Liquid Sprays of Formulation II	91
3.4	Discussion	95
3.4.1	Precipitation of Airborne Particles	95
3.4.2	Assessment of Investigation	98
3.4.3	Areas for Further Investigation	99
Chapter 4	Bioefficacy of Electrically Charged Insecticide Aerosols Generated by Pressure-pack Dispensers	100
4.1	Introduction	100
4.1.1	Domestic Pressure-Pack Insecticide Sprays	101
4.1.2	Factors Which Influence the Rate of Knockdown	102
4.1.3	Considerations for the Assessment of Electrostatically Charged Insecticides	104

4.1.4	Application of Electrostatic Spraying in Agriculture	105
4.1.5	Problems Associated With Domestic Flying Insects	106
4.1.6	Objectives	107
<b>4.2</b>	Materials and Methods	108
4.2.1	Culture of Houseflies, <i>Musca domestica</i>	108
4.2.2	Culture of Blow Flies, <i>Calliphora</i> species	108
4.2.3	Culture of Mosquitoes, <i>Culex quinquefasciatus</i>	109
4.2.4	Specifications of Pressure-pack Insecticide Sprays	109
4.2.5	Measurement of Charge-to-Mass Ratio	110
4.2.6	Deposition of Highly Charged Insecticide Sprays onto Tethered Flies	110
4.2.7	Assessment of Knockdown and Mortality - Direct Spray Protocol for Houseflies	113
4.2.8	Assessment of Knockdown and Mortality - Space Spray Protocol for Houseflies	115
4.2.9	Assessment of Knockdown and Mortality - Space Spray Protocol for Mosquitoes	116
4.2.10	Quantification of Spray Characteristics	116
<b>4.3</b>	Results	120
4.3.1	Deposition of Charged Insecticide Droplets onto Tethered Flies	120
4.3.2	Effect of Charge on Insecticide Aerosol Bioefficacy	121
4.3.3	Spray Characteristics of Insecticide Aerosols	124
<b>4.4</b>	Discussion	126
4.4.1	Deposition of Charged Insecticide Aerosol onto Tethered Flies	126
4.4.2	Effect of Charged Insecticide Droplets on Bioefficacy	128
4.4.3	Effects of Spray Characteristics on Bioefficacy	130
<b>Chapter 5</b>	Conclusions and Further Work	131
<b>Appendix A</b>	Statistical Analysis	136
<b>Appendix B</b>	Triboelectric Series	142
Publications arising from this work		143
Glossary		144
References		146

## List of Figures

---

Figure 1.1	Schematic drawing showing the main components of a pressure-pack dispenser	3
Figure 1.2a	Schematic illustration of pressure-pack dispenser valve in closed Position	4
Figure 1.2b	Schematic illustration of pressure-pack dispenser valve in open Position	4
Figure 1.3	Schematic diagram of internal surface of an actuator insert, Showing swirl chambers and terminal orifice	6
Figure 1.4a	Coulomb attraction force between oppositely charged objects and coulomb repulsion force between like charged objects	8
Figure 1.4b	Space charge force resulting from a cloud of like charged objects	8
Figure 1.4c	Image charge force resulting from charged objects approaching a grounded object	9
Figure 1.4d	Polarisation resulting from charged objects approaching a dielectric object	9
Figure 2.1	Schematic illustration of dipole orientation, anion binding and cation covering of the mobile double layer at the water-air interface	12
Figure 2.2	Schematic illustration of the distribution of charge in models of the electrostatic double layer at a solid-liquid interface	15
Figure 2.3	Actuator styles	22
Figure 2.4	Schematic illustration of actuator swirl chamber designs	23
Figure 2.5	Schematic diagram of novel actuator insert orifice shapes (B to M) and standard circular orifice (B)	27
Figure 2.6	Faraday cup and electrometer	29
Figure 2.7	Effect of dip tube diameter and material on the charge-to-mass ratio of formulations I, II and III, showing standard error bars	34
Figure 2.8	Effect of dip tube length on the charge-to-mass ratio of formulations I and II, showing standard error bars	34
Figure 2.9	Effect of tail piece orifice diameter on the charge-to-mass ratio of formulations I, II and III, showing standard error bars	35
Figure 2.10	Effect of total stem hole orifice area on the charge-to-mass ratio of formulations I, II and III, showing standard error bars	35
Figure 2.11	Effect of vapour phase tap diameter on the charge-to-mass ratio of formulation I, showing standard error bars	36
Figure 2.12	Effect of vapour phase tap diameter on the charge-to-mass ratio of formulation II, showing standard error bars	36
Figure 2.13	Effect of vapour phase tap diameter on the charge-to-mass ratio of formulation III, showing standard error bars	37
Figure 2.14	Effect of actuator orifice diameter on the charge-to-mass ratio of formulations I, II and II, showing standard error bars	41
Figure 2.15	Effect of actuator orifice taper direction on the charge-to-mass ratio of formulations I, III and III, showing standard error bars	41
Figure 2.16	Effect of actuator swirl chamber design in the charge-to-mass ratio of formulation I, showing standard error bars	42

Figure 2.17	Effect of actuator swirl chamber design in the charge-to-mass ratio of formulation II, showing standard error bars	42
Figure 2.18	Effect of actuator swirl chamber design in the charge-to-mass ratio of formulation III, showing standard error bars	43
Figure 2.19	Effect of actuator orifice taper direction and valve vapour phase tap diameter on the charge-to-mass ratio of Formulation III, showing standard error bars	48
Figure 2.20	Spray rates of formulation III when combining actuator orifice taper direction and valve vapour phase tap diameter modifications, showing standard error bars	48
Figure 2.21	Effect of actuator orifice taper direction and stem hole area on the charge-to-mass ratio of Formulation III, showing standard error bars	49
Figure 2.22	Spray rates of formulation III when combining actuator orifice taper direction and valve stem hole area modifications, showing standard error bars	49
Figure 2.23	Effect of actuator swirl chamber design and valve vapour phase tap diameter on the charge-to-mass ratio of Formulation III, showing standard error bars	50
Figure 2.24	Spray rates of formulation III when combining actuator swirl chamber design and valve vapour phase tap diameter modifications, showing standard error bars	50
Figure 2.25	Effect of actuator swirl chamber design and valve stem hole area on the charge-to-mass ratio of Formulation III, showing standard error bars	51
Figure 2.26	Spray rates of formulation III when combining with actuator swirl chamber design and valve stem hole area modifications, showing standard error bars	51
Figure 2.27	Effect of mean charge-to-mass ratio of formulation III of the circumference to area ratio of the novel actuator orifice shapes, showing standard error bars. Labels correspond to those of Fig 2.5	53
Figure 3.1	Reported sizes of some particles which may occur indoors	65
Figure 3.2	Total and regional deposition fractions for various sizes of inhaled spherical particles in the human respiratory tract. Based on nasal breathing at a rate of 15 breaths per minute and a tidal volume of 1450 cm <sup>3</sup>	67
Figure 3.3	Schematic illustration of the deposition mechanisms by which particles may naturally be removed from the air	68
Figure 3.4	Schematic drawing of the test chamber used to quantify the depletion rates of artificially generated dust aerosols	74
Figure 3.5	Sequence of events for the quantification of dust cloud settling rate, the effect on this of liquid aerosols and the contribution of liquid aerosol to particle count	75
Figure 3.6	Apparatus for measurement of droplet size distributions of liquid aerosols produced from pressure-pack dispensers	78
Figure 3.7	Pressure-pack dispenser support for high voltage application	80
Figure 3.8a	Depletion rates for airborne particles of 0.5 to 0.7 µm diameter during natural settling of dust and after treatment with uncharged and artificially	

charged liquid aerosols of an alcohol-based formulation. Standard error bars shown	84
Figure 3.8b Depletion rates for airborne particles of 0.7 to 1.0 $\mu\text{m}$ diameter during natural settling of dust and after treatment with uncharged and artificially charged liquid aerosols of an alcohol-based formulation. Standard error bars shown	84
Figure 3.8c Depletion rates for airborne particles of 1.0 to 2.0 $\mu\text{m}$ diameter during natural settling of dust and after treatment with uncharged and artificially charged liquid aerosols of an alcohol-based formulation. Standard error bars shown	85
Figure 3.8d Depletion rates for airborne particles of 2.0 to 5.0 $\mu\text{m}$ diameter during natural settling of dust and after treatment with uncharged and artificially charged liquid aerosols of an alcohol-based formulation. Standard error bars shown	85
Figure 3.8e Depletion rates for airborne particles of 5.0 to 10.0 $\mu\text{m}$ diameter during natural settling of dust and after treatment with uncharged and artificially charged liquid aerosols of an alcohol-based formulation. Standard error bars shown	86
Figure 3.9a Depletion rates for airborne particles of 0.5 to 0.7 $\mu\text{m}$ diameter during natural settling of dust and after treatment with charged liquid aerosols of formulations I, II and III. Standard error bars shown	88
Figure 3.9b Depletion rates for airborne particles of 0.7 to 1.0 $\mu\text{m}$ diameter during natural settling of dust and after treatment with charged liquid aerosols of formulations I, II and III. Standard error bars shown	88
Figure 3.9c Depletion rates for airborne particles of 1.0 to 2.0 $\mu\text{m}$ diameter during natural settling of dust and after treatment with charged liquid aerosols of formulations I, II and III. Standard error bars shown	89
Figure 3.9d Depletion rates for airborne particles of 2.0 to 5.0 $\mu\text{m}$ diameter during natural settling of dust, and after treatment with charged liquid aerosols of formulations I, II and III. Standard error bars shown	89
Figure 3.9e Depletion rates for airborne particles of 5.0 to 10.0 $\mu\text{m}$ diameter during natural settling of dust and after treatment with charged liquid aerosols of formulations I, II and III. Standard error bars shown	90
Figure 3.10 Droplet size distribution of formulations I, II and III, showing standard error bars	90
Figure 3.11a Depletion rates for airborne particles of 0.5 to 0.7 $\mu\text{m}$ diameter during natural settling of dust and after treatment with uncharged and naturally charged liquid aerosols of an emulsion with continuous water phase. Standard error bars shown	92
Figure 3.11b Depletion rates for airborne particles of 0.7 to 1.0 $\mu\text{m}$ diameter during natural settling of dust, and after treatment with uncharged and naturally charged liquid aerosols of an emulsion with continuous water phase. Standard error bars shown	92
Figure 3.11c Depletion rates for airborne particles of 1.0 to 2.0 $\mu\text{m}$ diameter during natural settling of dust and after treatment with uncharged and naturally	

charged liquid aerosols of an emulsion with continuous water phase. Standard error bars shown	93
Figure 3.11d Depletion rates for airborne particles of 2.0 to 5.0 $\mu\text{m}$ diameter during natural settling of dust, and after treatment with uncharged and naturally charged liquid aerosols of an emulsion with continuous water phase. Standard error bars shown	93
Figure 3.11e Depletion rates for airborne particles of 5.0 to 10.0 $\mu\text{m}$ diameter during natural settling of dust and after treatment with uncharged and naturally charged liquid aerosols of an emulsion with continuous water phase. Standard error bars shown	94
Figure 3.11f Droplet size distribution for uncharged and naturally charged liquid aerosols, with standard error bars	94
Figure 4.1 Schematic illustration of apparatus used to quantify liquid aerosol deposition onto electrically isolated flies	112
Figure 4.2 Schematic diagrams of the chamber used for the direct and space spray bioassays, showing dimensions and fly release positions A and B in aerial view	114
Figure 4.3 Schematic drawing of a pressure-pack dispenser and the spray characteristics, cone angle ( $\theta$ ), droplet size distribution (D) and plume throw ( $\tau$ )	117
Figure 4.4 Deposition of uncharged, negatively charged and positively charged liquid aerosols onto electrically isolated flies. Standard error bars shown	121
Figure 4.5 Knock down of houseflies, <i>Musca domestica</i> , by uncharged and naturally charged insecticide aerosol, using the CERIT direct spray protocol. Standard error bars shown	122
Figure 4.6 Knock down of houseflies, <i>Musca domestica</i> , by uncharged and naturally charged insecticide aerosol, using the CERIT space spray protocol. Standard error bars shown	122
Figure 4.7 Knock down of mosquitoes, <i>Culex quinquefasciatus</i> , by uncharged and naturally charged insecticide aerosol, using the CERIT space spray protocol. Standard error bars shown	123
Figure 4.8 Mortality of houseflies, <i>Musca domestica</i> , and mosquitoes, <i>Culex quinquefasciatus</i> , by uncharged and naturally charged insecticide aerosol, using the CERIT direct spray and space spray protocol. Standard error bars shown	123
Figure 4.9 Droplet size distribution of uncharged and naturally charged insecticide aerosol sprays, showing standard error bars	125

## List of Tables

---

Table 2.1	Composition of the three formulation types	20
Table 2.2	Pressure-Pack Dispenser Components for Formulations I and II, to Investigate the Effect of Valve Component Modifications	22
Table 2.3	Pressure-Pack Dispenser Components for Formulation III, to Investigate the Effect of Valve Component Modifications	24
Table 2.4	Pressure-Pack Dispenser Components for all Formulations, to Investigate the Effect of Actuator Component Modifications	25
Table 2.5	Pressure-Pack Dispenser Components for Formulation III, to Investigate the Effect of Combining Valve and Actuator Modifications	26
Table 2.6	Summary of the effect of modifications to the valve components of pressure-pack dispensers on the charge-to-mass ratio of formulations I, II and III	38
Table 2.7	Summary of the effect of modifications to the actuator components of pressure-pack dispensers on the charge-to-mass ratio of formulations I, II and III	44
Table 2.8	Flow Rate of Formulation III with the Novel Insert Orifice Designs	53
Table 4.1	Charge-to-mass ratio of insecticide sprays, standard error shown in brackets	120
Table 4.2	Calculated values for $KD_{50}$ and $KD_{95}$ for the three bioassays	124
Table 4.3	Spray Characteristics of Uncharged and Charged Insecticide Aerosols Standard Error in Brackets	125

## Preface

---

This research is multidisciplinary and draws from a number of engineering and biological subjects. Sufficient background information has been provided for comprehension by engineers and scientists of any discipline at the beginning of the appropriate chapter. The basic theory of electrostatics and domestic pressure-pack dispensers is provided in Chapter 1. Chapter 2 concerns the production of charged droplets by pressure-pack dispensers, and theory relating to the electrification of liquid during flow is presented in the introduction to this chapter. This phenomenon has been well characterised with respect to hydrocarbons flowing in pipes, due to the hazards associated with the operation of pumping fuels. Application of highly charged domestic sprays for the removal of particles from the air is discussed in chapter 3. Issues concerning indoor air quality, domestic air cleaning devices and industrial electrostatic pollutant scrubbers are relevant to this section of research. Chapter 4 concerns the application of highly charged aerosols to domestic insecticide sprays. The factors affecting the rate of knockdown and mortality of flying insects and the factors influencing deposition of highly charged droplets are discussed here. Chapter 5 draws conclusion on this work, and discusses the potential benefits that may be conferred to a broad range of domestic pressure-pack products by this novel technology.

All liquid aerosols sprayed from pressure-pack dispensers carry some level of electrostatic charge, which is usually too low to alter the trajectory of the droplets. The primary aim of this work was to enhance this naturally generated charge to a level that would alter the behaviour of the aerosol and improve product performance. In this thesis it has been necessary to distinguish between aerosol sprays with a conventional, low level of charge and those which have had the charge-to-mass ratio enhanced to a level exceeding  $1 \times 10^{-4}$  C.kg<sup>-1</sup>. Although all aerosols had some charge, conventional sprays with a low level of charge have been referred to as 'uncharged', while sprays whose charge was enhanced have been referred to as 'charged'.

## Acknowledgements

---

I would like to thank the following people for their constant support and encouragement during this work. My supervisor and friend, Professor John Hughes, whose original idea generated the concept for this research, provided continuous help, assistance and good ideas. Tom Gaunt, my fiancé, has been patient and supportive. His assistance with computer problems, experimental design and with writing this thesis has been invaluable. For this I am deeply grateful, and I hope I can be as supportive and helpful to him during his studies. Jenny Knapp, who has also supervised me, has been constructive in the production of this thesis and in the application of suitable statistical analyses. I would like to thank all my friends and in particular: Karen Jerrim, Andrew Barton, Colin Light, Gary Wills, Paul Gaynor, Jonathon Swingler, William Cheng and Trevor Williams who all contributed to my research in their own way. Karen Jerrim has been a good friend and helped enormously with my experiments. Paul Gaynor and Jonathon Swingler educated me in many technical electrostatic subjects, while Andrew Barton and Gary Wills provided much help with computer issues. Trevor Williams taught me how to make accurate droplet size distribution measurements. Graham Hearne and Reg Jones of Wolfson Electrostatics allowed me to use their equipment and facilities. I must also thank Mark Long, from the Engineering Design

and Manufacturing Centre Workshop for making many pieces of equipment and novel actuator components.

I would also like to thank the sponsors of this research, Reckitt and Colman Plc, and in particular members of the New Business Technology Group (NBTG): Neale Harrison, Rod Fox, Malcolm McKechnie, Duncan Harper, Gay Cornelius and Liz Foyston. Pressure-pack dispensers for all the experiments in this research were supplied by Reckitt and Colman Plc, with various formulation and packaging modifications. Members of NBTG suggested a number of novel terminal orifice designs, and organised manufacture of these for testing. Without this backing it would not have been possible to investigate this concept. The research and development team in Sydney, Australia provided the insecticide samples, and invited me to Sydney to conduct bioassay experiments in their facilities. I would also like to thank Patrick O'Rourke of CERIT (Centre for Entomological Research and Insecticide Technology), who helped perform these experiments.

Finally, I would like to thank my family for their continuous support and encouragement during these studies and the rest of my education. They have inspired me to work hard and always achieve the best possible.

# Chapter 1

---

## 1.1 Introduction

Pressure-pack dispensers, of the type commercially available for domestic use, are widely used to deliver air fragrances, insecticides, deodorants, household surface care and other products. They are known to generate droplets with a net electrostatic charge (Roberts and Hughes, 1979; Krämer and Fröchtenigt, 1993), although this is usually too low to modify the trajectory or behaviour of the liquid aerosol. It was the aim of this research to identify methods of enhancing the charge separation process (such that highly charged liquid droplets are produced during atomisation) and to investigate the benefits that this can bring to liquid aerosol products.

For the trajectory of a droplet to be substantially affected as a result of the charge it carries, a threshold level must be exceeded such that electrostatic forces exceed gravitational forces (Bailey, 1988). The relative magnitudes of these two forces are represented by the charge-to-mass ratio ( $q/m$ ). The charge-to-mass ratio required to elicit useful electrostatic behaviour from the droplets was expected to be in excess of  $\pm 1$  or  $2 \times 10^{-4} \text{ C.kg}^{-1}$ . This is the threshold for enhanced target coating by charged powders (Singh *et al.*, 1978) and has been found to increase deposition of agricultural sprays (Splinter, 1968).

Although the term ‘aerosol’ has been popularly used to describe pressure-pack dispensers, throughout this document the word aerosol will be used in its original meaning of ‘a solid or liquid suspended in gas’ (Hinds, 1982). Thus, the word aerosol will be used to refer to the mist of droplets produced by a pressure-pack dispenser (liquid aerosol) or disperse airborne particulates (dust aerosol).

## 1.2 Domestic Pressure-pack Dispensers

Pressure-pack dispensers are composed of a propellant, a solvent and an active ingredient, packaged in a container equipped with a valve for discharging the liquid formulation when required. Sanders (1970) gives a full explanation of pressurised spray products in his book on the subject, but a concise review of the main points is given here. The main components of a dispenser are shown in Figure 1.1. Figure 1.2 shows a typical valve and actuator assembly in more detail, illustrating the valve in the closed and open positions. In its simplest form, the valve is opened by depression of the actuator, allowing the liquid under pressure to be forced up the dip tube, into the valve housing, and through the now open valve stem holes into an expansion chamber. In this chamber a proportion of the liquefied propellant flashes into the gaseous phase due to the drop in pressure. On entering the actuator, the liquid travels to the terminal orifice. As the liquid formulation leaves this orifice, further liquid propellant flashes into a gas, causing break-up into fine droplets. When the actuator is released, the valve moves back up due to the action of the spring, so that the valve gasket covers the stem holes to prevent further flow of liquid. A vapour phase tap may be present in the valve housing, which allows gaseous propellant to pass into the valve chamber and mix with the liquid flowing through. This has the effect of producing a finer aerosol. The actuator may have a chamber prior to the terminal orifice, composed of a number of tangentially arranged channels that feed in to the orifice, which is illustrated in Figure 1.3. This is known as a swirl chamber or mechanical break-up unit (MBU), and by imparting a swirling motion to the liquid as it leaves the orifice enhances break-up of the liquid into a fine aerosol.

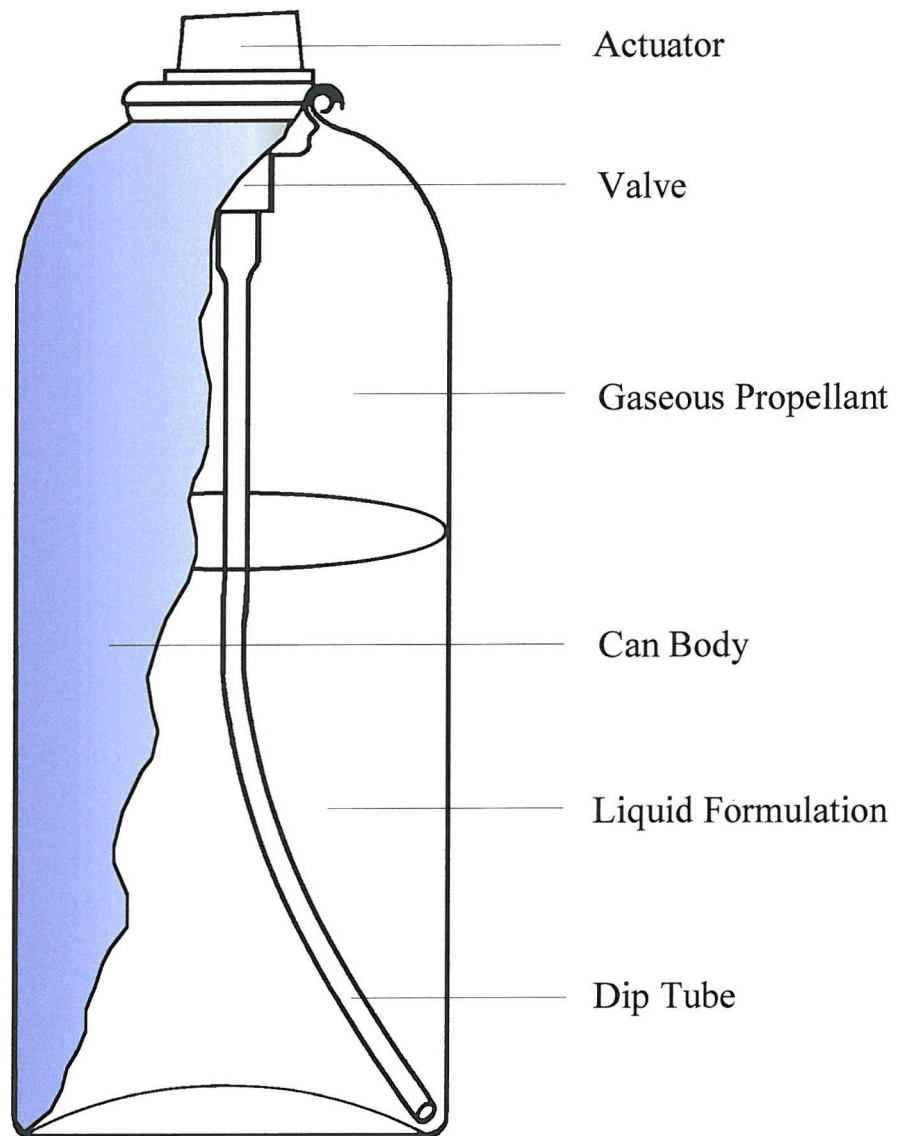


**Figure 1.1** Schematic drawing showing the main components of a pressure-pack dispenser

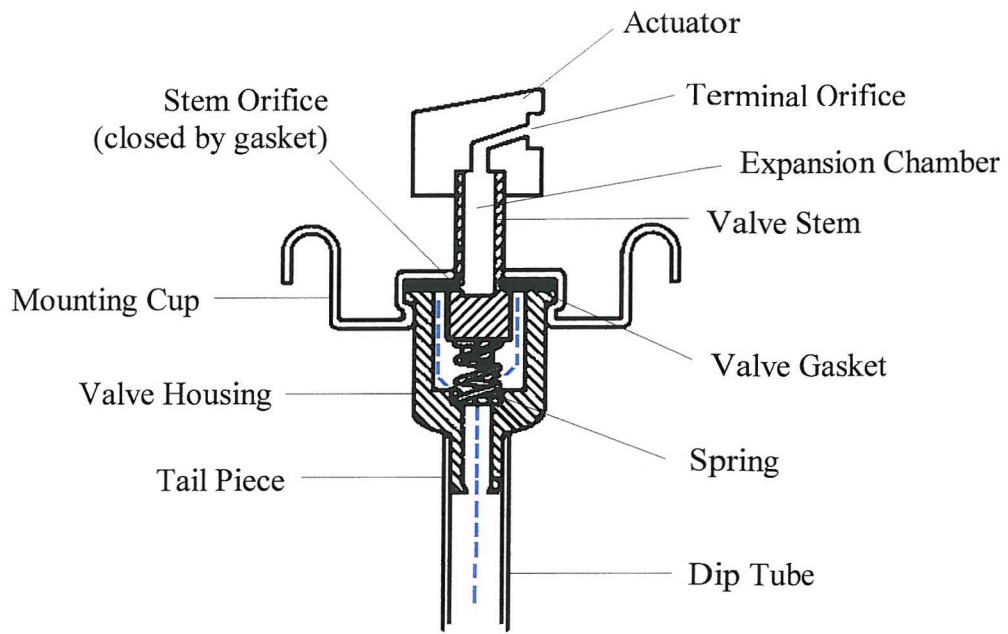


**Figure 1.2a** Schematic illustration of pressure-pack dispenser valve in closed position. Blue line represents flow of liquid formulation.

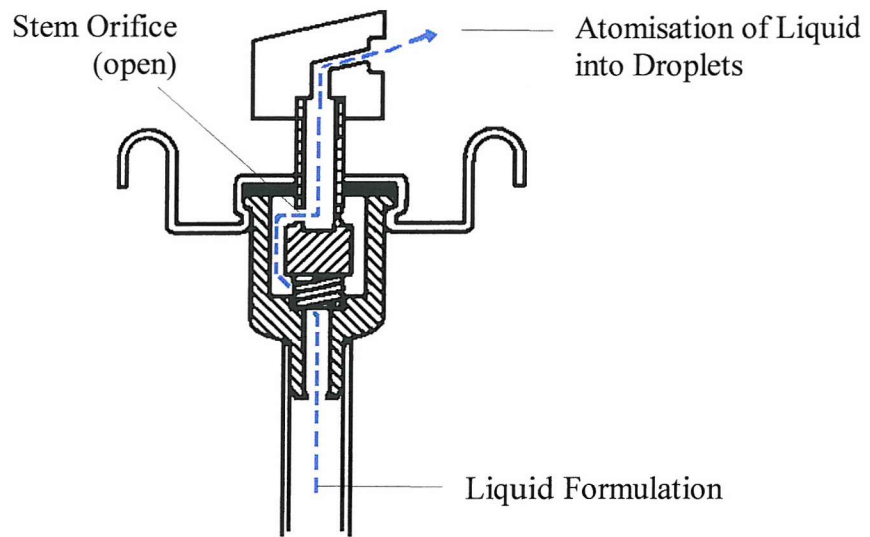


**Figure 1.2b** Schematic illustration of pressure-pack dispenser valve in open position. Blue line represents flow of liquid formulation.

The propellants commonly used in present day dispensers are liquefied hydrocarbons (butane/propane mixes) or compressed gases (air or carbon dioxide). All the dispensers used in this project contained hydrocarbon propellants. The formulation can be either homogeneous, in which all the ingredients are mutually soluble, or heterogeneous, in which they are not. The latter can be a suspension of an insoluble powder in the solvent/propellant mix or may contain immiscible liquids combined as an emulsion. Emulsions may be classified as either oil-in-water or water-in-oil, depending on which phase comprises the continuous phase.

The spray characteristics of liquid aerosols are important for the spray to achieve its objective. For example, air fragrance sprays are more efficient if they have small droplets dispersed in a broad angled plume, achieving wide dispersion of long lasting droplets. Surface sprays are composed of larger droplets, as these must settle quickly. For insecticide sprays, the droplet size distribution can be optimised for the size of flying insect being targeted (Tsuda *et al.*, 1987), and a long plume throw is beneficial in order to contact insects which may be a distance away.

Swirl chambers in the actuator (Fig. 1.3) generate a smaller sized aerosol, and a wider plume cone angle. Smaller aerosol droplets are also produced by more volatile solvents, due to their rapid evaporation after the spray has travelled only a short distance. Ambient conditions can influence the nature of an aerosol: as the temperature rises, the aerosol becomes finer because more propellant flashes from the liquid to a gaseous state during atomisation, and evaporation of the solvent occurs faster. Humidity also influences the aerosol spray, because evaporation is slower at higher relative humidity. Increasing the tailpiece orifice diameter or the stem hole orifice diameter allows a higher flow rate of liquid through the valve, so increases the spray rate (mass of liquid formulation dispensed per unit time). Spray rate can be decreased by the use of a vapour phase tap, which reduces the volume of liquid that can flow through the valve.

Spray characteristics could be affected when making modification to pressure-pack components, in the course of enhancing the charge-to-mass ratio ( $q/m$ ). If they are altered, then the effect of this on the aerosol performance must be considered, because the advantages that the charge confers could be negated.

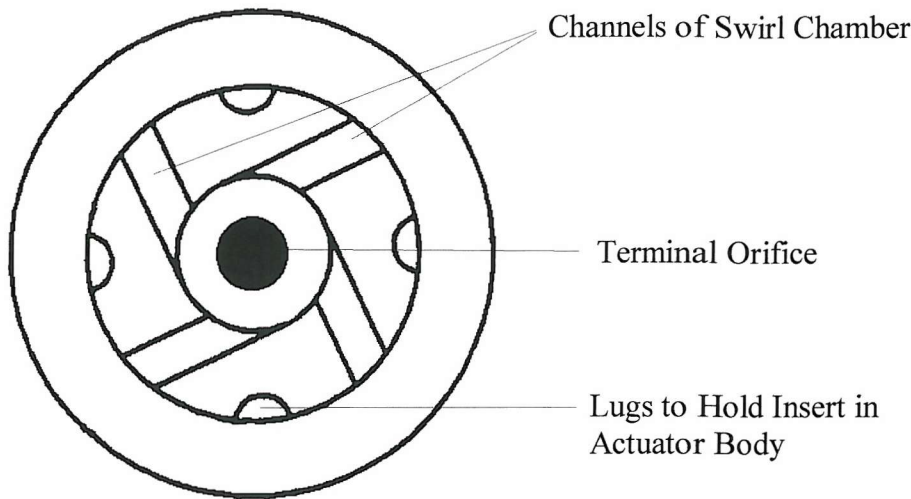


**Figure 1.3** Schematic diagram of internal surface of an actuator insert, showing swirl chambers and terminal orifice.

### 1.3 Electrostatic Principles

Electrostatics, for the current purpose, can be defined as the study of the causes and effects of charge accumulation in solids and liquids. A comprehensive review of the subject is given by Cross (1987). The basic electrostatic interaction can be defined by Coulomb's law, which states that like charges repel and unlike attract, the force depending upon the magnitude of the charges and the spatial separation according to the following equation:

$$F = \frac{qq'}{4\pi\epsilon\epsilon_0 d^2}$$

where  $F$  is the force,  $q$  and  $q'$  are point charges,  $\epsilon$  is the dielectric constant of the medium ( $\sim 1$  in air),  $\epsilon_0$  is the absolute permittivity of free space ( $8.85 \times 10^{-12}$  F/m) and  $d$  is the distance between the objects. From this, the concept of the electric field is derived, which is a region of space around a charged object in which electrical forces act. Electric field can be visualised in terms of field lines, which originate on a positive charge and terminate on a negative charge, all lines terminating at right angles at the electrode surface. The work done in moving a unit charge, unit distance, against unit electric field is defined as the electric potential, the unit of which is the volt (V).

Arising from the basic electrostatic interactions are a number of electrostatic forces, illustrated in Figure 1.4. Coulomb attraction and repulsion forces arise from the proximity of opposite and like charges respectively (Fig. 1.4a). A number of objects with like charges, such as a unipolar charged liquid aerosol, will repel each other, giving rise to a net outward force known as space charge (or diffusion) force (Fig. 1.4b). When a charged object approaches a grounded, conducting object, image charge forces arise (Fig. 1.4c), the magnitude of which can be expressed by the following equation:

$$F = \frac{q^2}{4\pi\epsilon\epsilon_0(2d)^2}$$

where  $d$  is the distance between  $q$  and the surface of the object. An equal and opposite charge is induced in the object, mirroring the approaching charge. There is then Coulombic attraction between the charged object and its oppositely charged image. If the charged object nears a surface of dielectric material, then the formation of dipoles are induced. If the dielectric material is polar then the rotation of permanent dipoles can also occur. There is now Coulombic attraction between the charged objects and the polar region of the surface (Fig. 4.1d). Electrostatic interactions occur over relatively short distances, as the force reduces rapidly as the distance between the objects increases. Electrification of solids and liquid occurs naturally through redistribution of charge carriers (ions or electrons), without the need for an external power supply. Where solids are concerned, charge reorganisation at the surfaces occurs when two materials are brought into contact. For insulating materials, charges are exchanged when the materials are separated, such that one may retain a net negative charge and the other a net positive charge. Both surfaces maintain positively and negatively charged areas, with one charge predominating. This phenomenon is known as triboelectric charging (Cross, 1987). For conducting materials, charge reorganisation occurs during contact, but relaxes as the surfaces are separated. Many factors can influence the polarity and magnitude of triboelectric charging, including temperature, humidity, rubbing or non-rubbing contact and impurities in the material, to the extent that it is not always possible to predict the nature of charge transfer.

Electrification of liquids also occurs through natural processes of charge reorganisation at phase boundaries. These mechanisms are believed involved in the generation of charged droplets by pressure-pack dispensers, so these will be discussed in Chapter 2.

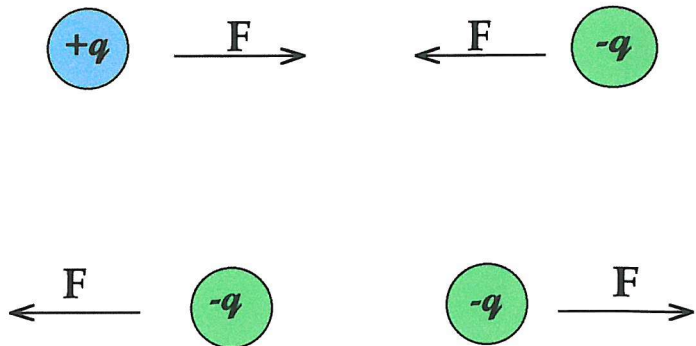


**Figure 1.4a** Coulomb attraction force between oppositely charged objects and Coulomb repulsion force between like charged objects

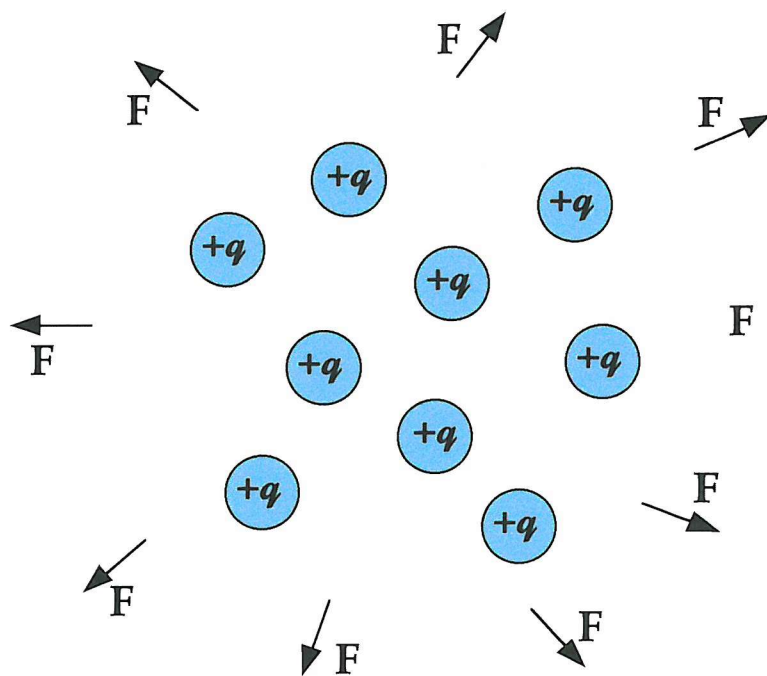


**Figure 1.4b** Space charge force resulting from a cloud of like charged objects

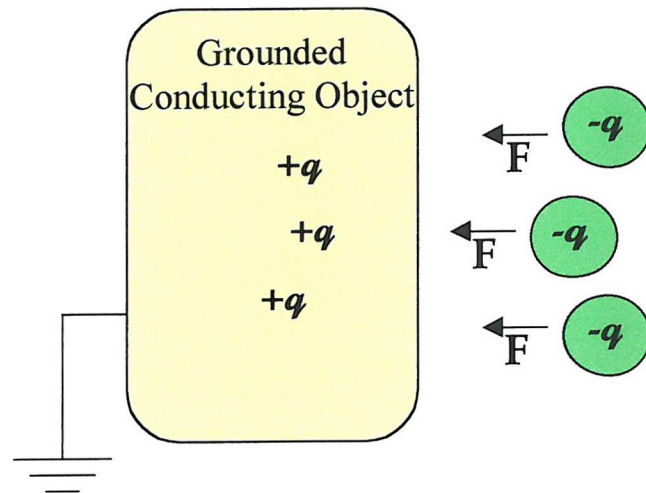


**Figure 1.4c** Image charge force resulting from charged objects approaching a grounded object

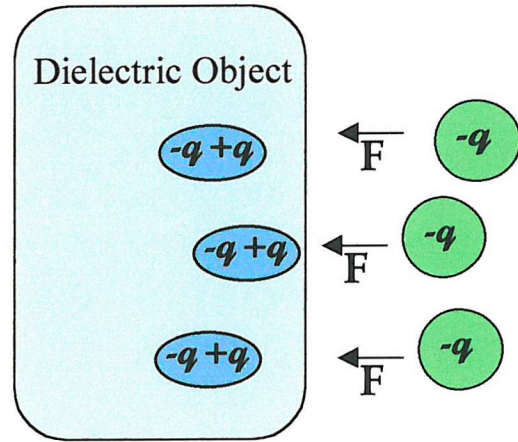


**Figure 1.4d** Polarization resulting from charged objects approaching a dielectric object

## Chapter 2

---

### Charge-to-Mass Ratio of Liquid Droplets Produced by Pressure-Pack Dispensers, and Enhancement of this Charge to an Electrostatically Useful Level

#### 2.1 Introduction

All liquids, when disrupted into droplets carry a net electrical charge, either positive or negative in polarity, although the level of charge is usually small (Bailey, 1988). This charge arises due to an imbalance of mobile charge carriers, such as ions or electrons. Droplets generated by pressure-pack dispensers are similarly electrostatically charged with the level usually being relatively low at a charge-to-mass ratio of  $10^{-10}$  to  $10^{-5}$  C.kg $^{-1}$ . The physical processes involved in generating charged droplets are extremely complex and only partially understood (Makin, 1975). Modern theories explaining droplet charging are based on an electrical double layer mechanism, where local separation of positive and negative charge occurs at liquid-solid, liquid-gas and liquid-liquid interfaces (Touchard, 1995). The aim of the work described in this chapter was to identify ways to enhance the charge-to-mass ratio imparted to droplets as they were generated by pressure-pack dispensers. Modification of standard components of pressure-pack dispensers and the formulation of

the liquid sprayed from them were considered. The charge-to-mass ratio required to elicit useful electrostatic behaviour from the droplets was expected to be in excess of  $\pm 2 \times 10^{-4}$  C.kg<sup>-1</sup>, as this is the threshold for charged powder applications (Singh *et al.*, 1978) and has been found to increase deposition of agricultural sprays (Splinter, 1968).

### 2.1.1 Generation of Charged Droplets Through the Spray Electrification Phenomenon

It has long been recognised that naturally generated sprays of water, such as those originating from waterfalls and in sea sprays, are composed of charged droplets and ions. The first observations of this phenomenon were made by Elster and Geitel (1890), who measured considerable amounts of electrical charge in the vicinity of waterfalls in the Austrian Alps. This phenomenon was subsequently studied in detail by Lenard (1892), and was termed spray electrification. Loeb (1958) provides an extensive review of these early experiments. Lenard measured that the fine droplets of waterfall spray were predominantly negatively charged, while the larger droplets were predominantly positively charged. Because the mist created by waterfalls is composed mainly of fine droplets, due to the larger ones settling quickly, the mists carried a net negative charge. Laboratory studies led Lenard to postulate an electrical double layer at a water-gas interface as an inherent characteristic of water (illustrated schematically in Figure 2.1). For pure water, Lenard measured this double layer to have an outer negative layer about  $5 \times 10^{-6}$  mm thick, with on average one additional electron to every  $10^4$  or  $10^5$  water molecules, and below this is a corresponding positive layer (Lenard, 1915). These double layers are believed to arise as a result of the orientation of some electrical dipoles (water molecules) at the interfaces, with the negative polarity outwards towards the gaseous phase and the positive polarity inwards towards the liquid phase, for most aqueous solutions (Currie and Alty, 1929). Dipoles orientated in this manner attract anions from the bulk of the liquid to their positive ends, as shown in Figure 2.1. Corresponding cations remain in dynamic equilibrium within the liquid bulk. There is now little doubt that electrical double layers exist at gas-liquid interfaces, the proof of which is discussed in detail by Loeb (1958, pp 61-74).

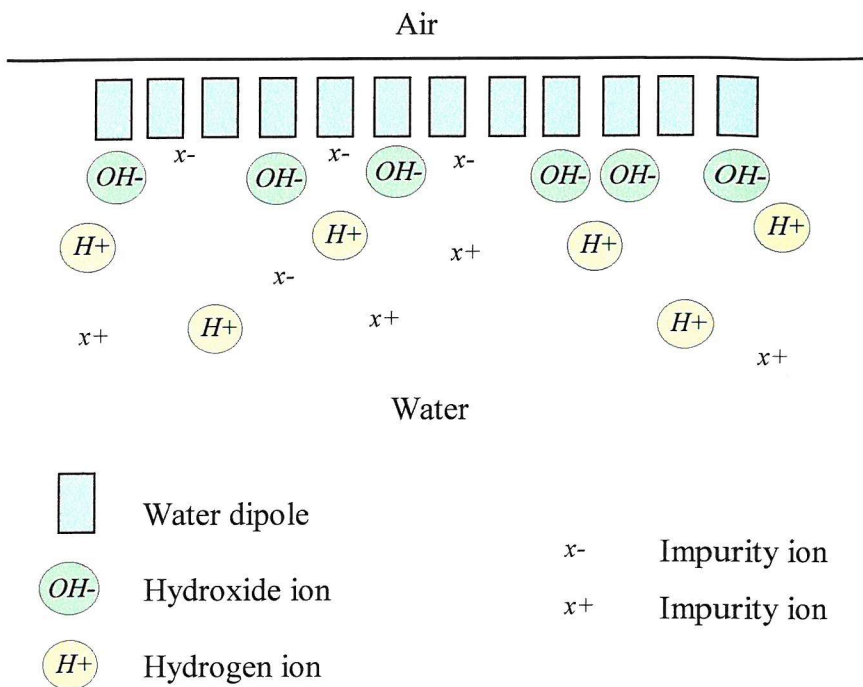


**Figure 2.1** Schematic illustration of dipole orientation, anion binding and cation covering of the mobile double layer at the water/air interface (Currie and Alty, 1929).

Iribarne and Mason (1967) conducted early fundamental research into the role of electrical double layers in droplet charging. They demonstrated that droplets produced by bubbles bursting on the surface of very pure water were always negatively charged. As conductivity of the solution was increased by the dissolution of carbon dioxide gas (up to concentrations of about  $10^{-4}$  M), the charge carried by resultant droplets was significantly reduced. At high solute concentrations, the droplet charge reversed sign to give droplets carrying a small positive charge. Using thin contaminated films on the water surface these authors were able to detect the contaminating material in the droplets produced. From these observations they assumed that during droplet formation a proportion of the liquid surface, containing a thickness of the electrical double layer, was skimmed off resulting in a droplet containing a surfeit of ions of one polarity. The ions more strongly attracted to the orientated dipole molecules of the surface would theoretically be sheared from the corresponding, loosely bound counter ions (ions of the opposite polarity). The double layer was thinner in solutions of higher concentrations, accounting for the smaller charges on these droplets. The charge carried by droplets depends on the mechanical processes of dispersion, ion concentration and charge relaxation times.

### 2.1.2 Separation of Charged Liquids Through the Flow Electrification Phenomenon

Electrical double layers also form at liquid-solid interfaces, where one polarity of ions become relatively tightly bound at the interface to form a compact layer, while counter ions form a diffuse layer extending into the bulk of the liquid. When liquid flows over a solid surface, separation of charge occurs as the tightly bound compact layer remains associated with the solid surface and the diffuse layer of ions is carried with the bulk of the liquid. This process of double layer shearing is known as flow electrification, and although the phenomenon has been extensively studied for a period of time, the mechanism is not fully understood (Koszman and Gavis, 1962b).

In contrast to the electrical double layer described for liquid-gas interfaces, ions at the liquid-solid interface form a double layer mainly through the transfer of charge across the interface, which can occur by several mechanisms (Ottewill, 1975; Parsons, 1971; Cross, 1987). Where the solid surface is metal there can be image forces between ions in the liquid and the surface, such that smaller ion species are more strongly held. Alternatively, preferential chemical adsorption of a specific ionic species from the liquid can occur, or metal ions can enter solution, resulting in the surface becoming charged (Cross, 1987). Where the surface is an insulating solid, chemical groups can become dissociated, altering the charge balance of the surface (Ottewill, 1975). By these mechanisms a potential difference is established across the interface causing a double layer of charge to form. The polarity of the two layers depends on the type of ions on the surface and the relative diffusivity and mobility of the ion species in the liquid (Cross *et al.*, 1977). Parsons (1971) and Haydon (1974) give comprehensive reviews of the electrochemical processes involved in double layer formation.

A number of models for the distribution of charge in the double layer have been postulated, and some of these are illustrated in Figure 2.2. Helmholtz (1879) hypothesised that counter ions were parallel to the charged surface at a distance of about one molecular diameter (Fig. 2.2a). This model was superseded by the Gouy-Chapman model (Gouy, 1910; Chapman, 1913), which postulated a less rigid, diffuse layer of counter ions, decreasing in concentration away from the surface (Fig 2.2b). This theory was later modified by Stern (1924), who proposed a tightly bound, single layer of counter ions close to the surface, and a further diffuse layer also of counter ions (Fig. 2.2c). Once the double layer has formed in a stationary liquid it is considered to be in an equilibrium condition, in

which diffusion of ions away from the interface is balanced by counter diffusion towards it (Gavis and Koszman, 1961).

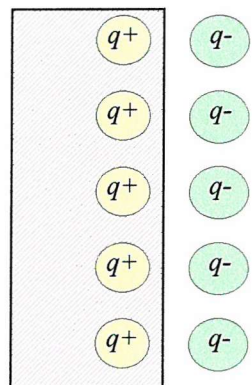
Where liquids flow through pipes, either conducting or electrically insulating, charge from the diffuse layer is conveyed with the liquid, resulting in a net charge in the bulk of the liquid. In any pipe there will, however, be another process occurring in addition to charge accumulation, and that is charge relaxation due to the resultant space charge field (Cross *et al.*, 1977). The process of charge accumulation can be continuous as long as charge is replenished by the flow of current to the pipe walls (Cross, 1987). Continuous electrification occurs in glass, rubber and plastic tubes, because these materials can conduct the small currents observed during flow electrification (Gavis and Koszman, 1961). Klinkenberg and van der Minne (1958, pp 154) determined that, from the point of view of static electricity, a rubber hose may be considered a conductor.

The main characteristics of this electrification phenomenon were summarised by Gavis and Koszman (1961), which were based upon observations from the preceding literature concerning charge separation in liquids flowing in pipes. Five factors were described which influenced charge separation:

1. Conductivity: as the conductivity of liquid is increased, charge separation increases. This continues up to a maximum, after which further increases in conductivity cause charge separation to decrease.
2. Flow characteristics of the liquid: generally, increasing velocity increases charge separation, and turbulent flow causes greater electrification than laminar flow.
3. Surface type: conducting pipes result in the highest levels of charge separation, although electrification also occurs in glass, plastic and rubber tubes.
4. Tube length: longer tubes cause greater charge separation than shorter tubes, proportionally at first. As tube length increases its influence on charge separation decreases.
5. The charge separation process is continuous; so surface charge must be replenished.

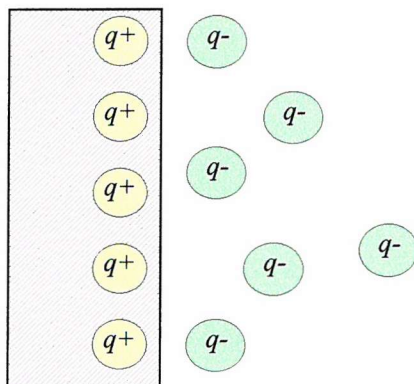
Since these observations were made, numerous theories and models for charge separation have been devised, although application of these to real systems is not always feasible without simplifying the system and ensuring that all components are well defined (Cross *et al.*, 1977).

Solid      Liquid



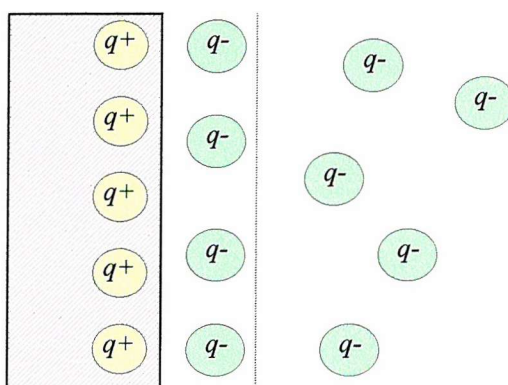
**(a) Helmholtz model,**  
with counter ions parallel to  
the charged surface.

Solid      Liquid



**(b) Gouy-Chapman model,**  
with diffuse layer of counter ions  
decreasing in concentration with  
distance from the surface.

Solid      Liquid



**(c) Stern model,**  
with a single layer of strongly  
associated counter ions close  
to the surface and a diffuse  
layer of the same polarity

**Figure 2.2** Schematic illustration of the distribution of charge in models of the electrostatic double layer at a solid-liquid interface.

### 2.1.3 Characteristics of Flow Electrification

The amount of charge which accumulates as liquids flow through pipes is dependent upon three main parameters: the electrochemical reaction at the interface, the thickness of the diffuse layer and the characteristics of flow (Touchard, 1995). The nature of the electrochemical reaction at the interface depends upon the interaction between the solid and liquid components, and this determines the net flux of electrical charges comprising the double layer. The rate of this reaction, and the resulting concentration of charge carriers, thus controls the process of flow electrification. Attempts have been made to model this reaction (Walmsley and Woodford, 1981; Touchard *et al.*, 1996) but since the electrochemistry of the boundary reactions is not well understood these rely on adjustable parameters (Cross, 1987).

The thickness of the double layer is largely determined by the conductivity of the liquid and charge relaxation time (Koszman and Gavis, 1962b). For aqueous solutions, where the conductivity is greater than  $10^{-6}$  S m<sup>-1</sup>, the diffuse layer is only a few molecules thick, while in less conducting liquids, such as hydrocarbons, it can extend a macroscopic distance into the liquid bulk (Koszman and Gavis, 1962a; Gavis and Koszman, 1961). Liquids with a conductivity of between  $10^{-13}$  and  $10^{-7}$  S m<sup>-1</sup> demonstrate charging, maximum charging occurring at about  $10^{-10}$  S m<sup>-1</sup>. In more conducting liquids charge relaxation times are very fast, and a high space charge cannot accumulate in the liquid bulk. In less conducting liquids the concentration of dissociated ions is insufficient to develop high levels of charge separation (Klinkenberg and van der Minne, 1958; Koszman and Gavis, 1962a).

Finally, the characteristics of flow, such as velocity, turbulence, pipe length, roughness and radius, influence the flow electrification process through the effect on double layer shearing. Turbulent flow is generally considered to generate more charge than laminar flow, and this is believed to be a result of the diffuse layer of charge being distributed across the bulk of the liquid by turbulent transport (Klinkenberg and van der Minne, 1958). During laminar flow there is little or no radial movement of the double layer, so the space charge density does not differ significantly from when the liquid is at rest (Touchard, 1995). The effect of higher flow velocity is to increase turbulence and reduce the thickness of the sub-layer of laminar flow at the pipe wall. Velocity dependence of flow

electrification is also related to liquid conductivity (Rutgers *et al.*, 1956; Klinkenberg and van der Minne, 1958). The flow velocity determines the degree of turbulence through any particular pipe, and thus the thickness of the sub-layer of laminar flow at the walls. Where turbulence is less, this sub-layer is thicker. Three scenarios are conceivable (Cross, 1987), depending upon the relative depths of the laminar sub-layer and the electric double layer. For liquids of low conductivity, the diffuse charged layer is very thick, and may extend uniformly across the diameter of a narrow pipe. Under these circumstances turbulent flow would have no influence over flow electrification, as charge would be distributed evenly through the pipe. At intermediate conductivity, the diffuse layer extends a finite distance from the wall of the pipe. As flow velocity increases, the depth of the laminar sub-layer decreases, and thus more of the diffuse layer is transported into the bulk of the liquid. The results of experimental work with hydrocarbon liquids flowing in metallic pipes by Klinkenberg and van der Minne (1958) show that with increases in conductivity (reduction in double layer thickness) the flow velocity required to demonstrate enhanced charge separation also increases. Charge separation in highly conducting liquids is largely unaffected by turbulent flow, because the diffuse charge layer resides wholly within the sub-layer of laminar flow. Pumping liquid through a pipe can have the effect of increasing electrification, as a result of the increased turbulence (Klinkenberg and van der Minne, 1958). The presence of a filter can enhance charging by several orders of magnitude due to the increase in turbulence, and the increase in surface contact in relation to the volume of liquid (Klinkenberg and van der Minne, 1958; Taylor and Secker, 1994).

Pipes with roughened surfaces have been observed to generate different levels of charge separation than those with smooth surfaces (Cross, 1987; Touchard *et al.*, 1989). The development of small eddies very close to the walls of the pipe are believed to disturb the double layer, influencing the shearing process. The effect on pipe diameter and length has also been studied and modelled (Touchard and Romat, 1981), indicating that longer pipes and pipes with narrower diameters develop higher levels of charge separation. Narrow pipes can develop higher levels of charge separation than wide pipes because they allow a larger proportion of liquid to contact the pipe wall for the development of double layers. Increasing pipe length can increase charge separation by allowing double layer searing to continue during flow until an equilibrium situation is reached, at which point charge separation and charge relaxation processes are balanced.

#### 2.1.4 Charged Liquid Droplets

Depending upon the method of droplet formation, four mechanisms can be responsible for the production of charge on liquid droplets (Cross, 1987):

1. Disruption of the double layer occurring at a liquid-gas interface,
2. Disruption of the double layer occurring at a liquid-solid interface,
3. Charge separation within the liquid due to an electric field,
4. Charge separation due to uneven division of ions randomly distributed in the liquid.

Disruption of the double layer at a liquid-gas interface is involved in the formation of charged droplets during bubble bursting (Iribarne and Mason, 1967), as discussed in Section 2.1.1. Where droplets are formed at an orifice however, disruption of the double layer of the liquid-solid interface (discussed in Section 2.1.2) is more important (Cross, 1987 p81). In mechanism 3, charge separation within the bulk of the liquid occurs due to an electric field, such that on disruption of the liquid, the resultant droplets are formed with a surplus of ions of one polarity. Mechanism 4 is also known as statistical charging, and refers to the production of droplets with a few ions more of one sign than the other, due to random distribution.

#### 2.1.5 Objectives

The low charge-to-mass ratio of the liquid aerosol generated by pressure-pack dispensers ( $10^{-10}$  to  $10^{-5}$  C.kg<sup>-1</sup>) is expected to be too low to cause any significant modifications to the trajectory or behaviour of the aerosol droplets. Shearing of the double layer at the solid-liquid interface is postulated to be the main mechanism responsible for this charge, although this is not a verifiable hypothesis in a system as complex as pressure-pack dispensers. The primary objective of this section of work was to enhance the charge-to-mass ratio of the aerosol droplets generated by pressure-pack dispensers to  $10^{-4}$  C.kg<sup>-1</sup>. This was to be achieved by modifying components of the dispensers, while maintaining the spray characteristics. A semi-empirical approach was adopted, due to the complexity of both the pressure-pack dispenser system and the formulations sprayed. It was predicted

that results would be consistent with the theory that shearing of the electrical double layer was the primary mechanism responsible for charge separation.

Initially, the effects of modifications to standard components of pressure-pack dispensers (described in Chapter 1) were investigated for their effect on the charge-to-mass ratio of three different commercial formulation types. The valve parameters investigated were:

1. dip tube diameter, material and length
2. stem hole diameter
3. vapour phase tap presence and diameter
4. stem hole number and diameter.

Actuator components investigated were:

1. terminal orifice diameter
2. orifice taper direction
3. swirl chamber type.

Three formulations were used in studying these modifications: a homogeneous alcohol-based solution, a heterogeneous emulsion with continuous water phase and a heterogeneous emulsion with continuous oil phase. Commercially, the different formulations perform different functions. The effects of valve and actuator parameters were first studied in isolation, and then selected parameters were combined for investigation. Some analysis of spray rates was also undertaken, as the function of the pressure-packs under investigation relies upon certain spray characteristics to be maintained, as discussed in Chapter 1. This indicated that spray rate was reduced in pressure-pack dispensers in which elevated charge-to-mass ratios had been achieved. In an attempt to overcome this, novel actuator orifice shapes were designed and manufactured, which attempted to combine high spray rates with a high charge-to-mass ratio.

## 2.2 Materials and Methods

The effect of modifying the specifications of some pressure-pack components on the charge-to-mass ratio ( $q/m$ ) of common pressure-pack formulations was investigated. Three formulation types were used, and are described in Section 2.2.1. Charge-to-mass ratios were measured according to the method described in Section 2.2.6 for the component variations described in Sections 2.2.2 to 2.2.5. The spray rate was also recorded when investigating valve and actuator combinations and novel actuator inserts, according to the method in Section 2.2.7, as an indication of the effect these modifications had on the spray characteristics.

### 2.2.1 Specifications of Pressure-Pack Formulations

Three formulation types commonly used in pressure-pack dispensers were used for the current experiments, and are described in Table 2.1.

**Table 2.1** Composition of the three formulation types

<b>Ingredient</b>	<b>Ingredients as percentage of total volume</b>		
	<b>Formulation I</b> Alcohol-based solution	<b>Formulation II</b> Oil in water emulsion	<b>Formulation III</b> Water in oil emulsion
<b>Butane/Propane Propellant</b>	28 (40 psi)	35 (40 psi)	40 (55 psi)
<b>Hydrocarbon Solvent</b>	57 (alcohol)	5 (C9 hydrocarbon)	8 (C13 hydrocarbon)
<b>Aqueous Solvent</b>	14	59	51
<b>Corrosion Inhibitor</b>	<1	<1	<1
<b>Surfactant/ Emulsifier</b>	<1	<1	<1
<b>Fragrance Component</b>	<1	<1	<1

Formulation I was a homogeneous, alcohol-based solution, with no emulsification, in which the components remained homogeneous in the dispenser. Formulation II was a heterogeneous emulsion with an aqueous continuous phase, in which the oil and water components separated over a period of minutes after mixing. Formulation III was a heterogeneous emulsion with an oil continuous phase, in which the oil and water components separated over a period of minutes after mixing. All dispensers containing formulations I and II were prepared and supplied by Reckitt and Colman Products Ltd, Hull, and all dispensers of formulation III were prepared and supplied by Reckitt and Colman Products Pty Ltd, Australia.

## 2.2.2 Effect of Valve Modifications on Charge-to-Mass Ratio - Specifications of the Pressure-Pack Dispensers

The components of the pressure-pack dispensers used in this investigation were all industry standard. The function of these components was described in Chapter 1 and illustrated in Figure 1.2. The valve parameters investigated were:

1. material, diameter and length of the dip tube
2. vapour phase tap orifice diameter
3. tailpiece orifice diameter
4. diameter and number of stem holes.

Table 2.2 lists the standard components used with formulations I and II, with the range of modifications investigated. In all cases, the valves of the dispensers were composed according to the standard description, with the exception of the component that was being varied. The only exception to this was in the investigation of the effect of dip tube diameter and material, where the tailpiece orifice was 1.27 mm in diameter instead of the standard 0.64 mm. The actuator used with formulations I and II was a button-style actuator illustrated in Figure 2.3 with a 0.66 mm diameter orifice and *Aqua*-type swirl chamber. The construction and function of swirl chambers was discussed in Chapter 1 and illustrated in Figure 1.3. The different commercial types used in the current investigation are illustrated in Figure 2.4. Table 2.3 lists the standard components used with formulation III and the range of modifications investigated. Not all valve parameters were investigated

with respect to formulation III, as insufficient components were available. The actuator used with formulation III was a single-piece overcap with a 0.85 mm diameter straight through orifice, with no swirl chamber, also illustrated in Figure 2.3.

**Table 2.2** Pressure-Pack Dispenser Components for Formulations I and II, to Investigate the Effect of Valve Component Modifications

Pressure-Pack Component	Description of Standard	Parameters Investigated
<b>Dip Tube Diameter and Material</b>	3.00 mm Polyethylene	3.00 mm Polyethylene 1.27 mm Polypropylene
<b>Dip Tube Length</b>	186 mm	186 mm 372 mm
<b>Tailpiece Orifice Diameter</b>	0.64 mm 1.27 mm*	0.64 mm 2.03 mm
<b>Stem Hole Orifice Diameter</b>	4 x 0.61 mm	4 x 0.61 mm 2 x 0.51 mm
<b>Vapour Phase Tap Orifice Diameter</b>	none	none 0.64 mm 1.02 mm 1.17 mm

\* Denotes component used in place of standard when studying dip tube effects

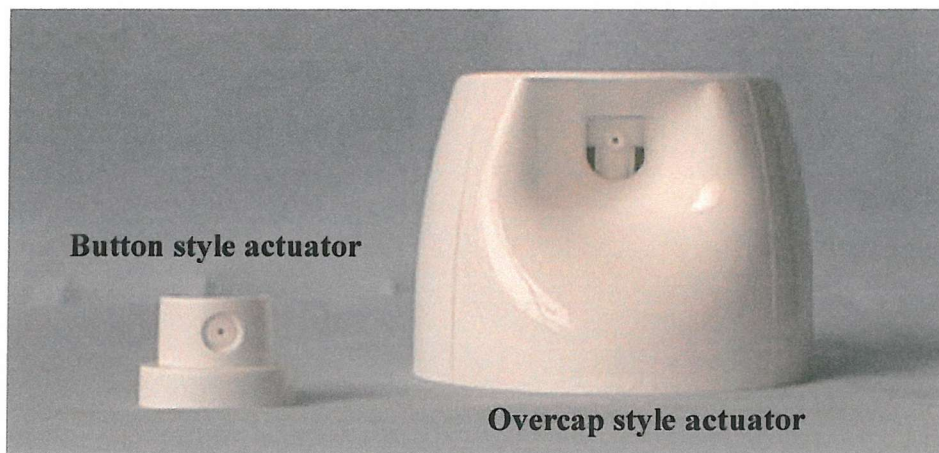
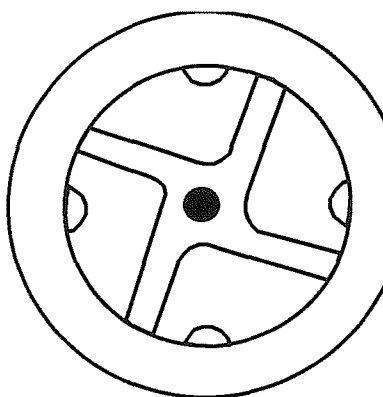
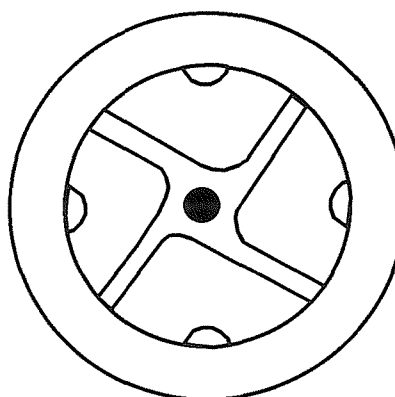


**Figure 2.3** Actuator styles



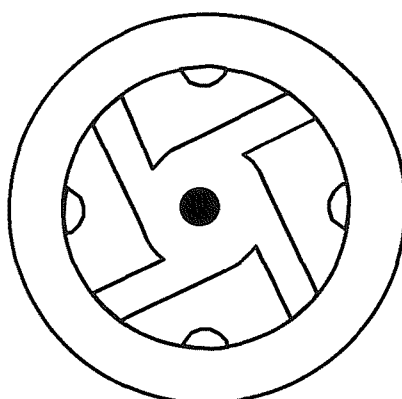
**MBU style swirl chamber**

Channel width: 0.4 mm, channel length: 1.7 mm



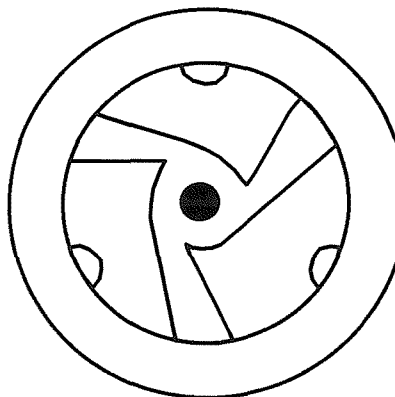
**MBU CO<sub>2</sub> style swirl chamber**

Channel width: 0.2 mm, channel length: 1.8 mm



**Aqua style swirl chamber**

Channel width: 0.55 mm, channel length: 1.7 mm



**MBU Soft style swirl chamber**

Channel width: 0.5 mm at widest and 0.2 mm at narrowest, channel length: 1.0 mm

**Figure 2.4** Schematic illustration of actuator insert swirl chamber designs

**Table 2.3** Pressure-Pack Dispenser Components for Formulation III, to Investigate the Effect of Valve Component Modifications

Pressure-Pack Component	Description of Standard	Parameters Investigated
<b>Dip Tube Diameter and Material</b>	3.00 mm Polyethylene	3.00 mm Polyethylene 1.27 mm Polypropylene
<b>Dip Tube Length</b>	163 mm	-
<b>Tailpiece Orifice Diameter</b>	1.27 mm	-
<b>Stem Hole Orifice Diameter</b>	2 × 0.51 mm	2 × 0.51 mm 2 × 0.61 mm 3 × 1.27 mm
<b>Vapour Phase Tap Orifice Diameter</b>	0.64 mm	0.41 mm 0.76 mm

### 2.2.3 Effect of Actuator Modifications on Charge-to-Mass Ratio - Specifications of the Pressure-Pack Dispensers

Table 2.4 lists the standard valve components used with the three formulations, and the range of actuator modifications investigated. In all cases, the dispensers were composed according to the standard description, with the exception of the component that was being varied. The actuator parameters investigated were:

1. orifice diameter
2. orifice taper direction
3. effect of swirl chamber geometry.

A two-piece button-style actuator as shown in Figure 2.3 was used; the standard parameters for which were a 0.46 mm diameter orifice and no swirl chamber. Unless the taper direction was under investigation, all orifices were straight through, without any angle.

**Table 2.4** Pressure-Pack Dispenser Components for all Formulations, to Investigate the Effect of Actuator Component Modifications

Pressure-Pack Component	Formulation I	Formulation II	Formulation III
<b>Dip Tube Diameter</b>	3.00 mm Polyethylene	3.00 mm Polyethylene	3.00 mm Polyethylene
<b>Dip Tube Length</b>	186 mm	186 mm	163 mm
<b>Tail piece Orifice</b>	0.64 mm	0.64 mm	1.27 mm
<b>Stem Holes</b>	4 × 0.61 mm	4 × 0.61 mm	4 × 0.61 mm
<b>Vapour Phase Tap</b>	None	None	0.64 mm
<b>Swirl Chamber Type</b>	MBU, MBU CO <sub>2</sub> , MBU soft Aqua	MBU MBU CO <sub>2</sub> MBU soft Aqua	MBU MBU CO <sub>2</sub> MBU soft Aqua
<b>Actuator Orifice Diameter</b>	0.46 mm 0.64 mm	0.46 mm 0.64 mm	0.46 mm 0.64 mm
<b>Actuator Orifice Taper</b>	5.5° Narrowing 5.5° Widening	5.5° Narrowing 5.5° Widening	5.5° Narrowing 5.5° Widening

#### 2.2.4 Effect of Combining Valve and Actuator Modifications on Charge-to-Mass Ratio - Specifications of the Pressure-Pack Dispensers for Formulation III

The two valve and two actuator components which had the greatest effect on the q/m of formulation III were selected and combined, in order to investigate the relationship between components with respect to charge separation. Only formulation III was used for this part of the study. Modifications to the number and diameter of the stem holes and the diameter of the vapour phase tap were the valve parameters selected, while the actuator parameters were the orifice taper direction and the swirl chamber type. The investigation was restricted to these combinations because they appeared to have the greatest effect during the previous investigations. Table 2.5 describes the specifications of the pressure-pack dispensers.

**Table 2.5** Pressure-Pack Dispenser Components for Formulation III, to Investigate the Effect of Combining Valve and Actuator Modifications

Pressure-Pack Component	Description of Standard	Component Investigated
<b>Dip Tube Diameter and Material</b>	3.00 mm Polyethylene	-
<b>Tail piece Orifice Diameter</b>	1.27 mm	-
<b>Stem Hole Diameters</b>	2 × 0.61 mm	2 × 0.51 mm 3 × 1.27 mm
<b>Vapour Phase Tap Diameter</b>	0.64 mm	0.41 mm 0.76 mm
<b>Actuator Body</b>	Button-type	-
<b>Swirl Chamber Type</b>	None	<i>MBU CO2</i> <i>Aqua</i>
<b>Orifice Diameter</b>	0.46 mm	-
<b>Orifice Taper</b>	Straight-Through	5° Narrowing 5° Widening

## 2.2.5 Effect of Novel Actuator Orifice Designs on the Charge-to-Mass Ratio of Formulation III - Specifications of the Pressure-Pack Dispensers

A range of novel actuator orifice shapes were designed, such that the perimeter of the shape which forms the surface for the liquid to contact was larger than that of a circular orifice with the same cross-sectional area. This can be defined as the circumference length to cross-sectional area ratio (C;a) of the actuator orifice. These shapes are labelled B to M in Figure 2.5, and the shape labelled A is the circular orifice with which these were compared. The purpose of these shapes was to investigate whether the increased contact area between solid and liquid in the actuator orifice would increase the charge-to-mass ratio achieved, whilst maintaining the spray rate of liquid from the pressure-pack dispenser. Only formulation III was used to investigate the effect of these shapes, which all had a cross-sectional area of 0.567 mm<sup>2</sup>, the same as a circular orifice 0.85 mm in diameter.

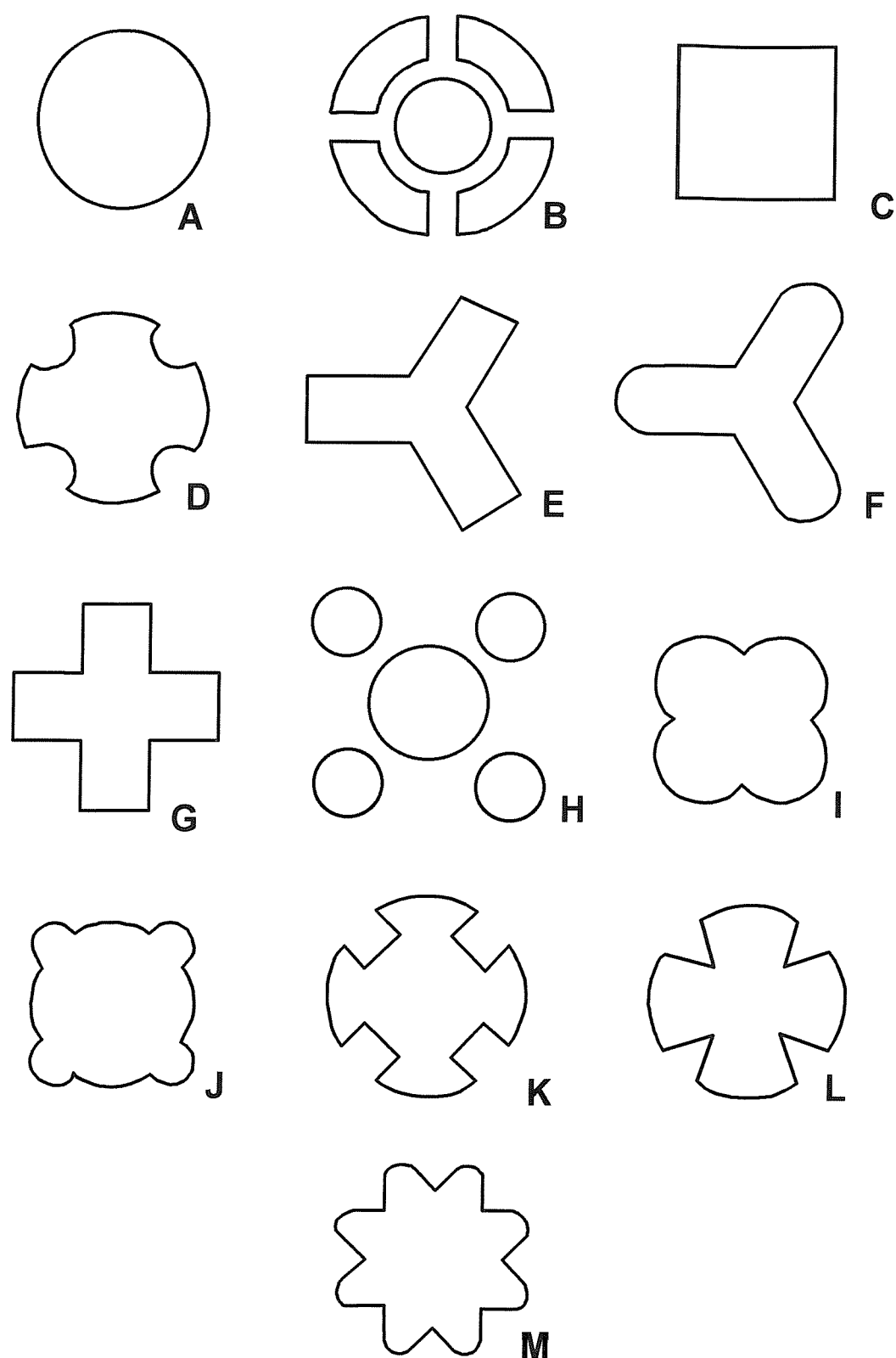


**Figure 2.5** Schematic diagram of novel actuator insert orifice shapes (B to M) and standard circular orifice (A)

The pressure-pack dispenser for formulation III comprised the same valve components indicated in Table 2.4, while the actuator used was the button-type (Fig. 2.3). The novel orifice shapes all had a 5.5° widening orifice taper and were incorporated into actuator inserts with *Aqua*-style swirl chambers (Fig. 2.4).

#### 2.2.6 Measurement of Charge-to-Mass Ratio of Liquid Aerosols Generated by Pressure-Pack Dispensers

The charge-to-mass ratio of the droplets generated from pressure-pack dispensers was measured using a Faraday cup, which is shown in Figure 2.6. The pressure-pack dispensers were accommodated within the Faraday cup, and actuation was achieved using an electrically insulating rod inserted through orifices in the top of the cup. The actuator of the pressure-pack dispenser directed the plume of droplets out of the Faraday cup. The orifices in the lids of the cup measured 32 mm in diameter, while the orifice in the front of the Faraday cup measured 47 mm in diameter. At the orifice in the front of the Faraday cup a ring of PTFE (Teflon) separated the outer and inner compartments. This prevented liquid droplets falling between the outer and inner compartments, which would have created an electrical connection between the inner and outer cups, rendering the apparatus ineffective. The Faraday cup was connected to an electrometer (Keithley Instruments, 610C solid state electrometer), which registered the charge, in Coulombs, on the dispenser during actuation. It was assumed that the net charge carried by the liquid aerosol generated was equal in magnitude and opposite in electrical polarity to the charge recorded on the pressure-pack dispenser inside the cup. The total mass of the droplets produced was calculated by weighing the pressure-pack dispenser before and after the spraying procedure. The  $q/m$  was then calculated by dividing the charge in Coulombs by the mass in kilograms, to give  $q/m$  in Coulombs per kilogram ( $C\cdot kg^{-1}$ ). Before each measurement, the pressure-pack dispensers were shaken for 5 seconds. The mean and standard error of five measurements was calculated for each pressure-pack combination.

The accuracy of the measurements taken in this way was dependent upon the assumption that there was no net electrical charge present on the insulated rod used to actuate the pressure-pack dispenser when inside the Faraday cup. Charge could not be

carried down the rod into the Faraday cup, but any charge residing on the surface of the rod would have been recorded on the electrometer, affecting the charge recorded for the pressure-pack dispenser. Precautions were taken against this occurrence by checking that there was no deflection of the electrometer recording needle when the rod was inserted.



**Figure 2.6** Faraday cup and electrometer

### 2.2.7 Measurement of Spray Rate

The spray rate ( $R$ ) is defined as the mass of formulation dispensed per second ( $\text{g.s}^{-1}$ ). The dispenser was first weighed, and then sprayed by hand for about 3 seconds. A stopwatch was used to measure the duration of the spray. The dispenser was then reweighed, and the mass dispensed divided by the measured duration of the spray, giving the mass sprayed per second. The average of at least three replicates was calculated.

The spray rate of pressure-pack dispensers was only measured during the investigation into the effects of valve and actuator parameter combinations (2.2.4), and of the effects of novel terminal orifice designs (2.2.5).

## 2.3 Results

### 2.3.1 Effect of Valve Modifications on Charge-to-Mass Ratio

In the following comparisons, the effect on the charge-to-mass ratio ( $q/m$ ) of aerosol droplets of using different valve component variables within pressure-pack dispensers was investigated. Only industry standard components were selected, which occasionally limited the parameters that could be investigated. The components used are shown in Table 2.2 for formulations I and II and in Table 2.3 for formulation III. Formulation I generated charge sometimes with a positive polarity and sometimes with a negative polarity, depending on the component combinations. This tendency to switch polarity will be discussed later, but for the analysis of results, polarity was ignored. This decision was based on the assumption that only the polarity of the charge, and not the magnitude, was affected.

#### Effect of Modifications to the Dip Tube Parameters

The effect on charge-to-mass ratio of modifying the diameter and length of the dip tube and the material of construction were investigated. Comparisons were made between a 3.00 mm polyethylene tube and a 1.27 mm polypropylene tube. The standard length of a dip tube was 186 mm for formulations I and II, and to investigate the effect of a longer tube this was replaced by one of 372 mm, by coiling it around to reach the bottom of the body of the dispenser. Polyethylene tubes 3.00 mm in diameter were used. Figure 2.7 compares the effect of dip tube diameter and material on the  $q/m$  of formulations I, II and III, while Figure 2.8 compares the effect of dip tube length on the  $q/m$  of formulations I and II. Both Figures show standard error bars, and are based on 5 replicates.

Figure 2.7 shows that generally the  $q/m$  is lower when a 3.00 mm diameter polyethylene dip tube is used, than with a 1.27 mm diameter polypropylene tube, but the level of this increase differed according to the formulation. These differences were statistically analysed using t-tests, although it was necessary to first transform ( $\log_{10}$ ) the data in order to stabilise the variance. All statistical procedures are described in Appendix A. These analyses implied that the increases in  $q/m$  observed with the 1.27 mm

polypropylene dip tube in formulations I and II were highly statistically significant ( $p < 0.01$ ). There was no significant difference with formulation III.

The effect of using a dip tube of twice the usual length was also to increase the  $q/m$  of formulations I and II, as shown in Figure 2.8. Statistical analysis (t-test) suggested that the increase was highly statistically significant for formulation I ( $p < 0.01$ ), but not for formulation II.

#### Effect of Modifications to the Tailpiece Orifice Diameter

The effect on charge-to-mass ratio of tailpiece orifice diameter was investigated by comparing orifices of 0.64 mm and 2.03 mm in diameter, with formulations I and II. The results are shown in Figure 2.9, with standard error bars.

The results indicated that although the smaller orifice achieved a slightly higher  $q/m$  on formulation I, the difference was not statistically significant (t-test). There was no statistically significant difference in  $q/m$  between 0.64 mm and 2.03 mm orifice diameters for formulation II.

#### Effect of Modifications to the Stem Hole Area

The effect on charge-to-mass ratio of modifying the number and diameter of the stem holes in the valve was investigated. Standard valve components allowing the number of stem holes and their diameter to be varied independently were not available. Thus, the overall area given by the various combinations in number and diameter of stem holes was compared to changes in the  $q/m$ . Pressure-pack dispensers of formulations I and II were prepared incorporating stem holes of either  $4 \times 0.61$  mm diameter or  $2 \times 0.51$  mm diameter in the valve. The stem hole orifice area was  $1.169 \text{ mm}^2$  and  $0.409 \text{ mm}^2$  respectively. Formulation III was prepared in pressure-packs with either  $3 \times 1.27$  mm diameter,  $2 \times 0.61$  mm diameter or  $2 \times 0.51$  mm diameter format stem holes. The total orifice area of these was  $3.800 \text{ mm}^2$ ,  $0.584 \text{ mm}^2$  and  $0.409 \text{ mm}^2$  respectively. Figure 2.10 compares the mean  $q/m$  generated on the droplets sprayed from these dispensers based on five replicates, showing standard error bars.

The results for the three formulations show a trend for a larger total area of stem hole to generate a lower q/m than a smaller area. Statistical analysis for formulation I (t-test) indicated that the smaller stem hole area gave a significantly ( $p < 0.05$ ) higher q/m than the larger area. For formulation II, analysis suggested that there was no significant difference in q/m. ANOVA statistical analysis (Appendix A) was conducted for formulation III, which suggested a statistically significant difference. A subsequent Tukey test (Appendix A) showed that only the  $3.800 \text{ mm}^2$  ( $3 \times 1.27 \text{ mm}$ ) and the  $0.409 \text{ mm}^2$  ( $2 \times 0.51 \text{ mm}$ ) combinations differed significantly ( $p < 0.05$ ).

#### Effect of Modifications to the Diameter of the Vapour Phase Tap

The effect of the diameter of the vapour phase tap (VPT), and the effect of the absence of a vapour phase tap, on the charge-to-mass ratio was compared. With formulations I and II, comparisons were made between dispensers with vapour phase taps of 0.64 mm diameter, 1.02 mm diameter and 1.17 mm diameter, and with no VPT. With formulation III VPTs of 0.41 mm diameter and 0.76 mm diameter were compared

The results shown in Figures 2.11, 2.12 and 2.13 for formulations I, II and III respectively demonstrate a trend for the use of a VPT to increase the q/m achieved. A larger diameter VPT tended to give a higher charge than VPTs of smaller diameter. ANOVA statistical analysis was performed for formulations I and II. With formulation I, there was a highly significant difference ( $p < 0.01$ ) and a subsequent Tukey test showed that the mean q/m was different for all VPT diameters, with the exception of the 1.02 mm diameter and 1.17 mm diameter VPTs. For formulation II, there was also a highly significant difference ( $p < 0.01$ ) in the mean values for q/m, and a subsequent Tukey test showed that only the 0.64 mm diameter and 1.02 mm diameter VPT gave values for q/m not significantly different from each other. The difference in q/m of formulation III with the 0.41 mm diameter and 0.76 mm diameter VPTs was analysed (t-test) which suggested the difference observed to be highly statistically significant ( $p < 0.01$ ).

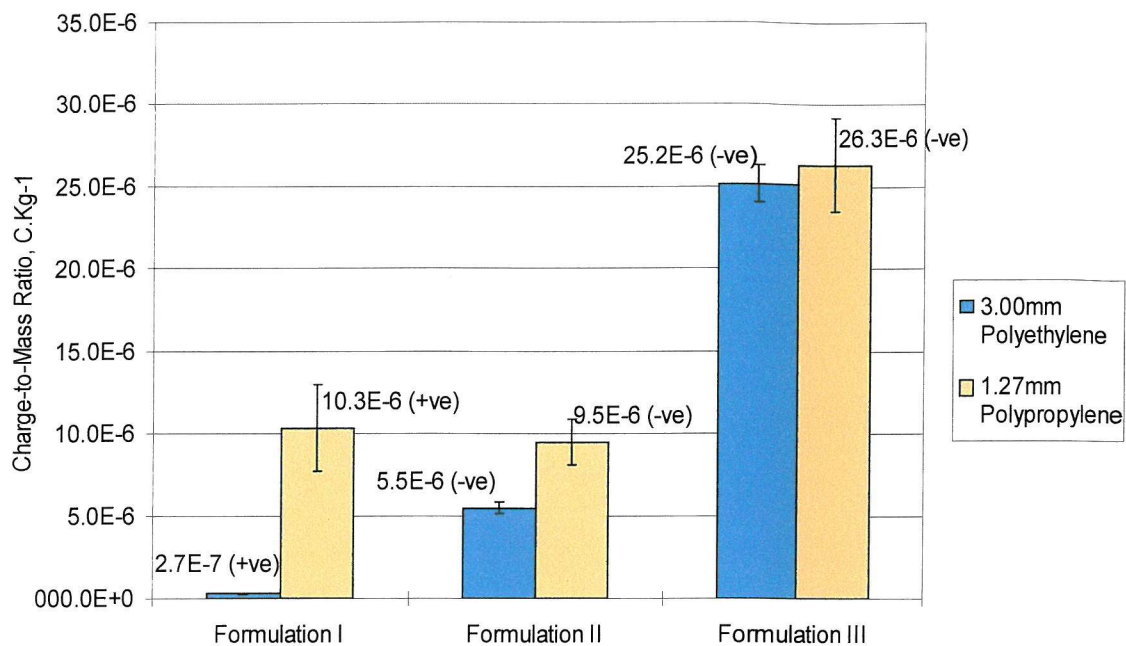


**Figure 2.7** Effect of dip tube diameter and material on the charge-to-mass ratio of formulations I, II and III, showing standard error bars

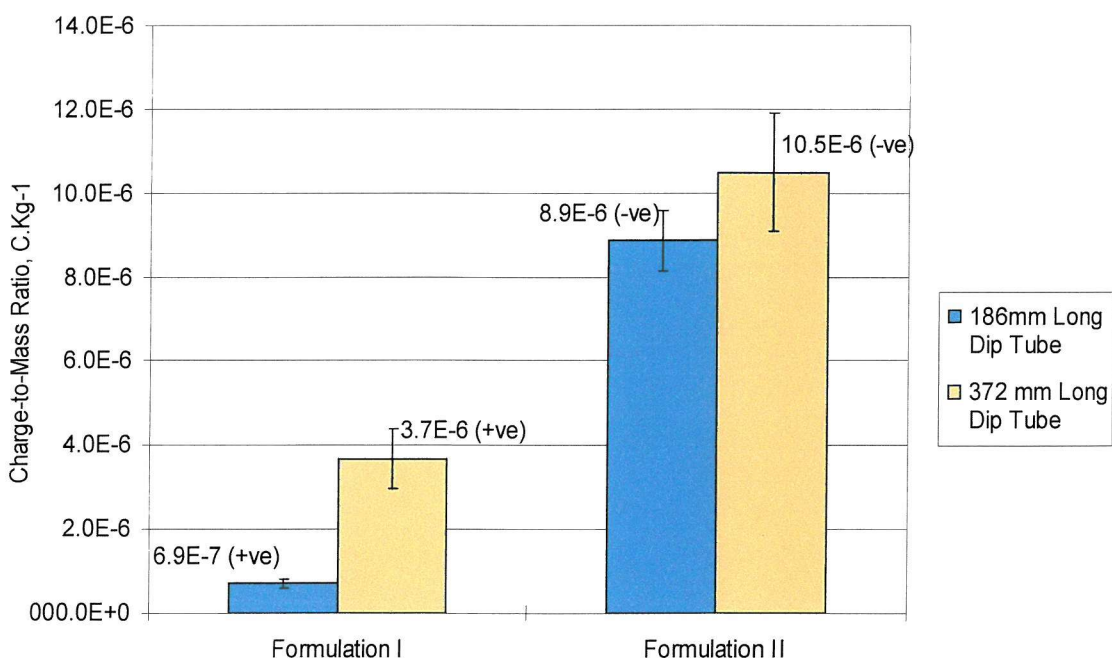


**Figure 2.8** Effect of dip tube length on the charge-to-mass ratio of formulations I and II, showing standard error bars

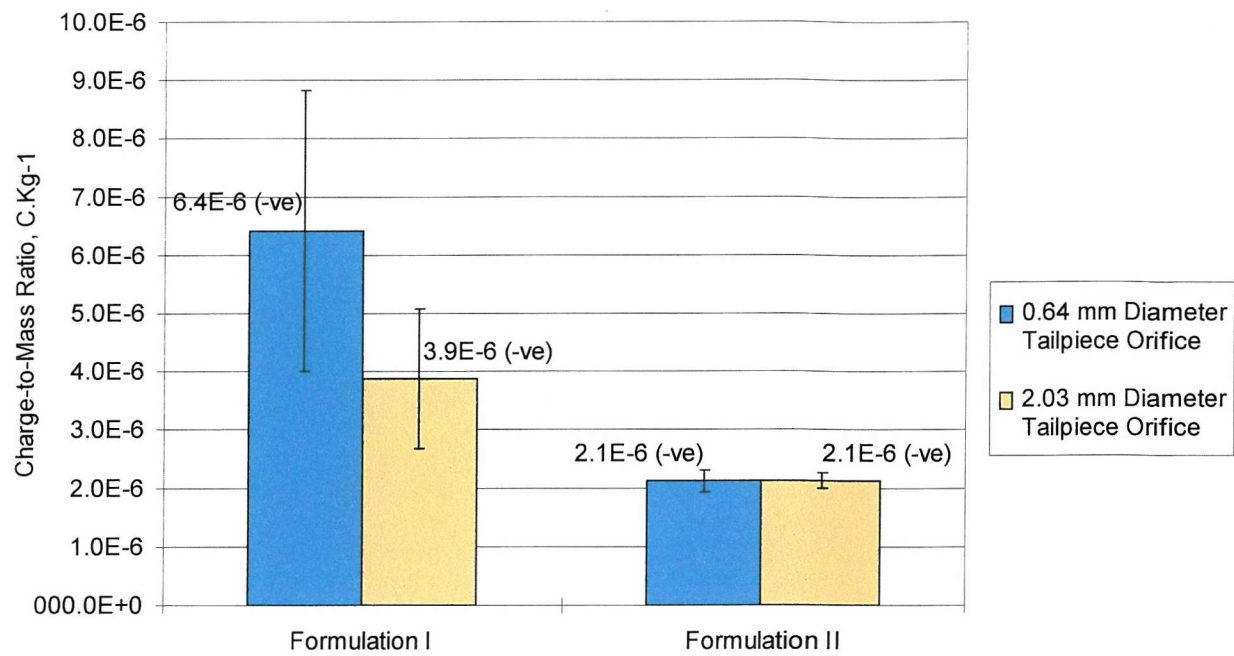


**Figure 2.9** Effect of tail piece orifice diameter on the charge-to-mass ratio of formulations I, II and III, showing standard error bars

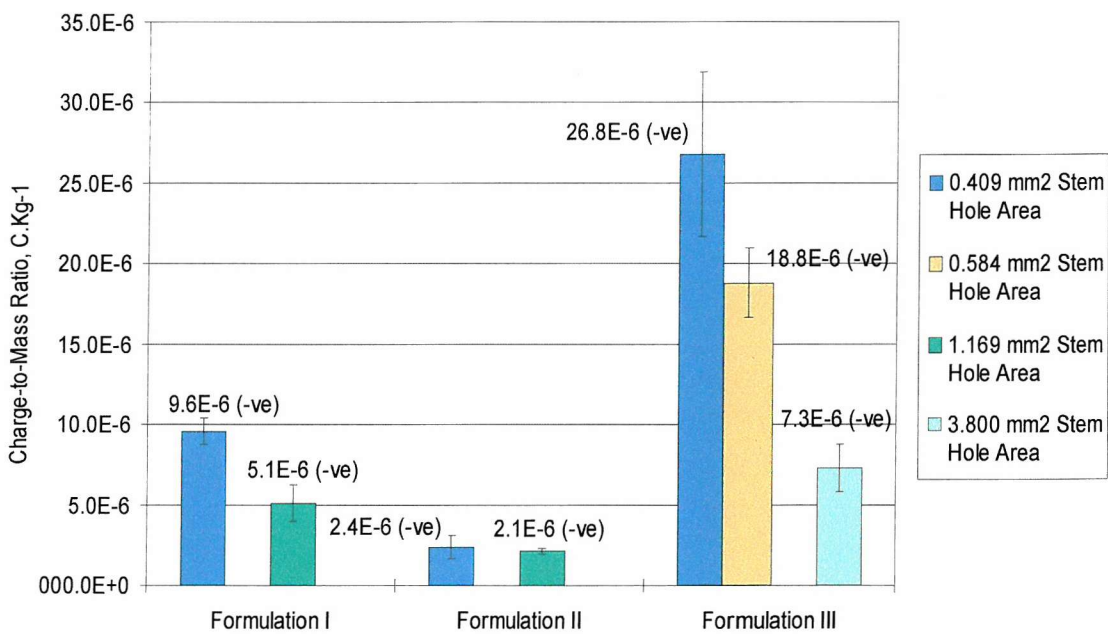


**Figure 2.10** Effect of total stem hole orifice area on the charge-to-mass ratio of formulations I, II and III, showing standard error bars

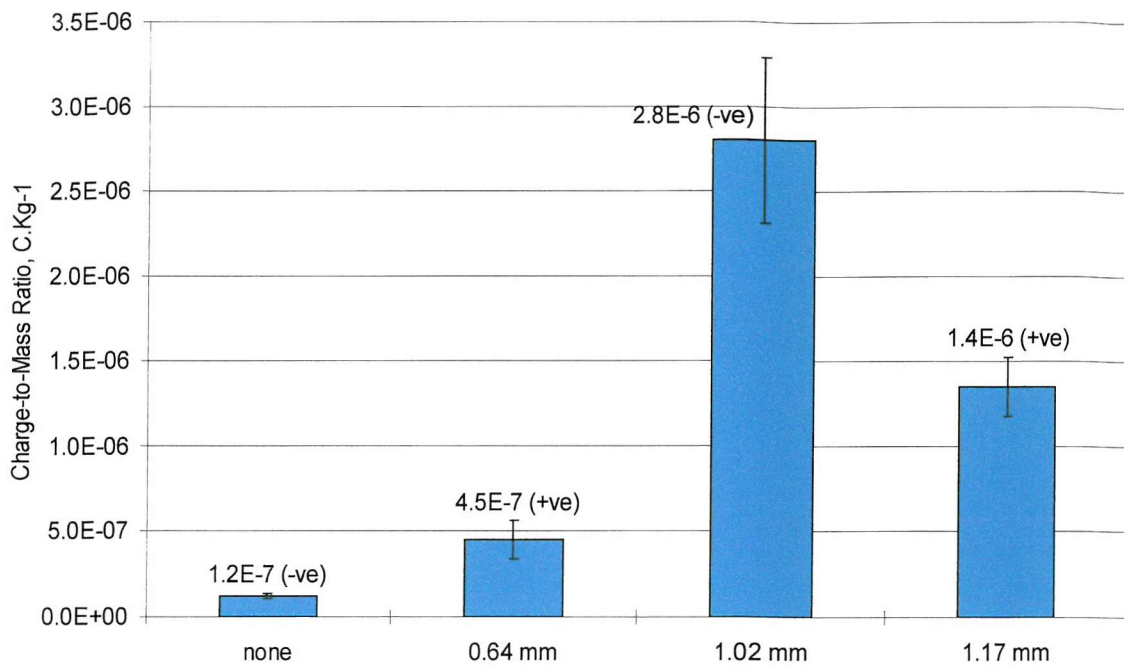


**Figure 2.11** Effect of vapour phase tap diameter on the charge-to-mass ratio of formulation I, showing standard error bars

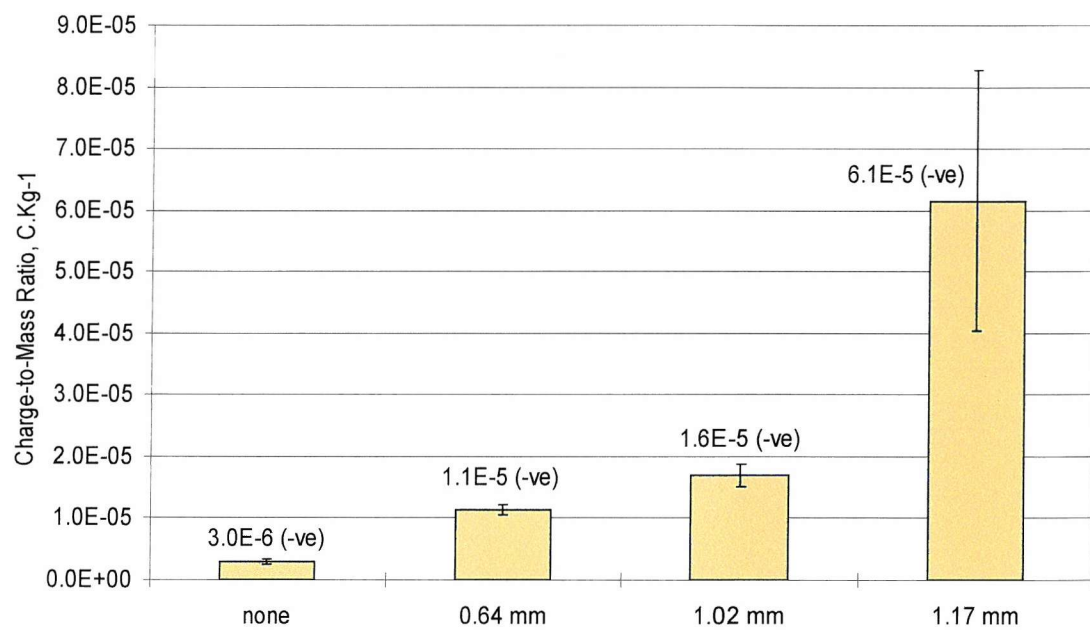


**Figure 2.12** Effect of vapour phase tap diameter on the charge-to-mass ratio of formulation II, showing standard error bars

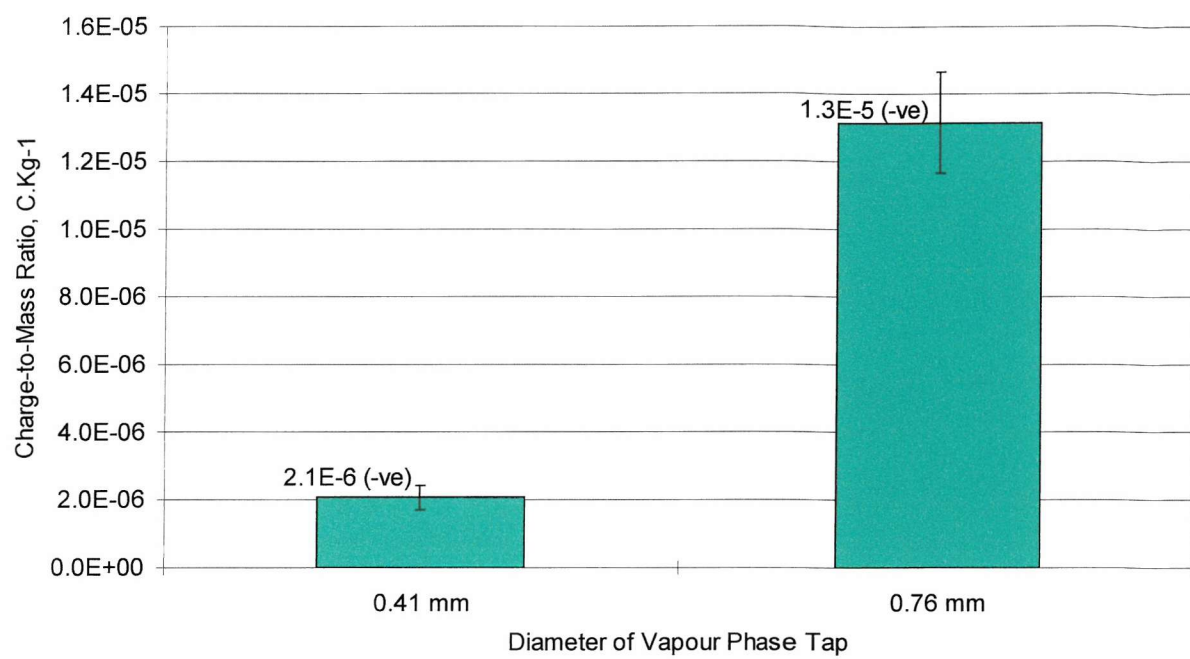


**Figure 2.13** Effect of vapour phase tap diameter on the charge-to-mass ratio of formulation III, showing standard error bars

## Summary of the Effect of Valve Modifications on Charge-to-Mass Ratio

The effect of dip tube diameter, material and length, tailpiece orifice diameter, stem hole number and diameter, and vapour phase tap diameter on the charge-to-mass ratio of formulations I, II and III have been investigated. The effect of variations in these components was not always the same for all formulations. The trends and effects are summarised briefly in Table 2.6.

**Table 2.6** Summary of the effect of modifications to the valve components of pressure-pack dispensers on the charge-to-mass ratio of formulations I, II and III

Component	Formulation I	Formulation II	Formulation III
<b>Dip tube diameter and material</b>	1.27 mm polypropylene gave a higher q/m ( $p < 0.01$ )	1.27 mm polypropylene gave a higher q/m ( $p < 0.01$ )	No significant difference
<b>Dip tube length</b>	Long tube gave a higher q/m than short tube ( $p < 0.01$ )	Trend for long tube to give a higher q/m than the short tube Not statistically significant	Not known
<b>Tail piece orifice diameter</b>	Trend for 0.64 mm diameter to give a higher q/m than 2.03 mm Not statistically significant	Trend for 0.64 mm diameter to give a higher q/m than 2.03 mm Not statistically significant	Not known
<b>Total stem hole area</b>	Smaller total stem hole area gave a higher q/m than larger total areas ( $p < 0.05$ )	Trend for smaller total stem hole area to give a higher q/m than larger total areas Not statistically significant	0.409 mm <sup>2</sup> total stem hole area gave a higher q/m than a 3.800 mm <sup>2</sup> area ( $p < 0.05$ )
<b>Vapour phase tap presence and diameter</b>	Larger diameter VPT gave a higher q/m than smaller ones, and no VPT gave the lowest q/m ( $p < 0.01$ )	Larger diameter VPT gave a higher q/m than smaller ones, and no VPT gave the lowest q/m ( $p < 0.01$ )	0.41 mm diameter VPT gave a higher q/m than 0.76 mm ( $p < 0.01$ )

### 2.3.2 Effect of Actuator Modifications on Charge-to-Mass Ratio

In the following comparisons, components of the actuator were modified. The components used are described in Table 2.4 for the three formulations. The actuator used was of the button-style shown in Figure 2.3, with 0.46 mm diameter, straight through orifice and *MBU*-type swirl chamber (Fig. 2.4) unless otherwise specified.

#### Effect of Modifications to the Diameter of the Actuator Orifice

Two diameters of actuator orifice; 0.46 mm and 0.64 mm were compared for their effect on the charge-to-mass ratio of formulations I, II and III.

The mean values for  $q/m$ , based on 5 replicates, are shown in Figure 2.14, with standard error bars. The trend for formulations I and II was for the smaller orifice to achieve a higher  $q/m$ , while for formulation III the opposite trend was observed. Statistical analysis (t-test) suggested these trends to be highly statistically significant ( $p < 0.01$ ) for all three formulations.

#### Effect of Modifications to the Taper Direction of the Actuator Orifice

The charge-to-mass ratio of formulations I, II and III with widening and narrowing orifices was measured. The orifices were 0.46 mm in diameter at the narrowest point, and the tapers were  $5.5^\circ$ . The results, based on 5 replicates, are shown in Figure 2.15 with standard error bars. For formulations I and II there was a trend for the widening orifice to generate a higher  $q/m$ . Statistical analysis (t-test) suggested that only the difference with formulation II was significant ( $p < 0.05$ ). With formulation III the trend was more exaggerated, and was highly statistically significant ( $p < 0.01$ ).

## Effect of Modifications to the Swirl Chamber Type

The effect of various commercially available swirl chamber designs on the charge-to-mass ratio of formulations I, II and III was measured. The swirl chambers used (*MBU*, *MBU CO<sub>2</sub>*, *MBU soft* and *AQUA*) were described in Figure 2.4.

The mean q/m generated using these swirl chambers is shown in Figures 2.16, 2.17 and 2.18 for formulations I, II and III respectively, with standard error bars. The results are based on 5 replicates. ANOVA statistical analyses were performed, followed by Tukey tests, to show which pairs were significantly different from each other. With formulation I (Fig. 2.16) the *MBU* and *AQUA* swirl chamber types generated a statistically significantly larger q/m than the *MBU CO<sub>2</sub>* type. With formulation II (Fig. 2.17) the *MBU* type chamber generated a significantly larger q/m than the others ( $p < 0.05$ ). The *MBU CO<sub>2</sub>* type gave a significantly higher q/m than the *MBU Soft* and the *Aqua* types ( $p < 0.05$ ). For formulation III, the q/m with the *AQUA* type swirl chamber was significantly lower than that with the other three, and the q/m with the *MBU CO<sub>2</sub>* chamber was significantly higher than that with the *MBU Soft* type.

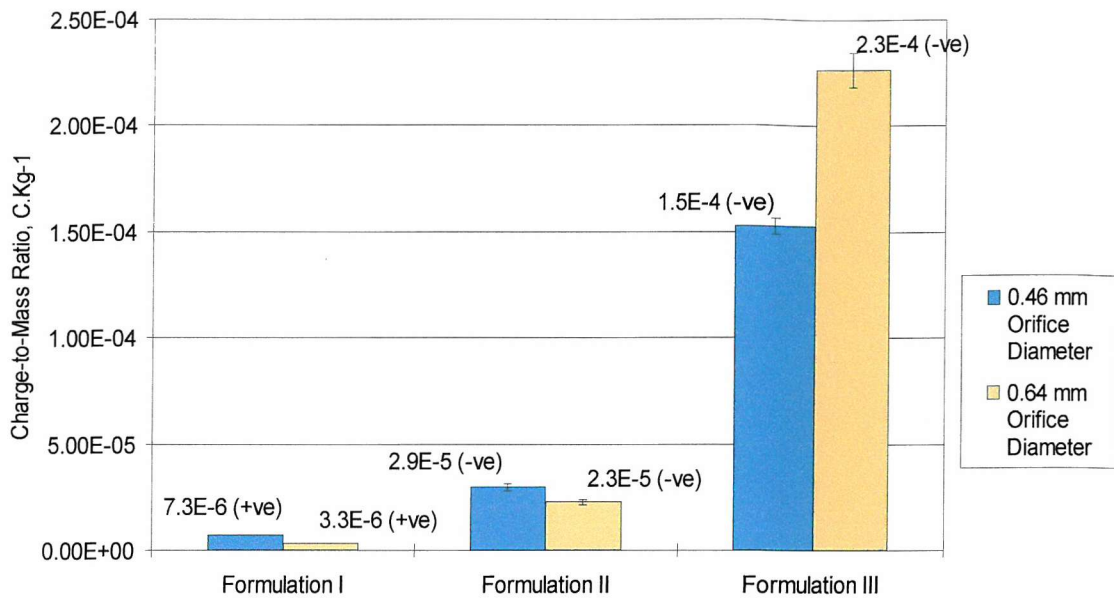


**Figure 2.14** Effect of actuator orifice diameter on the charge-to-mass ratio of formulations I, II and III, showing standard error bars

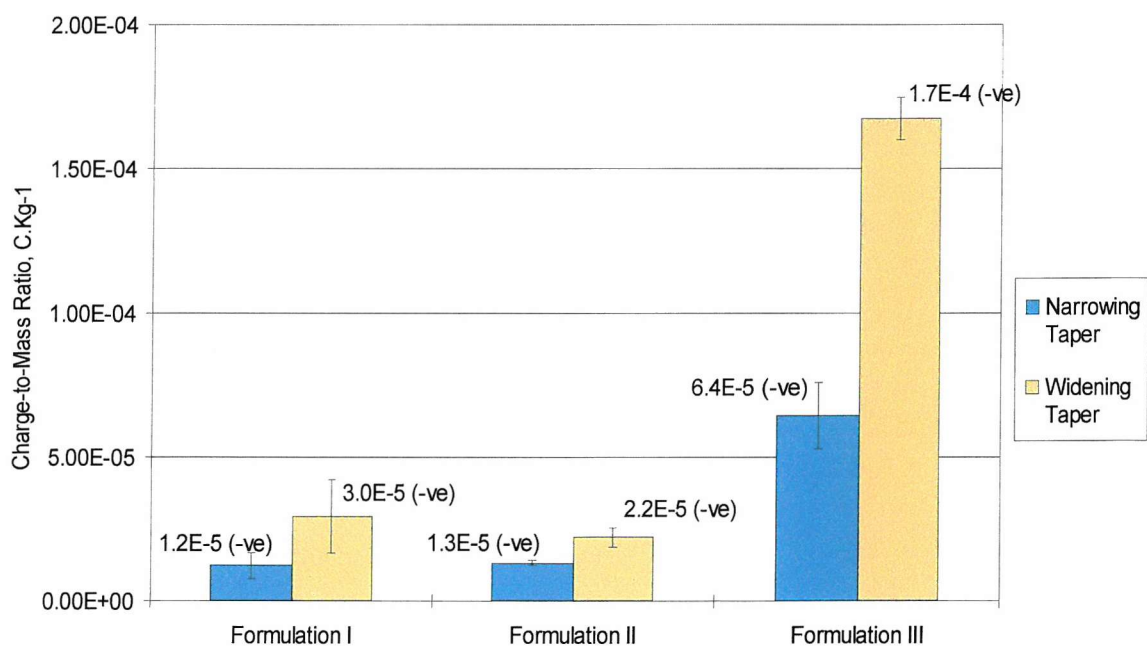


**Figure 2.15** Effect of actuator orifice taper direction on the charge-to-mass ratio of formulations I, II and III, showing standard error bars

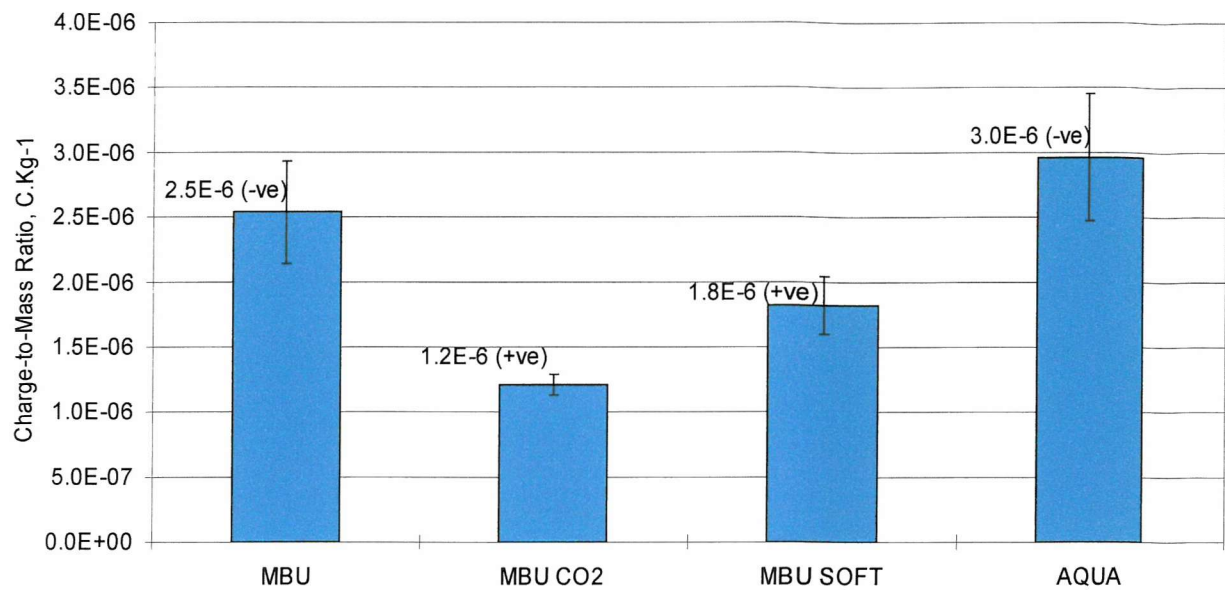


**Figure 2.16** Effect of actuator swirl chamber design on the charge-to-mass ratio of formulation I, showing standard error bars

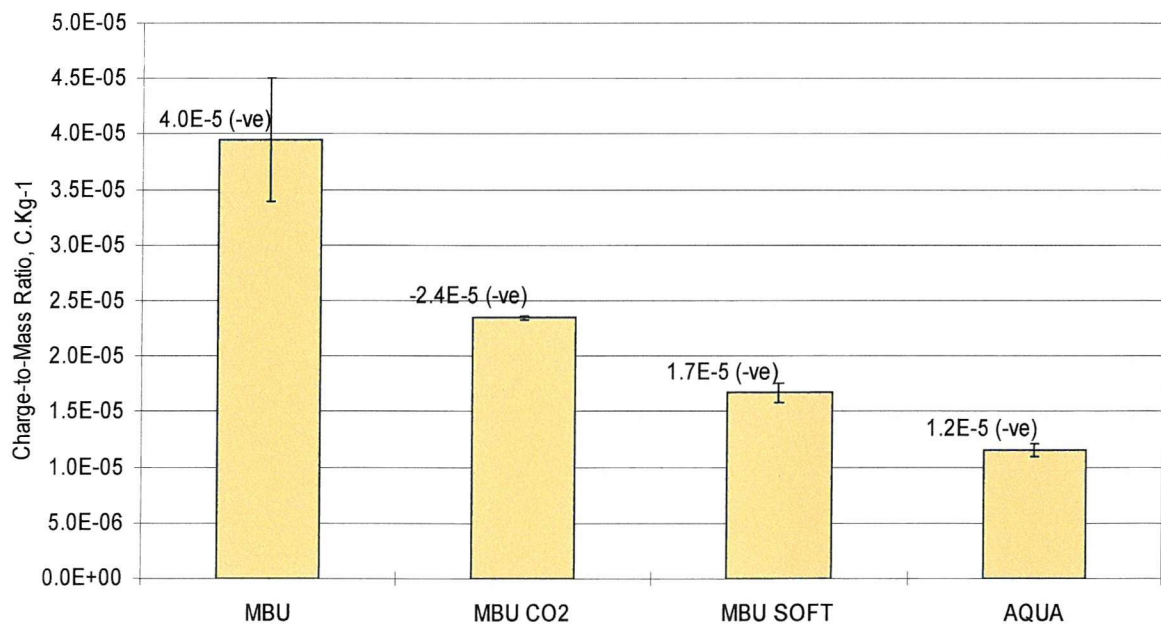


**Figure 2.17** Effect of actuator swirl chamber design on the charge-to-mass ratio of formulation II, showing standard error bars

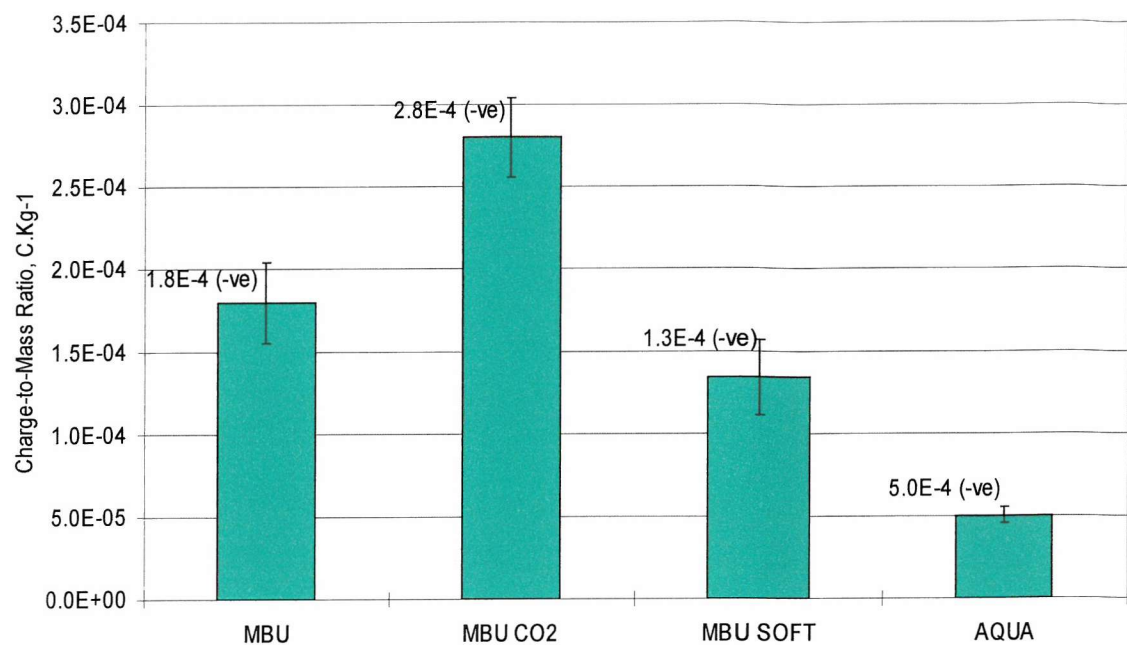


**Figure 2.18** Effect of actuator swirl chamber design on the charge-to-mass ratio of formulation III, showing standard error bars

## Summary of the Effect of Actuator Modifications on Charge-to-Mass Ratio

The effect of actuator orifice diameter and taper and the effect of various swirl chamber geometry designs on the charge-to-mass ratio of formulations I, II and III have been investigated. As with modifications to the valve components, the effect of a particular parameter was not always the same for all formulations. These effects are summarised in Table 2.7.

**Table 2.7** Summary of the effect of modifications to the actuator components of pressure-pack dispensers on the charge-to-mass ratio of formulations I, II and III

Component	Formulation I	Formulation II	Formulation III
Terminal orifice diameter	Smaller diameter orifice gave a higher q/m ( $p < 0.01$ )	Smaller diameter orifice gave a higher q/m ( $p < 0.01$ )	Smaller diameter orifice gave a lower q/m ( $p < 0.01$ )
Orifice taper direction	Trend for widening orifice to give a higher q/m Not statistically significant	Widening orifice gave a higher q/m ( $p < 0.05$ )	Widening orifice gave a higher q/m ( $p < 0.01$ )
Swirl chamber type	<i>MBU</i> and <i>Aqua</i> gave a higher q/m than <i>MBU CO<sub>2</sub></i> ( $p < 0.05$ )	<i>MBU</i> gave a higher q/m than <i>MBU CO<sub>2</sub></i> , <i>Aqua</i> gave the lowest q/m ( $p < 0.05$ )	<i>MBU CO<sub>2</sub></i> gave a higher q/m than <i>MBU Soft</i> , <i>Aqua</i> gave the lowest q/m ( $p < 0.05$ )

### 3.2.3 Effect of Combining Valve and Actuator Modifications on Charge-to-Mass Ratio

The aim of the work presented in this chapter was to enhance the naturally generated charge-to-mass ratio of the liquid aerosol sprayed from pressure-pack dispensers to a level in the region of  $10^4 \text{ C.kg}^{-1}$ . In order to do this successfully it was expected that a number of modifications would have to be made. Therefore, the next step in this work was to investigate whether combinations of valve and actuator modifications, which had significantly enhanced the q/m alone, could be used to enhance the q/m further.

Important factors to consider when attempting to identify dispenser modifications that enhance the q/m are the spray characteristics. These must be maintained within desirable boundaries in order for the spray to fulfil its function, as discussed in Chapter 1. One of the most important spray characteristics is the spray rate, which defines the quantity of formulation dispensed from the pressure-pack per unit length of time (Saunders, 1970). It is usually expressed in units of grams per second ( $\text{g.sec}^{-1}$ ). For this reason, the spray rates for combinations of valve and actuator modifications were measured, in addition to the q/m.

To investigate the effect of combining valve and actuator modifications, the parameters that significantly influenced the q/m formulation III were selected and combined. Only formulation III was used for this part of the investigation because it appeared to achieve the required level of charge more readily than formulations I and II. A spray rate of about  $2.0 \text{ g.sec}^{-1}$  is needed.

Modifications to the actuator orifice taper direction and the swirl chamber type of the actuator significantly affected the charge-to-mass ratio of formulation III. The valve parameters that significantly influenced the q/m were the diameter of the vapour phase tap and the area of the stem holes. Therefore, button-style actuators with an orifice of 0.46 mm diameter and either a  $5.5^\circ$  widening or narrowing orifice taper, and with either an *MBU CO<sub>2</sub>* or *Aqua* style swirl chamber were selected. These were used to actuate pressure-pack dispensers of formulation III with either 0.41 mm diameter or 0.76 mm diameter VPT and with stem holes of either  $3.800 \text{ mm}^2$  ( $3 \times 1.27 \text{ mm}$  diameter),  $0.584 \text{ mm}^2$  ( $2 \times 0.61 \text{ mm}$  diameter) or  $0.409 \text{ mm}^2$  ( $2 \times 0.51 \text{ mm}$  diameter) in area. Other components were as described in Table 2.5.

Figure 2.19 shows the mean  $q/m$ , with standard error bars, achieved when combining VPT and actuator taper modifications, and Figure 2.20 the corresponding spray rates. The  $q/m$  shows a small decrease with the 0.76 mm VPT compared to the 0.41 mm diameter VPT, and a small decrease with the narrowing actuator orifice compared to the widening one when the 0.76 mm diameter VPT was used. These data were analysed using two-way ANOVA, which suggested that in this combination VPT diameter has a highly statistically significant effect on  $q/m$  ( $p < 0.01$ ), taper direction had no significant effect and there was no interaction between these variables. The spray rate was lower with the wider 0.76 mm diameter VPT, and with the narrowing orifice taper. Statistical analysis (two way ANOVA) suggested that VPT diameter had a highly significant effect ( $p < 0.01$ ) and taper direction also a significant difference ( $p < 0.05$ ), but there was no interaction between these factors.

Figure 2.21 shows the mean  $q/m$ , with standard error bars, achieved when combining actuator orifice taper and stem hole modifications, and Figure 2.22 the corresponding spray rates. There was a trend for a narrowing orifice to give a smaller  $q/m$  than a widening orifice, while stem holes with a total area of  $0.580 \text{ mm}^2$  appeared to give a  $q/m$  higher than those with an area of  $0.409 \text{ mm}^2$  or  $3.800 \text{ mm}^2$ . Two-way ANOVA suggested that in this combination a widening orifice taper significantly increased  $q/m$  ( $p < 0.01$ ), stem hole area had no effect and there was no interaction between these variables. Spray rate was again slightly lower with the narrowing orifice taper than the widening taper. There was very little difference in flow with the  $0.409 \text{ mm}^2$  and  $0.580 \text{ mm}^2$  stem hole areas, but the largest  $3.800 \text{ mm}^2$  stem holes did tend to increase flow rate slightly. Statistical analysis (two way ANOVA) on the spray rate data suggested that both these factors have a highly significant effect ( $p < 0.01$ ), but there is no interaction.

The effect on  $q/m$  of swirl chamber type and VPT diameter are shown in 2.23, with standard error bars, and the corresponding flow rates in Figure 2.24. There is a distinct trend for the 0.76 mm diameter VPT to give a larger  $q/m$  than the 0.41 mm diameter VPT, but the effect of the swirl chamber type was different depending on the diameter of the VPT. With the wider diameter VPT, the *MBU CO<sub>2</sub>* swirl chamber gave a much higher  $q/m$  than the *Aqua* type, but with the smaller diameter VPT the *Aqua* type gave a slightly higher  $q/m$ . These data were statistically analysed (two-way ANOVA) showing that both swirl chamber type and VPT diameter significantly affected  $q/m$  ( $p < 0.01$ ), and that there was a significant interaction between them. As previously observed, the wider 0.76mm diameter

VPT gave a reduced flow rate compared to the smaller 0.41 mm, and there was also a slight increase in flow when using the *Aqua* type swirl chamber. Both these factors had a highly significant effect on flow rate ( $p < 0.01$ ), but there was no interaction shown by statistical analysis (two way ANOVA).

The mean q/m (based on 5 replicates) generated using the two swirl chamber types in combination with the three stem hole area variants is shown in Figure 2.25, with standard error bars, and the corresponding flow rates in Figure 2.26. The *Aqua* type swirl chamber gave a lower q/m than the *MBU CO<sub>2</sub>* type, but there was no clear trend for the influence of stem hole area. Two-way ANOVA suggested that in this combination, swirl chamber type significantly affected the q/m ( $p < 0.01$ ), but stem hole area did not, and there was no interaction between the variables. As previously observed there was a trend for larger total stem hole areas to increase flow rate, and for the *Aqua* type swirl chamber to demonstrate a greater flow than the *MBU CO<sub>2</sub>* type swirl chamber. These trends were statistically significant ( $p < 0.01$ ), but there was no interaction between swirl chamber design and stem hole area.

The aim of this work was to generate an aerosol with a q/m greater than  $1 \times 10^{-4}$  C.kg<sup>-1</sup> and a spray rate of about 2.0 g.sec<sup>-1</sup>. The q/m achieved by combining the *MBU CO<sub>2</sub>* swirl chamber design and any stem hole configuration was above  $1 \times 10^{-4}$  C.kg<sup>-1</sup>, but the spray rate was only between 0.5 and 0.6 g.sec<sup>-1</sup>.

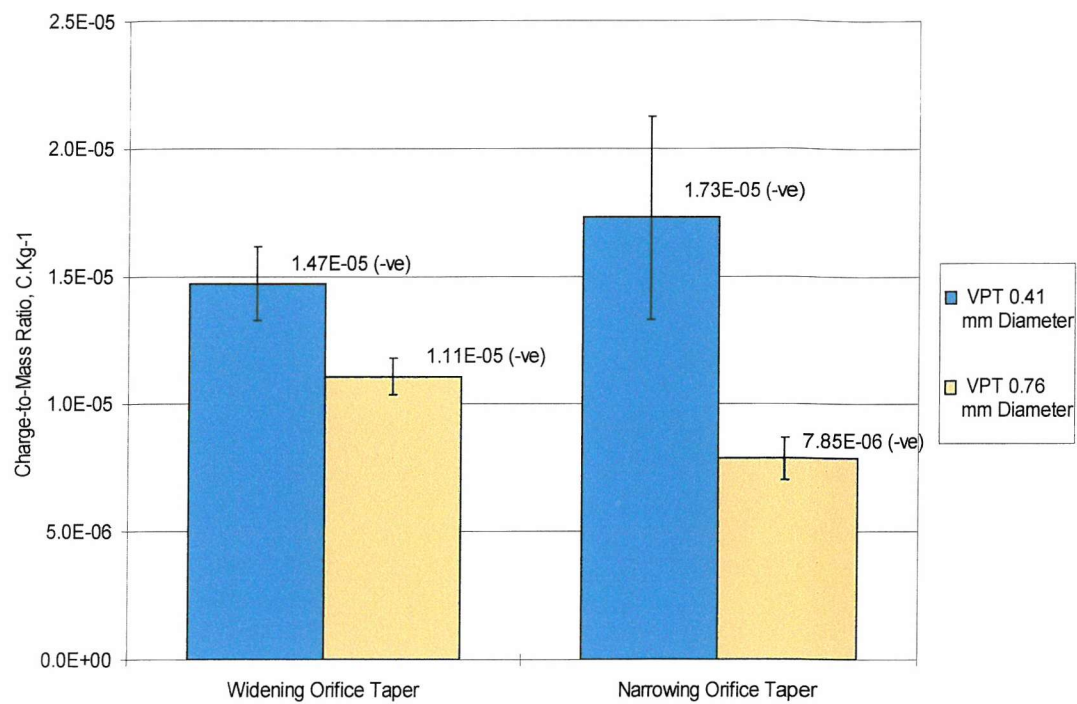


**Figure 2.19** Effect of actuator orifice taper direction and valve vapour phase tap diameter on the charge-to-mass ratio of Formulation III, showing standard error bars

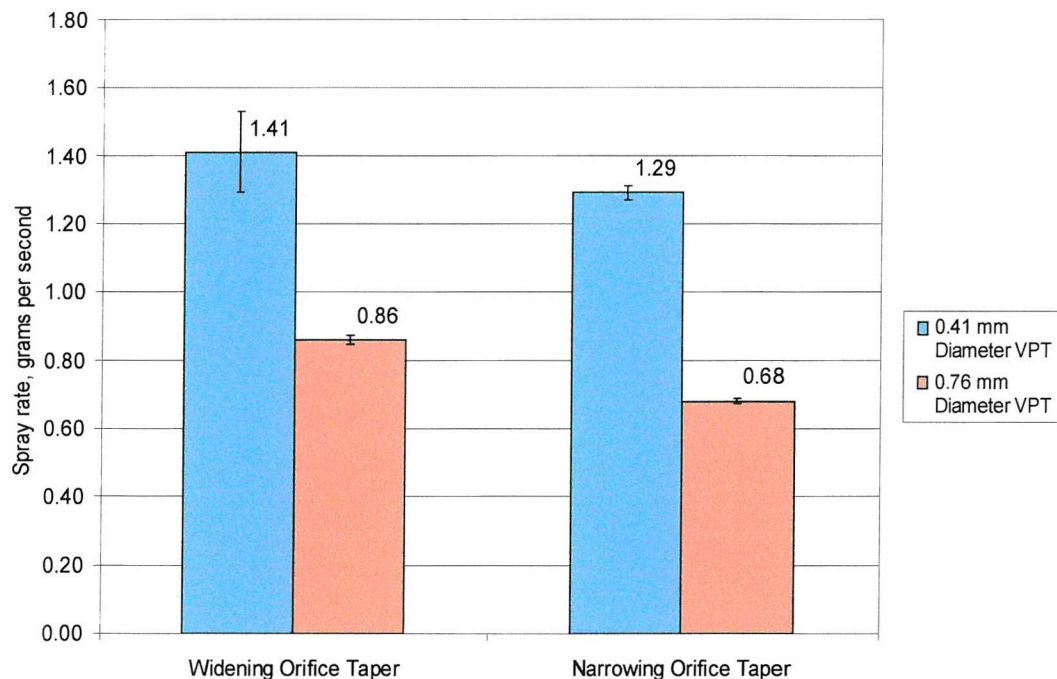


**Figure 2.20** Spray rates of formulation III when combining actuator orifice taper direction and valve vapour phase tap diameter modifications, showing standard error bars

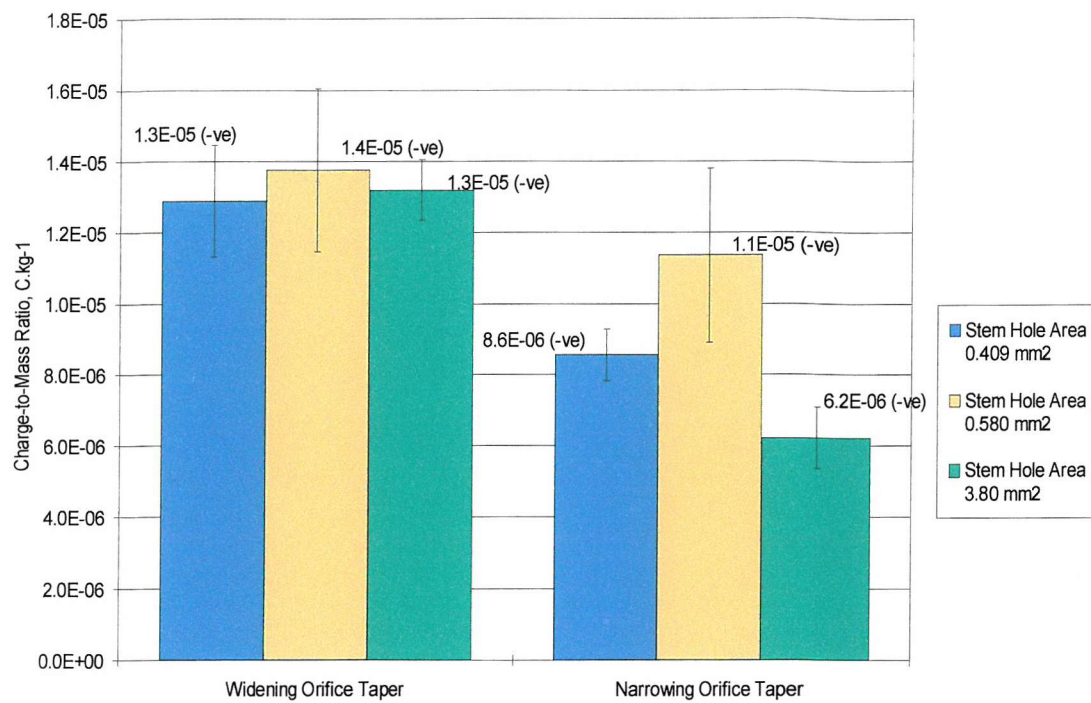


**Figure 2.21** Effect of actuator orifice taper direction and stem hole area on the charge-to-mass ratio of Formulation III, showing standard error bars

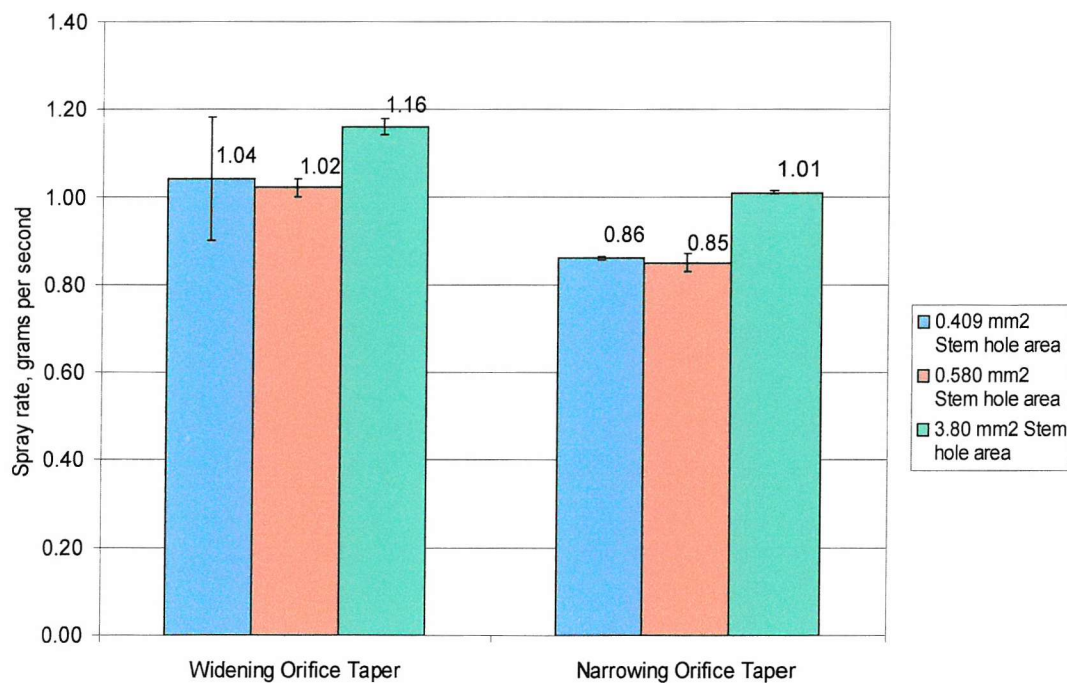


**Figure 2.22** Spray rates of formulation III when combining actuator orifice taper direction and valve stem hole area modifications, showing standard error bars

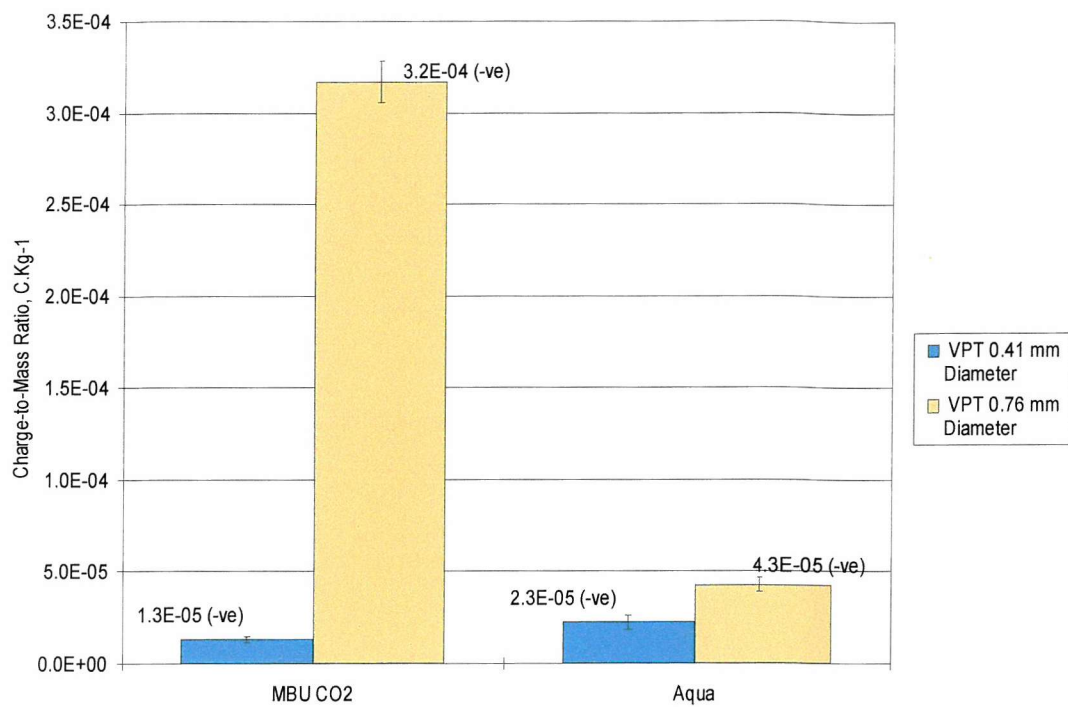


**Figure 2.23** Effect of actuator swirl chamber design and valve vapour phase tap diameter on the charge-to-mass ratio of Formulation III, showing standard error bars

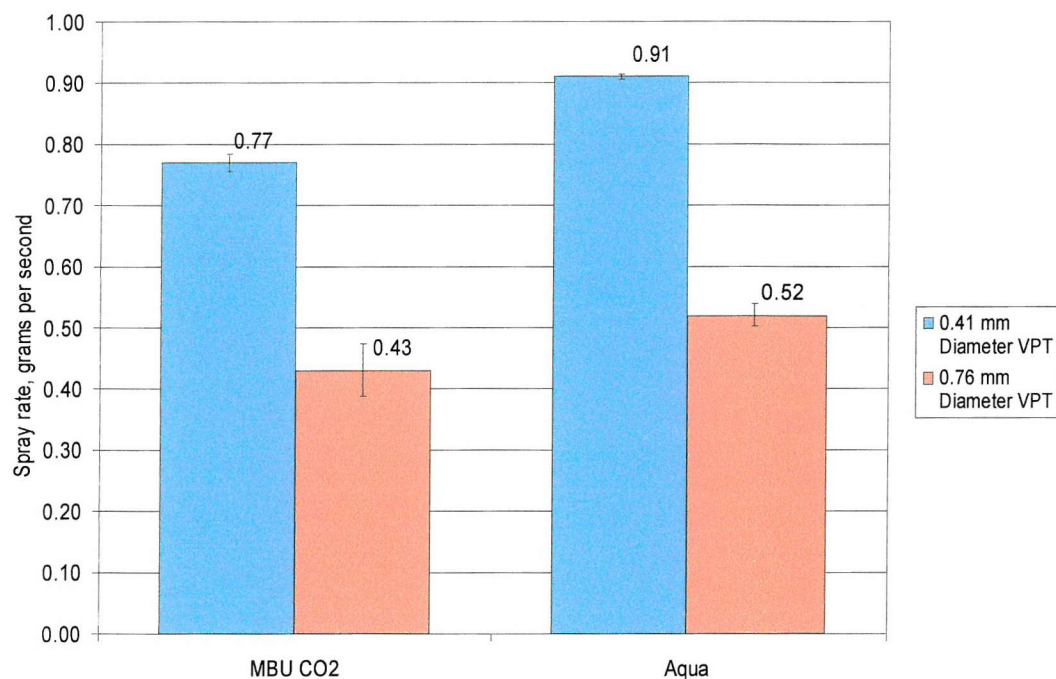


**Figure 2.24** Spray rates of formulation III when combining actuator swirl chamber design and valve vapour phase tap diameter modifications, showing standard error bars

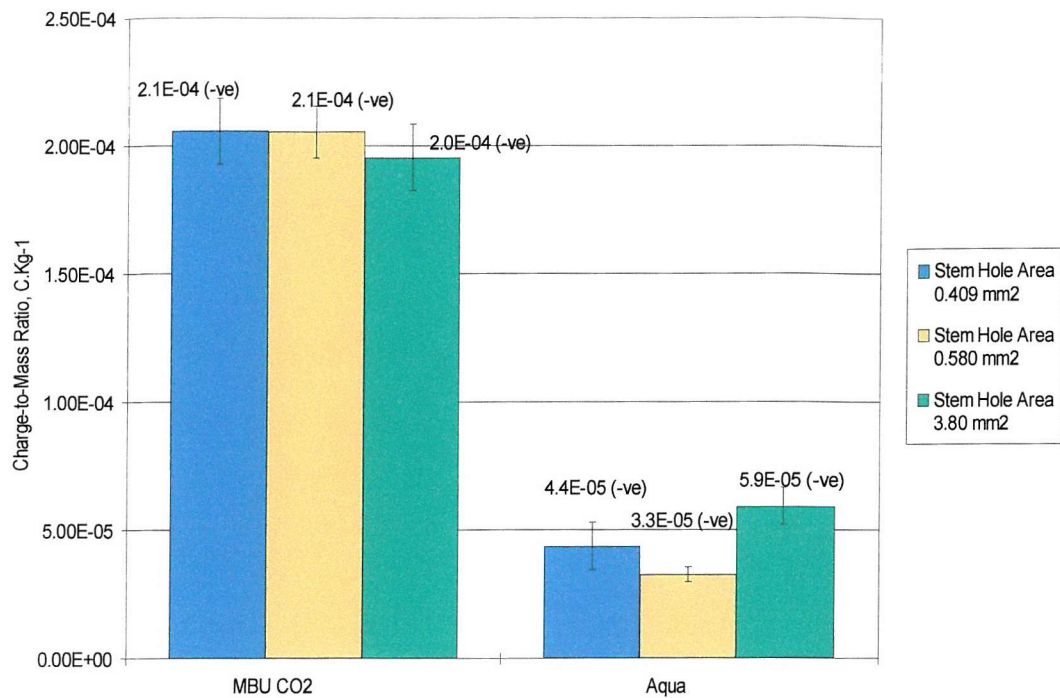


**Figure 2.25** Effect of actuator swirl chamber design and valve stem hole area on the charge-to-mass ratio of Formulation III, showing standard error bars

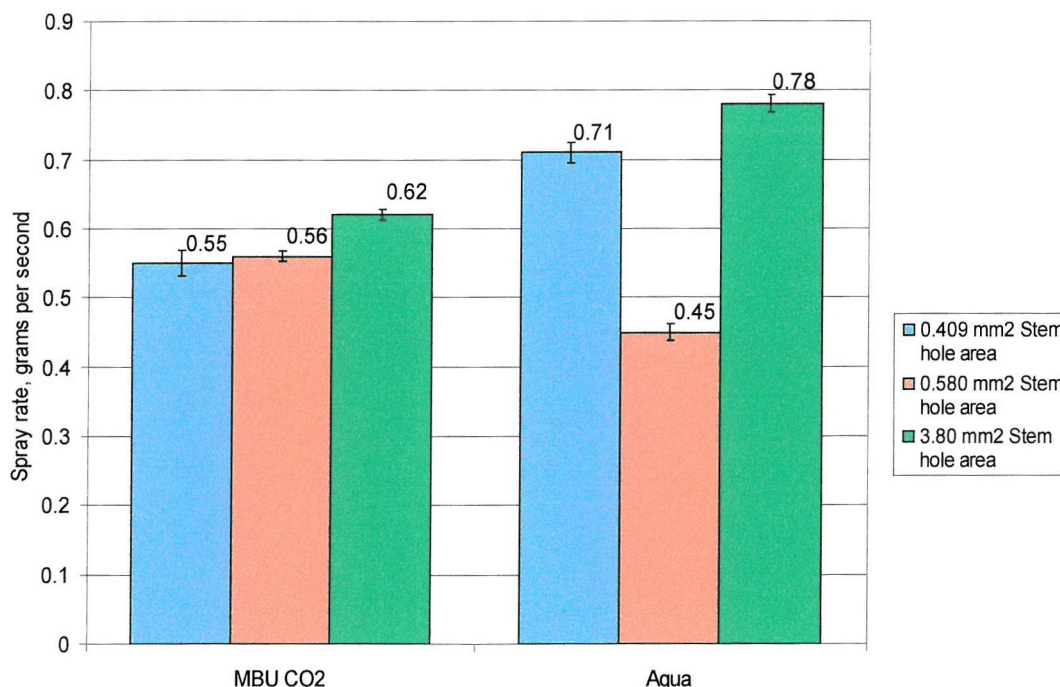


**Figure 2.26** Spray rates of formulation III when combining with actuator swirl chamber design and valve stem hole area modifications, showing standard error bars

#### 2.3.4 Effect of Novel Actuator Orifice Designs on Charge-to-Mass Ratio

Charge-to-mass ratios in excess of  $10^{-4}$  C.kg<sup>-1</sup> were achieved using standard industry components with formulation III, but the spray rate with these modifications was invariably far below the desired level of about 2.0 grams per second, required for domestic applications. Smaller diameter actuator orifices had achieved higher values for q/m (Section 2.3.2). It was hypothesised that this resulted from the large surface area of contact available at the point of atomisation, with respect to the volume of liquid passing through the orifice. Hence it was postulated that alternative orifice shapes could be designed which would allow a high degree of contact between the surface of the orifice and the liquid flowing through. A number of such designs were proposed to test this theory, and were manufactured into standard actuator inserts. This was achieved using laser machining technology, and performed by 'Exitech Limited' Oxford, UK. The inserts into which the novel orifice designs were machined utilised the *Aqua* type swirl chamber, because only this provided space between the feed channels to accommodate the novel orifice shapes (see Fig. 2.4). The inserts were used in button style actuator bodies (Fig.2.3).

The q/m and spray rate of formulation III was measured using 12 novel actuator orifice designs described in Figure 2.5 and a circular orifice of 0.85 mm diameter manufactured using the same technique. The mean q/m based on 5 measurements, using each design is shown in Figure 2.27, with standard error bars. The mean flow rates are shown in Table 2.8. The product moment correlation coefficient (Appendix A) was calculated to identify whether increasing the circumference to area ratio of the orifice designs increased the q/m of formulation III. The correlation coefficient calculated was 0.649, which exceeds the tabulated value for 13 samples of 0.514 ( $p=0.05$ ), so it is suggested that there is a modest correlation between circumference to area ratio and q/m.

**Table 2.8** Flow Rate of Formulation III with the Novel Insert Orifice Designs

Design Label (Fig. 2.5)	Circumference to Area Ratio	Mean Charge-to-Mass Ratio, C.kg <sup>-1</sup>	Mean Spray Rate, grams per second (standard error)
<b>A</b>	4.706	$-1.69 \times 10^{-5}$	1.83 (0.031)
<b>B</b>	12.064	$-1.06 \times 10^{-4}$	1.93 (0.020)
<b>C</b>	5.317	$-1.79 \times 10^{-5}$	1.86 (0.044)
<b>D</b>	5.908	$-2.77 \times 10^{-5}$	1.82 (0.072)
<b>E</b>	7.335	$-3.31 \times 10^{-5}$	1.65 (0.048)
<b>F</b>	6.929	$-4.78 \times 10^{-5}$	1.82 (0.057)
<b>G</b>	7.245	$-2.26 \times 10^{-5}$	1.88 (0.038)
<b>H</b>	10.385	$-1.26 \times 10^{-5}$	1.64 (0.058)
<b>I</b>	5.292	$-3.22 \times 10^{-5}$	1.75 (0.053)
<b>J</b>	5.470	$-4.39 \times 10^{-5}$	1.73 (0.030)
<b>K</b>	7.568	$-5.03 \times 10^{-5}$	1.75 (0.036)
<b>L</b>	6.842	$-2.36 \times 10^{-5}$	1.87 (0.048)
<b>M</b>	6.329	$-2.82 \times 10^{-5}$	1.65 (0.024)

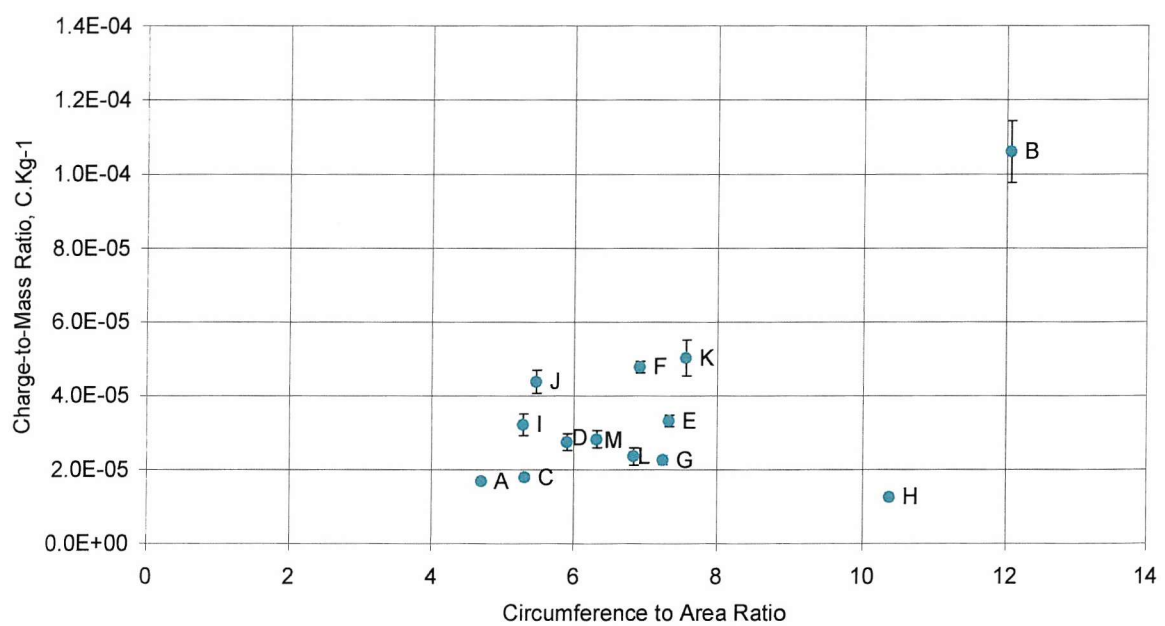


**Figure 2.27** Effect of mean charge-to-mass ratio of formulation III of the circumference to area ratio of the novel actuator orifice shapes, showing standard error bars. Labels correspond to those of Fig 2.5

## 2.4 Discussion

The trends observed resulting from modifications to pressure-pack dispenser parameters were mostly consistent with the theory that charge is generated primarily through shearing of electrical double layers. This is suggested because charge separation appears to be sensitive to factors such as the pipe radius (degree of contact between the liquid and the internal surfaces of the dispenser), flow turbulence, and by the nature of the liquid, as has been observed for double layer shearing in flow electrification (Klinkenberg and van der Minne, 1958; Koszman and Gavis, 1962a and b). Charge separation on the aerosol droplets due to other processes, such as the presence of a strong electric field or statistical charging can be eliminated as possible mechanisms, as will be discussed shortly. Although considerable effort has been devoted by researchers to explain charge separation in liquids flowing in pipes and tubes, invoking double layer shearing as the mechanism, these mainly concern simple, well defined systems. The system under consideration here is complex, involving liquids under pressure flowing in polymer pipes and mechanical atomisation. However, comparisons will be drawn between the observed data and published work.

Shearing of electrical double layers formed at liquid-solid interfaces is postulated to be the most probable mechanism of charge separation in this system. Of the 4 mechanisms by which charged droplets could be produced, described in Section 2.1.4, only shearing of electrical double layers could explain the significant net electrical charges measured on the aerosols produced by pressure-pack dispensers. Induction charging as a result of electric field (mechanism 3), can be discounted, as no external sources of charge existed during spraying. No significant electric field was present to cause separation of charges within the bulk of the liquid. Mechanism 4 describes random distribution of ions in the liquid, but this would not account for the level of net charge consistently measured, although it could explain some variability in the data.

If a mechanism similar to spray electrification (as described by Lenard for waterfalls) was responsible for the charge measured on the aerosol droplets, then droplets of both polarities would exist, and little or no net electrical charge would be exhibited. Under these circumstances, one would not expect to measure a net charge on the pressure-pack dispenser. However, the generation of a largely uni-polar aerosol, with equal and

opposite charge residing on the pressure-pack dispenser formed the basis of the measurement technique employed. It was not determined whether the aerosol was unipolar, so it could have consisted of droplets of both polarities. However, significant levels of net charge were measured on the pressure-pack dispensers, which suggests shearing of the double layer at the solid-liquid interface to be the predominant, if not the sole mechanism.

For many parameters, the effect on charge-to-mass ratio was the same for the three formulations investigated, but in some instances different trends were observed. A source of error in the following comparisons arises as a consequence of the pressure-pack dispensers being formulated and assembled by hand, rather than on a production line. The proportion of ingredients in the formulated liquid, the volume of liquid measured into the containers and the level of pressurisation achieved during filling would consequently be more variable. These factors could significantly influence charge separation, but were not controllable. The trends observed will now be discussed.

#### 2.4.1 Modifications to Components of the Valve Assembly of Pressure-Pack Sprays

All components of the valve assembly affected the charge-to-mass ratio of aerosol droplets generated by pressure-pack dispensers, with the exception of the tailpiece orifice diameter. Formulations II and III were always observed to give rise to droplets negative in polarity, while formulation I sometimes generated negative and sometimes positive droplets. This observation will be discussed in Section 2.4.6.

The trends for modifications in dip tube parameters were for 1.27 mm polypropylene dip tubes to generate a higher  $q/m$  than 3.00 mm polyethylene tubes. Dip tubes of twice the normal length gave a higher  $q/m$  than conventional tubes. The former trend could be attributed to the effects of increased velocity, and narrower tubes allowing a higher proportion of the liquid volume to contact a surface where double layers form. Velocity dependence is considered a characteristic of the flow electrification phenomenon. It has been observed experimentally by a number of investigators (Klinkenberg and van der Minne, 1958; Koszman and Gavis, 1962a) and modelled theoretically (Koszman and Gavis, 1962b; Touchard *et al.*, 1996). However, because the 3.00 and 1.27 mm dip tubes also differed in material, such conclusions cannot be made. Although tubes of Pyrex glass, gold,

silver and stainless steel have experimentally yielded similar flow electrification tendencies to each other (Koszman and Gavis, 1962a), dielectric materials may give different results, and surface roughness can be influential (Touchard *et al.*, 1989). The observation that longer dip tubes increase charge separation was also consistent with double layer shearing models. It is postulated that continued shearing of the electrical double layer along the length of the tube occurs, until an equilibrium condition is reached (Touchard and Romat, 1981). The effect of coiling the long dip tube inside the dispenser would also be to cause different rates of flow at the inner and outer edges of the bends. Faster flow at the inner edge would increase charge separation, but this could be balanced by the reduction in charge separation at the outer edge, due to slower flow.

Tailpiece orifice diameter did not appear to significantly influence  $q/m$ . The effect of other components could have masked the influence this orifice had on the  $q/m$ , or relaxation of charge later in the system could have negated any effect. Charge relaxation during flow of dielectric liquids through complex circulating systems has been experimentally observed (Cross *et al.*, 1977).

The area provided by the stem holes for liquid to flow into the actuator did influence  $q/m$ . For all three formulations the trend was for a smaller area to increase the level of charge generated, although the magnitude of the effect differed between formulations. There are two factors to be considered here: the effect of the number and of the diameter of these orifices. The effect of smaller orifices could have been to increase the velocity and hence the turbulence of flow. Both of these factors are considered instrumental in the flow electrification phenomenon. As discussed in Section 2.1.3, the effects of velocity and turbulence are interrelated, in that increases in velocity increase turbulence, which increases electrification (Klinkenberg and van der Minne, 1958). The effect of increasingly turbulent flow is not only to remove a greater depth of the diffuse part of the double layer, but also to bring more liquid closer to the surfaces and involved in formation of the double layer. Smaller orifices also increase the area of contact for the formation of double layers (Taylor and Secker, 1994). The number of stem hole orifices could also influence  $q/m$  by creating turbulence through the tangential arrangement of the converging liquid streams. However, because it was not possible to compare the effects of hole diameter and number separately, it is difficult to attribute the effects observed to either of these factors.

The effect of the presence of a vapour phase tap was very important in relation to a high  $q/m$  with all three formulations. The effect of gaseous propellant entering through the VPT, mixing with the liquid formulation as it flows through the valve and actuator assembly would be expected to increase turbulence. Klinkenberg and van der Minne (1958) observed increased charge separation when gas was injected into dielectric liquids flowing in pipes. They attributed this to the influence of turbulence rather than electrokinetic effects between the liquid and gas phases, because the charge levels increased almost immediately as gas injection commenced, and fell again when it was stopped.

It is possible that the double layers formed at the gas-liquid interfaces (as described in Loeb, 1958) may play a part in the enhanced electrification. The surface area of the interfaces formed in this way would be substantial. However, as this double layer is wholly contained within the liquid phase, it is difficult to envisage shearing of these layers to produce droplets with a net electrical charge.

For most comparisons, the valve and actuator parameters were standardised for the three formulations, with only one component undergoing modification at a time. However, the effect of the component under investigation could be masked or influenced by other components in the assembly. For example, the presence of a VPT could influence the outcome of changes to the stem holes. It should also be considered that use of different actuator types could result in different trends being observed. Actuator components have an important role to play in the separation of charge, as discussed in the next section.

#### 2.4.2 Modifications to Actuator Components of Pressure-Pack Sprays

The actuator components investigated for their effects on charge-to-mass ratio all had significant effects on the  $q/m$  of the three formulations.

For all formulations, a smaller actuator orifice tended to generate a higher  $q/m$  on the aerosol than larger orifices. A smaller orifice has a higher flow velocity, and a larger area of contact, which are both expected to increase electrification (Touchard and Romat, 1981). In addition, charge developed during flow through the actuator has little time to relax, as it does in the valve and dip tube.

Taper direction also had a significant effect on the separation of charge in formulations II and III, the widening taper giving a higher  $q/m$  than the narrowing. If

atomisation begun at the narrowest point of the orifice, this would allow an opportunity for further contact and charge separation between the newly formed droplets and the surface of the widening orifice. Double layer formation and separation could occur at the instant of contact with the surface, resulting in charge exchange, as described in Section 2.1.1. However, the precise mechanism of droplet formation in these actuator orifices is not documented.

The final component studied was swirl chamber design, the function of which is to break-up the liquid stream mechanically, by imparting a swirling motion to the liquid as it leaves the orifice. The flow of liquid would become highly turbulent through the action of the swirl chambers. In addition, the feed channels allow a large proportion of the liquid to contact solid surfaces and become involved in double layer formation. Both of these factors are known to enhance electrification. The difference between swirl chambers can be attributed to the different arrangement and dimensions of the feeder channels. With Formulations II and III the *MBU* and *MBU CO<sub>2</sub>* style swirl chambers achieved the highest charge-to-mass ratios, and this may have been due to the narrowness of the channels (shown in Fig. 2.4) increasing the surface area for contact with the liquid.

#### 2.4.3 Differences Between Formulations

It is apparent from the results that modifications to parameters such as actuator orifice diameter or vapour phase tap diameter did not lead to the same level of electrification for all formulations. Generally, the aerosol of formulation I was generated with a lower charge-to-mass ratio than formulation II, which had a lower q/m than formulation III. Conductivity of the formulations could greatly affect the charge generated, through its influence on the thickness of the double layer (Koszman and Gavis, 1962b). However, it was not possible as part of this study to measure conductivity of the formulations, due to the integral part in the formulation played by the propellant, maintained in a liquefied state only by high pressure within the dispenser. Charge separation could also have been influenced by the type of liquid being sprayed. Formulation I was a single phase liquid consisting mostly of water and alcohol, and probably highly conducting. Thus, the comparatively low q/m of this aerosol could have been due to a relatively thin double layer available for shearing, and rapid relaxation of

charge. Formulations II and III were both emulsions, which have been observed to generate higher charges than single-phase liquids (Klinkenberg and van der Minne, 1958; Krämer, 1981). However, formulation III tended to generate a higher  $q/m$  than formulation II, and this could be associated with the nature of the external phase of the emulsion. The conductivity of the continuous phase is believed to be of primary importance in influencing charging (Krämer, 1981). The continuous phase of formulation II was water and for formulation III; oil. Therefore, the conductivity of the continuous phase of formulation III may have been closer to the optimum observed by others (Klinkenberg and van der Minne, 1958; Koszman and Gavis, 1962a).

#### 2.4.4 Combinations of Modifications to the Valve and Actuator Parameters of Pressure-Pack Dispensers

The valve parameters investigated were VPT diameter and stem hole area, and these were combined with actuator swirl chamber designs (*MBU CO<sub>2</sub>* or *Aqua*) and terminal orifice taper direction variants (widening or narrowing). Although some of the trends observed in Sections 2.4.1 and 2.4.2 were reiterated in combination, it was also noted that the influence of components could be different when other components were varied. For example, the effect of taper direction on  $q/m$  differed for a 0.76 mm diameter VPT and a 0.41 mm diameter VPT. The consequence of this is that the trends recorded when investigated in isolation should only be interpreted with respect to the set of components used. Thus, these recorded trends would be useful in proposing component parameters that could aid the production of highly charged liquid aerosols, but the optimum configuration must still be identified empirically.

The effect of total stem hole area on  $q/m$  when studied in isolation was not seen in combination. This suggests that the effect of one component can mask or negate the influence that another has on charging. For example, Figure 2.21 shows almost no difference in  $q/m$  between the three stem hole variants in combination with a widening orifice. With the narrowing orifice the  $q/m$  is generally lower however, and the trend for larger stem hole areas to reduce  $q/m$  is seen. However, no significant interaction between these factors was found. It is possible for charge to relax at certain points in the dispenser system, such as in the valve. Charge separation occurring in the actuator has less

opportunity to relax, however, so can be more influential in determining the  $q/m$ . Relaxation of charge has been recorded in other examples of flowing liquid systems (Cross *et al.*, 1977). In addition, the charge separation that occurs within the actuator could be more significant, and exceed any occurring previously during flow.

There was a significant interaction recorded when different VPT diameters and swirl chamber designs were combined (Figure 2.23). The VPT diameter determined the proportion of gaseous propellant mixing with the liquid formulation (Saunders, 1970), which would affect the turbulence arising in the feed channels of the swirl chamber, and thus interact to determine the charge level achieved. In addition, a greater proportion of air in the liquid flow will reduce the volume of liquid (Sanders, 1970), thus increasing the proportion of the liquid volume contacting the surfaces of the insert for double layer formation.

However, when VPT diameter variants were combined with actuator orifice taper direction variants, different trends were observed. Previously with formulation III, a larger diameter VPT had recorded higher charges than a smaller VPT, but here the opposite was observed. This is probably another example of the interaction between VPT and swirl chamber, as the widening and narrowing actuators did not have swirl chambers. For the charge-to-mass ratio to be increased by the inclusion of a VPT, it appears to be necessary for a swirl chamber to be used, in which turbulence is increased.

Trends in the effect of these modifications on the flow rate were more consistent than for  $q/m$ . Statistical analysis suggested these effects to always be significant, and for there to be no interactions between the components. Thus, the effect of a component on flow rate can be predicted. Larger diameter VPTs always reduced flow rates, due to the gaseous propellant reducing the proportion of liquid passing through the valve (Saunders, 1970). Flow rate was always higher with larger stem hole areas, as these determine the volume of formulation that can flow from the valve. Narrowing terminal orifices always gave lower flow rates than widening orifices, and the *Aqua* type of swirl chamber (Figure 2.4) allowed greater flow, probably due to wider channels.

The spray rates suggested that valve and actuator combinations which achieved a  $q/m$  in excess of  $1 \times 10^{-4} \text{ C}.\text{kg}^{-1}$  did not deliver suitable rates of liquid flow (in the region of 2.0 g/s). Therefore, the design of the actuator orifice was selected for special consideration in achieving these objectives, as discussed in the following section.

#### 2.4.5 Novel Actuator Orifice Designs

The effect of circumference length to cross-sectional area ratio (C:a) of the actuator orifice on the charge-to-mass ratio is shown in Figure 2.27. There is a trend for an elevated C:a ratio to generate a slightly higher  $q/m$ , and most novel orifices generated a  $q/m$  a little higher than the equivalent circular orifice (*A*). The orifice labelled *H* gave a  $q/m$  lower than *A*, despite the ratio C:a being much greater. The orifice labelled *B* gave a  $q/m$  much higher than the others, and exceeded  $1 \times 10^{-4} \text{ C.kg}^{-1}$ . The product moment correlation coefficient suggested a statistically significant correlation. It was expected that increasing C:a could increase the  $q/m$ , due to a contact effect with the surface where the electrical double layer forms. It is interesting to note that orifice shape *B* gave a much higher  $q/m$  than the other shapes, out of proportion with its C:a ratio. This could have been because most other shapes had a central core for liquid flow. Shape *B*, however, was segmented into five channels that allowed electrical double layers to extend a greater proportion across the width of these channels than the other shapes. However, orifice *H* was also segmented into five channels, although of different shapes, yet gave a  $q/m$  much less than expected according to the C:a ratio. Therefore, other mechanisms must also be involved, which could account for this. Possibly, flow through the rectangular sections of *B* is more turbulent than through the circular sections of *H*.

Spray rates were approximately the same for the 12 novel orifice designs, suggesting that there is little impedance to flow due to the increased contact.

#### 2.4.6 Other Observations

On occasions, changes in polarity were observed with formulation I. This is believed to occur due to the sensitivity of the double layer charging process on the properties of the solid surfaces and the liquid (Cross *et al.*, 1977). Additives have been found to influence the polarity (Goodfellow and Graydon, 1968) and magnitude of charge (Gibson and Lloyd, 1970; Cross *et al.*, 1977) during flow electrification. Thus, impurities or poor mixing of the formulation could account for some variation in charge. It is also possible for the polarity of charge in the bulk of the liquid to reverse as it undergoes double

layer formation and separation (Cross *et al.*, 1977). Actuators were interchanged between formulations, providing opportunity for adsorption of impurities onto the surfaces. This could have been avoided. It is interesting to note that the other formulations were not subject to polarity reversal, although apparently subject to similar levels of impurities and variation. These formulations could have been less sensitive due to a better developed electrification process, suggested by the higher charge-to-mass ratios achieved.

Mixing of the emulsion by shaking the dispenser prior to spraying is another source of variation, which could cause some differences in the composition of liquids sprayed. A standard method of shaking was adopted throughout the work in an attempt to overcome this. The composition of the liquid also changes slightly over the lifetime of a pressure-pack dispenser, because the concentration of liquid propellant is reduced as more is converted to the gas phase to maintain pressure following use.

#### 2.4.6 Areas for Further Investigation

All tubing and most small components used in the pressure-pack dispensers were made from dielectric materials. The effect of components being made from conducting materials was not investigated, although metal pipes can generate higher charge levels than insulating materials such as glass, rubber and plastic (Cross, 1987; Gavis and Koszman, 1961). Identification of zones in which charge separation primarily occurs would provide a better understanding of the processes involved in the generation of charged aerosols from pressure-pack dispensers. Investigation into whether the aerosol is unipolar or bipolar, and whether charge is evenly distributed across the droplet size ranges, could help confirm double layer separation as the primary mechanism. If the aerosol had a considerable bipolar component or carried the charge on a certain size fraction of the aerosol, other mechanisms such as statistical charging or disruption of the double layer at the liquid-gas interface could also be invoked. This depth of understanding of the charge separation mechanisms occurring in pressure-pack dispensers could considerably aid further enhancement of the process.

## Chapter 3

---

### Precipitation of Airborne Particles by Electrically Charged Aerosols Generated by Pressure-pack Dispensers

#### 3.1 Introduction

Indoor air quality is an important issue, as exposure to indoor allergens has been associated with recent increases in the prevalence of allergic disease (Gergen and Weiss, 1992; Blumenthal *et al.*, 1993). In a recent survey of allergic patients in Quebec, Canada, the majority of allergic individuals were sensitised to indoor allergens (92.7%). 21.1% of allergic individuals were sensitised exclusively to indoor allergens and only 5.8 % exclusively to outdoor allergens (Boulet *et al.*, 1997). This study stresses the role of indoor allergens in the development of asthma, and thus the importance of preventative measures for these allergens. A number of portable air cleaning devices are available for home use which claim to reduce airborne particle concentrations (Nelson *et al.*, 1988; Fox, 1994). Clinical studies, however, have failed to substantiate a significant impact on asthma patients' symptoms (Fox, 1994). As soft furnishings, carpets and bedding provide a large reservoir for domestic allergens, air cleaning alone would not be expected to reduce concentrations sufficiently to ameliorate atopic symptoms (Nelson *et al.*, 1988). If liquid

aerosols generated by domestic pressure-pack dispensers can deplete airborne particles conveniently, indoor air quality would be improved on a local scale by this inexpensive means. This would provide a method by which aeroallergens can be reduced following dust disturbances, such as vacuuming or cleaning. This chapter describes investigations into this concept, and the importance of an electrostatic charge on the droplets in achieving airborne particle depletion.

### 3.1.1 Composition and Origin of Domestic Airborne Particles

Airborne particles found in domestic environments can originate indoors, or enter from outdoors through building openings. These particles can be plant or animal bioaerosols, combustion or mineral aerosols or be generated by home/personal care products (Owen *et al.*, 1992). The size ranges of a variety of indoor particles are summarised in Figure 3.1.

Mineral aerosols make up the bulk of house dust, and are largely produced outdoors through natural (e.g. weathering) or artificial (e.g. grinding) processes. They can vary greatly in shape and size, and may be carcinogenic or mutagenic (Owen *et al.*, 1992). Bioaerosols, which include pollen, spores, animal dander, bacteria and insect parts, also vary in size and shape. Cat allergen (Fel dI) is predominantly carried on particles of less than 2  $\mu\text{m}$  and remains airborne with little reduction for hours (Luczunskia *et al.* 1990). Alternatively, house dust mite allergen (Der pI) occurs mostly on particles of 10  $\mu\text{m}$  in diameter and larger, and settles out of still air in 15 to 35 minutes (Platts-Mills *et al.*, 1986).

The main sources of combustion aerosols in the domestic environment are tobacco products, cooking units and heating appliances. Most of the particles thus produced are sufficiently small to remain airborne and be inhaled into the lungs (Owen *et al.*, 1992). In households containing one or more smokers, tobacco smoke can be the main source of suspended particulate matter (Boleij and Brunekreef, 1982). Domestic spray devices and humidifiers are the main sources of home and personal care aerosols, and although these contribute only a relatively small mass to the air, their size and local concentration make them highly respirable (Owen *et al.*, 1992).

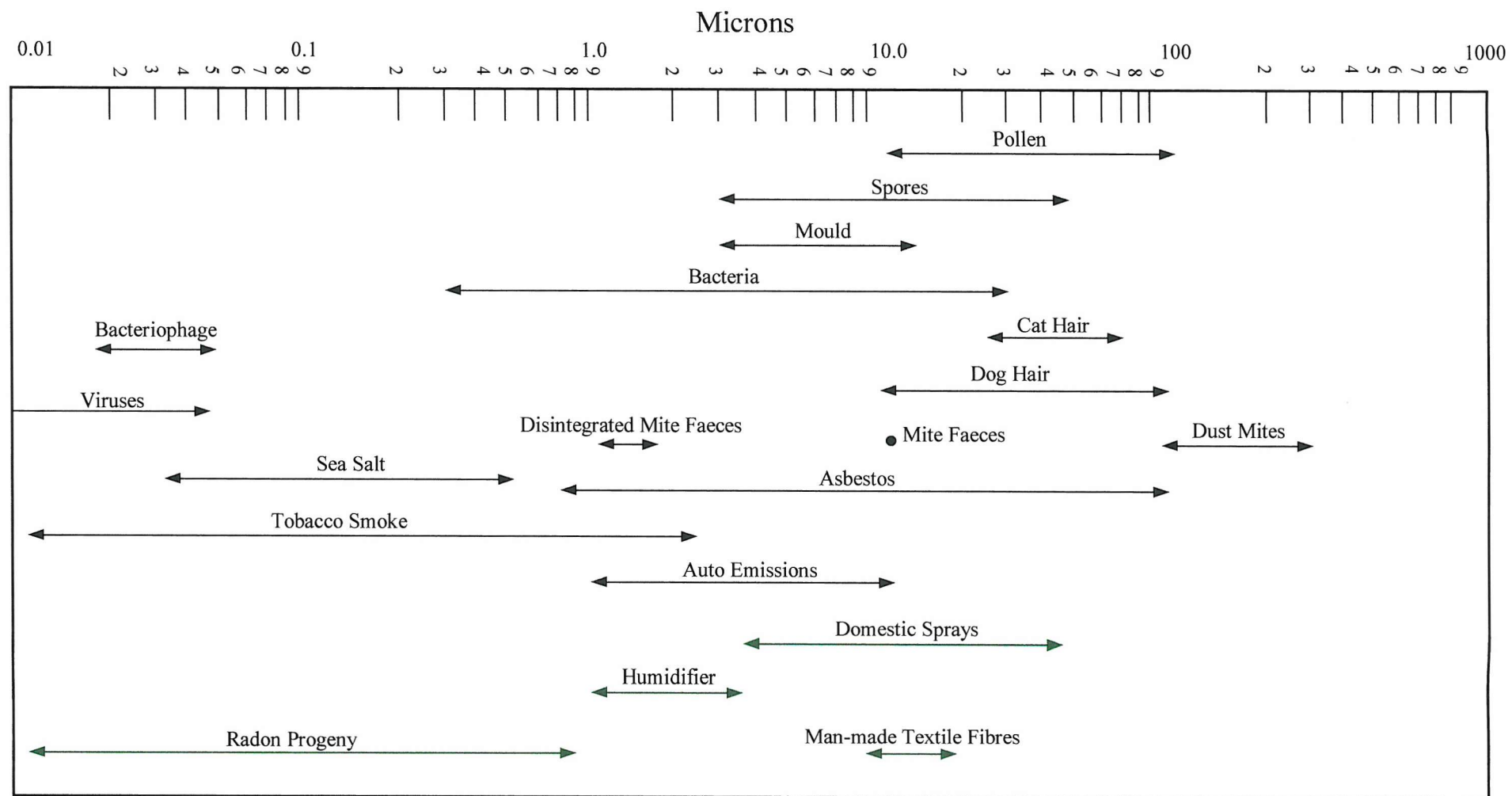


**Figure 3.1** Reported sizes of some particles which may occur indoors (after Owen *et al.*, 1992)

### 3.1.2 Health Implications of Domestic Particulates

Inhalation of airborne particles can carry a risk of infection or allergic reaction, the level of hazard depending on the composition of the particles and the site of deposition in the respiratory tract (Hinds, 1982). Deposition in the human airways is dependent largely on particle size, although the complexity of the respiratory tract and variation in breathing patterns make full characterisation of aerosol deposition impossible. Figure 3.2 summarises general trends for regional deposition, based on modelled data (Raabe, 1982). Airborne bacteria and viruses can be inhaled, but only pathogenic organisms, such as measles and influenza, can cause disease in this manner (Burge, 1990). A variety of common bioaerosols, including animal dander, pollen and insect parts and faeces can act as allergens in sensitive individuals, triggering atopic responses such as asthma, rhinitis or hayfever. Although house dust mite allergen and pollen grains are predominantly associated with particles of  $>10 \mu\text{m}$  in diameter, some particles of this size are known to enter the lungs. The high concentration of allergen in these particles means only a few are needed to trigger an allergic reaction (Platts-Mills *et al.*, 1986).

Information concerning regional deposition in the lungs is important for assessing the potential hazard of inhaled particles. Respirable particles are considered to be less than about 10 to 15  $\mu\text{m}$  in diameter, as few particles larger than this enter the respiratory tract (Hinds, 1982). Thus, it is particles below this size which are particularly important when assessing the reduction of airborne particle concentrations.

### 3.1.3 Natural Mechanisms of Particle Settling

The size and shape of airborne particles largely determine their motion and behaviour. The processes by which particles interact and are naturally lost from the air are classified as: sedimentation, impaction, interception, diffusion, and electrostatic. These mechanisms are widely reviewed (Hinds, 1982; Owen *et al.*, 1992), and only a brief summary is provided here. Figure 3.3 illustrates sedimentation, impaction, interception and diffusion schematically, while electrostatic interactions are described in detail in Section 1.3.

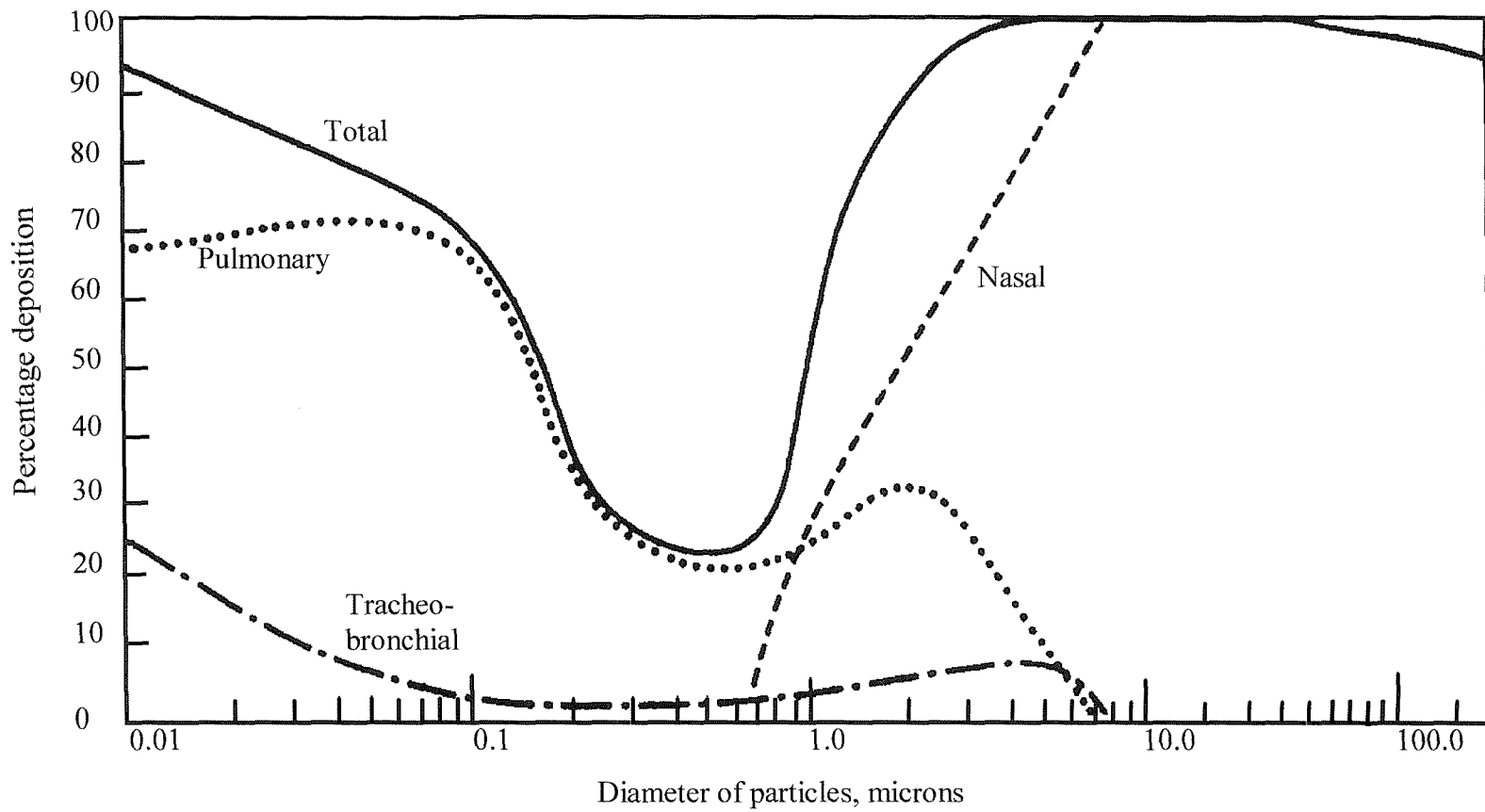
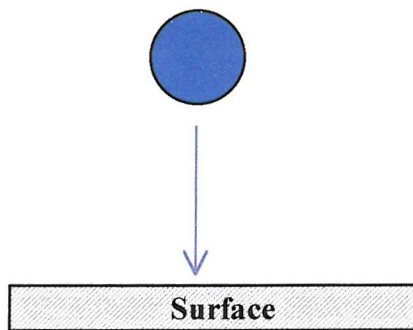
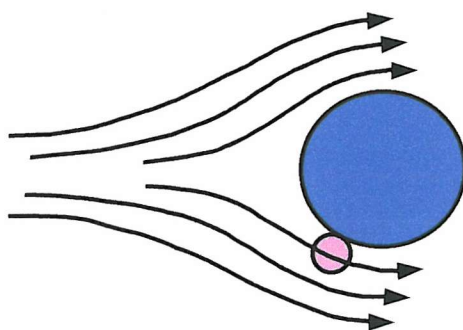


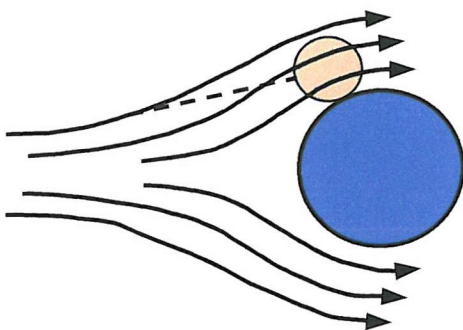
**Figure 3.2** Total and regional deposition fractions for various sizes of inhaled spherical particles in the human respiratory tract. Based on nasal breathing at a rate of 15 breaths per minute and a tidal volume of  $1450 \text{ cm}^3$ . (Raabe, 1982)



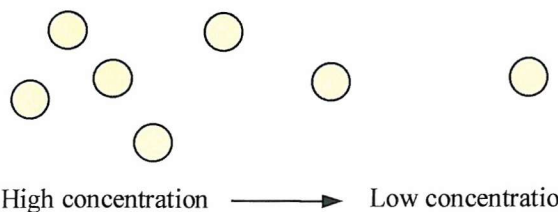
**Sedimentation** Particles settle onto horizontal surfaces as a result of gravity. Settling velocity increases with increasing particle size.



**Interception** Small particles with low inertia are carried in the gas stream around the obstacle, but will be brought into contact if the gas stream passes within one particle radius.



**Inertial Impaction** Particles in the gas flow with sufficient inertia are unable to be carried around an object in the gas stream, so impacts with the obstacle.



**Diffusion** The movement of particles undergoing Brownian motion, down a concentration gradient.

**Figure 3.3** Schematic illustration of the deposition mechanisms by which particles may naturally be removed from the air

Sedimentation occurs as a result of gravity and causes particles to settle onto horizontal surfaces. The settling velocity of particles increases with particle size, and is theoretically directly proportional to the square of particle diameter (spherical particles).

Interception occurs when a particle comes within one particle radius of the surface of an object. For true interception the particle has negligible inertial or Brownian motion, and hence does not deviate from its original gas streamline, resulting in its capture on the object surface. Impaction also occurs due to collision of particles with obstacles in the flow path, but in this case the particle deviates from its original gas stream, due to its inertia, resulting in the collision. This mechanism is relevant to larger particles with greater inertia, as smaller particles can be conveyed with the airflow around objects.

For particles of less than 1.0  $\mu\text{m}$ , diffusion is a primary mechanism of transport, and can be responsible for the collection of small particles onto surfaces in close proximity (Hinds, 1982). Diffusion is defined as the net transport of particles in a concentration gradient, from an area of high concentration to one of low concentration. Particle motion results from incessant bombardment by gas molecules, which causes an irregular action known as Brownian motion (Owen *et al.*, 1992). Mobility through Brownian motion decreases rapidly with increasing diameter. Diffusion can cause deposition of sub-micron particles over short distance, such as in filters and the lower respiratory tract. Collision of particles by diffusion can also lead to coagulation, and the formation of larger particles, which are then removed by impaction or sedimentation.

Electrostatic interactions occur when either the particle or the surface at close proximity is charged. Coulombic attraction forces exist between objects with opposite charges, while weaker image charge forces occur where one object is charged, and the other grounded, as described fully in Section 1.3. Electrostatic interactions occur over relatively short distances, because the force reduces rapidly as the distance between the objects increases (Taylor and Secker, 1994).

The production of airborne particles can occur through either dispersion or condensation. Condensation of vapours into discrete particles occurs during cooking, smoking and other combustion processes. Dispersion of particles in the home can occur through activities such as sweeping, dusting, vacuuming, movement and by air currents and drafts. Research has shown that vacuuming can significantly raise the concentration of cat

aeroallergen, through leakage from bag and connections, and through the disturbances created by the cleaning head, tube and wheels (Woodfolk *et al.*, 1993; deBlay *et al.*, 1998).

### 3.1.4 Domestic Particle Reduction Strategies

There are three strategies in the abatement of indoor air quality problems. The first is to control or eliminate the source of pollution, the second is to increase ventilation in order to dilute contaminant concentration and the third is the use of air cleaning devices (Fox, 1994). Removal of airborne particles by liquid aerosols falls into the third strategy, so air-cleaning devices will be discussed further.

A variety of air-cleaning devices are available which claim to deplete airborne particles in the domestic environment. These can be incorporated into mechanical ventilation systems or portable units that can be moved from room to room. Broad classifications can be made into 1) mechanical units, incorporating filters and often a motorised fan, and 2) electrostatic units such as ion-generators or precipitators. A study of portable air-cleaners using tobacco smoke as a particle source, found that while electrostatic precipitators removed particles at a substantial rate (often removing all particulate matter but leaving gas-phase odours) negative ion generators removed particles slowly (Offermann *et al.*, 1985). Mechanical units with simple panel filters were also generally ineffective in removing particles. Mechanical units with extended surface area HEPA (High-efficiency particulate air) filters were very efficient, however. These filters have a minimum removal efficiency of 99.97% for particles down to 0.3  $\mu\text{m}$  in diameter and efficiency actually improves with use, as captured particles reduce inter-fibre distances (Nelson *et al.*, 1988; Fox, 1994).

There are currently no standard evaluation procedures for portable air cleaners, although manufacturers make general claims and there are some published evaluations (Offermann *et al.*, 1985; Nelson *et al.*, 1988; Fernández-Caldas and Fox, 1992; Fox, 1994). Where tested for their ability to ameliorate atopic respiratory disease, portable air cleaning devices generally fail to achieve clinically significant results (Nelson *et al.*, 1988). The exceptions are mechanical units with HEPA filters. Where these units were used over the

beds of asthmatic children, less medication was required, although symptom amelioration was not observed (Verrall *et al.*, 1988).

Air cleaning devices fail to reduce air pollutant concentrations enough to effect clinical improvement of atopic disease due to the large reservoirs of particulates in the domestic environment (Fernández-Caldas and Fox, 1992). For example, large quantities of house dust mite and animal dander allergens accumulate in soft furnishings, carpets and bedding, readily becoming airborne during disturbance. For this reason, use of air cleaners is not advisable for aeroallergen reduction, unless in conjunction with appropriate environmental control of the particular allergen source (Nelson *et al.*, 1988).

### 3.1.5 Objectives

The aim of this section of research was to investigate whether liquid aerosols generated by domestic pressure-pack dispensers remove airborne dust particles, and whether this effect could be enhanced if the droplets carried an electrostatic charge. An air particle counter was used to quantify airborne particle concentration, so that the effect of liquid aerosol droplets on concentration could be quantified. The effect of uncharged and charged droplets was compared, initially using artificially charged dispensers. The effects of three different formulation types were compared, for which the charge-to-mass ratio of each was increased artificially to the same level. This was followed with a comparison using a dispenser that generated the level of charge naturally during atomisation. Precipitation of considerable quantities of airborne particles by highly charged liquid aerosol would provide a cheap and convenient method of cleaning the air in the home. Although this would not confer the longer-term benefits of portable air cleaning devices, it may provide an additional approach, which would be immediately effective.

## 3.2 Materials and Methods

### 3.2.1 Preparation of Standard House Dust

House dust was prepared from vacuum cleaner bags collected from local domestic residences. The bag contents were sieved to produce a fine dust fraction, using a mechanical siever and a series of Endecott sieves ranging from 500 to 63  $\mu\text{m}$ . The course dust from the vacuum cleaner bags was placed in the largest mesh sieve at the top of the stack, and the fibres teased apart to aid particle release. Dust passing through the finest sieve (63  $\mu\text{m}$ ) at the bottom was stored in a glass jar, and vigorously shaken to achieve a homogeneous mix. This was stored at -20 °C until required. Freezing had the effect of preventing biological activity in the dust, such as house dust mite or fungal growth, which could alter the nature of particulates over time. House dust to be used in a series of experiments was sieved and stored in advance, so that all aliquots were drawn from the same homogenous reservoir, which was not added to in the course of the experiment. This ensured continuity between tests, because house dust collected from different sources at different times has the potential to vary enormously in composition.

This method of domestic dust collection may not generate samples representative of airborne dust in domestic environments. The finer dust particles constituting airborne dust probably remain within the carpet or soft furnishings, pass through the vacuum cleaner bag and filters or are re-entrained during the vacuuming process. Dust collected from vacuum cleaners will contain more of the heavy, non-organic components and less of the fine particles like skin cells, pollen and combustion particulates.

### 3.2.2 Quantification of the Precipitation Rate of Airborne Particulates by Liquid Aerosols

The concentration of an artificially created aerosol of dust particulates was measured using an air particle counter (Malvern Instruments), and the effect of liquid aerosol on the concentration of this aerosol quantified. This was conducted in a booth measuring  $1.8 \times 1.2 \times 1.0$  metres, which was constructed from sheets of transparent plastic held together by metal supports. The front panel of the booth was removable to allow

access for cleaning between experiments. This front panel had two square orifices, measuring  $0.3 \times 0.3$  m, with doors for access. All fixed joints were sealed with silicon sealant, and the interface between the front panel and the main body of the booth sealed with adhesive foam strips. This apparatus is shown in Figure 3.4.

An air particle counter, APC 300A (Malvern Instruments, Malvern, UK) was used to measure the concentration of airborne particulates in seven user-selected size ranges between  $0.3 \mu\text{m}$  and  $25 \mu\text{m}$  diameter. The sample flow rate was 28.3 litres per minute (one cubic foot per minute), and measurements were taken using an isokinetic sampling probe placed inside the booth. Two ten-times dilutors (Palas VKL-10 S) were fitted in series between the sampling probe and the APC, to achieve a one hundred-fold dilution of the incoming aerosol sample. This was necessary in order to bring the particle concentration within the working range of the counter, which was  $1.2 \times 10^6$  particles per 28.3 litres. The APC was controlled by an internal microprocessor, which counted and sized particles suspended in air, processed and stored the data. A user-defined measurement sequence was created, which ran a specific series of measurements for each experiment. In this way, sampling was automated once the program sequence had commenced.

An aerosol of dust particulates was generated in the chamber using  $2.0 \pm 0.1\text{g}$  of dust (Section 3.2.1). This was placed on a metal platform held 0.75 m above the floor of the booth, and 0.35 m from the end and side walls. The dust was then blown off the platform using compressed air from a hand-held air gun, at 2.5 psi. Immediately after the dust aerosol had been generated the sampling program of the APC was started. This program took ten, one-minute samples, with a 30 second interval between samples. There was a 120 second delay before commencement of the first sample, to allow the aerosol concentration to become homogenous within the chamber. Offermann *et al.* (1985) also found a settling period necessary in their test of portable air-cleaner efficiencies, due to changing concentration of particles that was attributed to coagulation. Ten samples were taken to produce a series of particle concentration measurements, within the selected size ranges, over the period of the experiment. The sequence of events and sampling are illustrated in Figure 3.5. The average of a minimum of five replicates was calculated for each size band. This was the reference dust-settling rate, with which precipitation rates achieved by the pressure-pack sprays were to be compared.

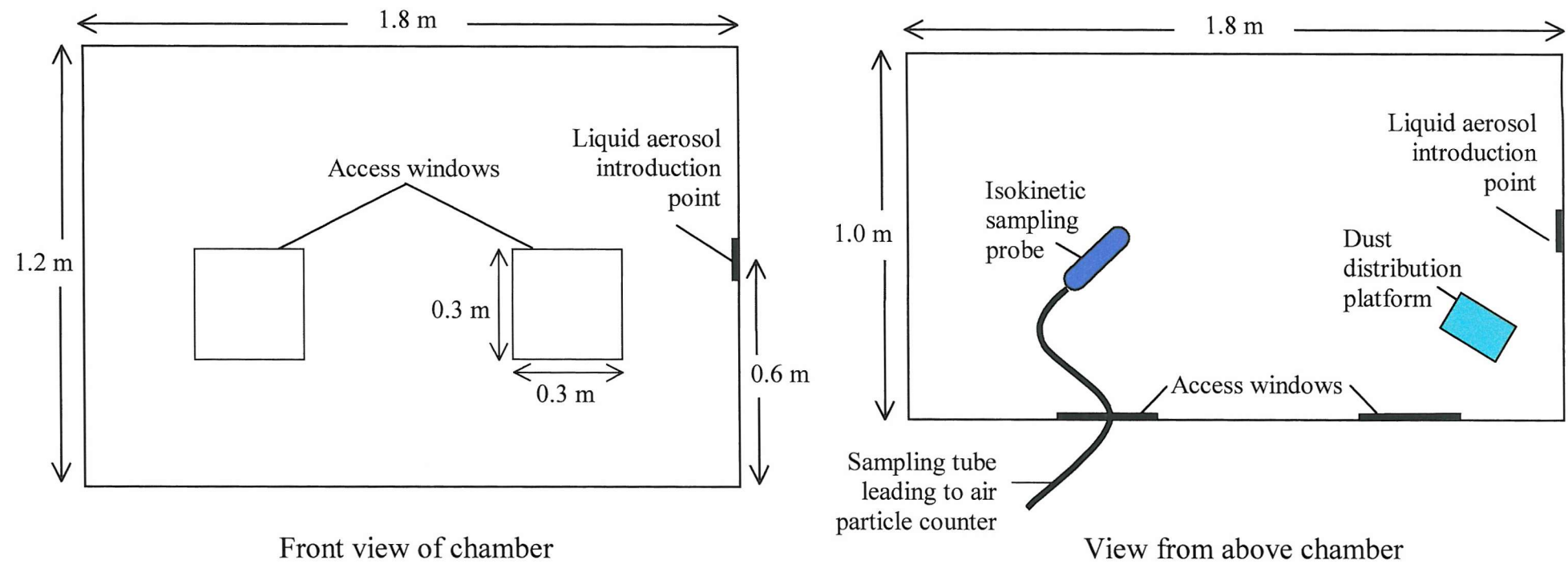


**Figure 3.4** Schematic drawing of the test chamber used to quantify the depletion rates of artificially generated dust aerosols.

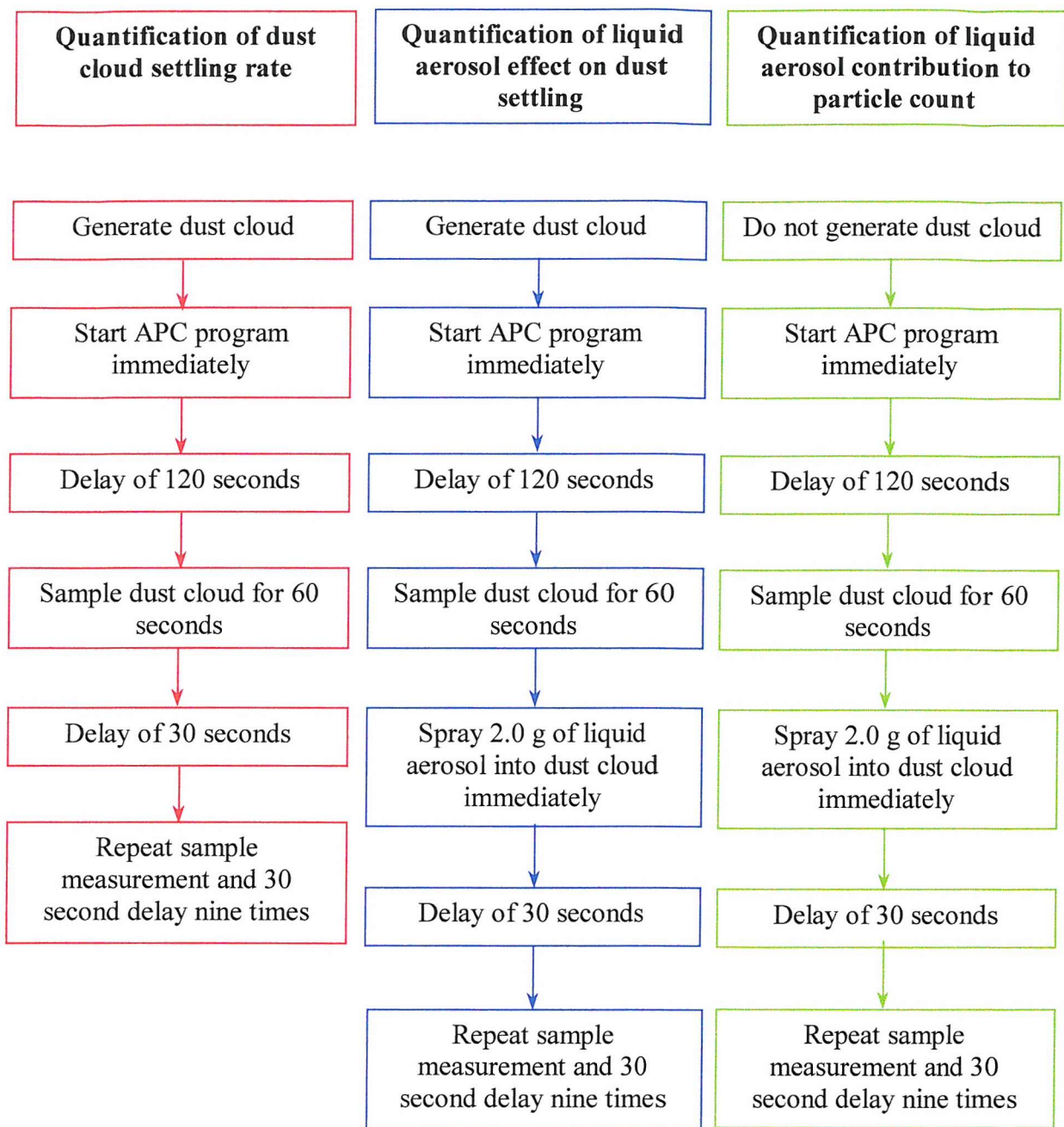


**Figure 3.5** Sequence of events for the quantification of dust cloud settling rate, the effect on this of liquid aerosols and the contribution of liquid aerosol to particle count

To quantify the effect of a pressure-pack liquid spray on the settling rate of dust, the dust aerosol was generated in the manner previously described. The APC program was immediately initiated. A  $2.0 \pm 0.2$  g spray from the pressure-pack dispenser was introduced into the chamber immediately following completion of the first sample in the

program sequence. The pressure-pack dispenser was sprayed through an opening in the end wall of the booth, central along the width of the booth and 0.6 m above its floor, as indicated in Fig 3.4. If the mass of liquid formulation did not fall within the defined range, then the test was discounted. The first sample taken in the APC program gave a value for the original concentration of the dust aerosol, and subsequent concentrations after treatment with the spray were expressed as a percentage of this concentration. Five replicates were conducted.

After each measurement, the chamber was ventilated and cleaned. Removing the front panel from the chamber allowed ventilation while the floor and side-walls of the chamber were cleaned with a damp cloth to remove most dust particles, to prevent re-entrainment during subsequent tests. A minimum of 2 hours passed between tests.

The APC counted both solid and liquid aerosols, so samples taken after the liquid droplet spray was introduced included a contribution from this source. It was therefore necessary to correct measurements to take account of this. To achieve this no dust aerosol was generated in the booth, but the APC program was initiated and  $2.0 \pm 0.2$  g of spray introduced immediately following completion of the first sample. This produced a set of measurements corresponding to the number of droplets during the dust quantification test. The first measurement gave a value for the concentration of the background of dust aerosol, and the subsequent nine measurements gave values for the number of liquid droplets in the air over the duration of the experiment. The background was subtracted from all the subsequent measurements, leaving only values representing liquid droplet numbers for each size band throughout the experiment. The average of five replicates was calculated, and converted to the number of droplets in 1 gram of liquid, by dividing by the mean mass of liquid aerosol sprayed. A correction factor was then calculated for each precipitation experiment replicate, by multiplying droplet number by the mass of liquid aerosol dispensed. This was subtracted from the measurement taken during dust aerosol precipitation experiments for the corresponding size band and sample number, to leave values representing the concentration of dust aerosol alone. The results were expressed as a percentage of the original dust aerosol concentration, and compared to particulate concentration during natural settling.

### 3.2.3 Measurement of Droplet Size Distribution of Liquid Aerosols

A Malvern droplet and particle sizer, Series 2600c (Malvern Co. Ltd, England), controlled by a microcomputer, was used to analyse the diameter of the droplets produced by pressure-pack dispensers. This instrument measured the percentage of droplets, by volume, falling into 15 size bands by laser diffraction. The size bands into which droplets were measured were determined by the lens used. For this purpose a 300 mm lens was used, which measured droplets of between 5.8 and 564 microns in diameter.

Initially a background was measured, which allows imperfections in the optical system to be taken into account during the experiment. The main sources of background are dirt or scratches on the lenses and ambient daylight or fluorescent light. The effect of these factors was minimised by keeping lenses clean and dust free, and by eliminating as much light as possible from the chamber housing the droplet and particle sizer.

It was important that the pressure-pack dispenser was positioned correctly with respect to the laser beam and the detector lens in order for accurate measurements to be taken. The concentration of the plume of droplets passing through the laser beam must be correct. If the concentration is too high multiple scattering of the laser beam can occur, and this causes the droplet size distribution to appear finer than it really is. If the concentration of the sample is too low, statistical errors occur. The sample must also pass within the focal length of the lens, because droplets outside this range will cause diffraction of the laser light beyond the lens, and the data to be lost. The focal length of the lens used was 300 mm, so the plume of droplets was positioned within 300 mm of the detector lens. To avoid deposition of droplets onto the lenses the plume was screened, such that only a 40 mm wide portion from the centre of the plume passed through the laser beam. This was achieved by placing metal cylinders around both lenses, such that the path of the laser beam was not obscured, and only 40 mm of the plume was sampled. It was found that the dispensers needed to be positioned about 450 mm from the laser path in order to achieve an acceptable droplet concentration. This apparatus is illustrated in Figure 3.6.

To measure the size distribution, the aerosol plume was sprayed continuously through the laser for about 3 seconds, while 75 measurement sweeps were made by the instrument. The data collected was compiled by the computer, and corrected for background. The data was then presented as the percentage, by volume, of droplets falling into the 15 size bands. A minimum of three replicates was conducted for each dispenser.

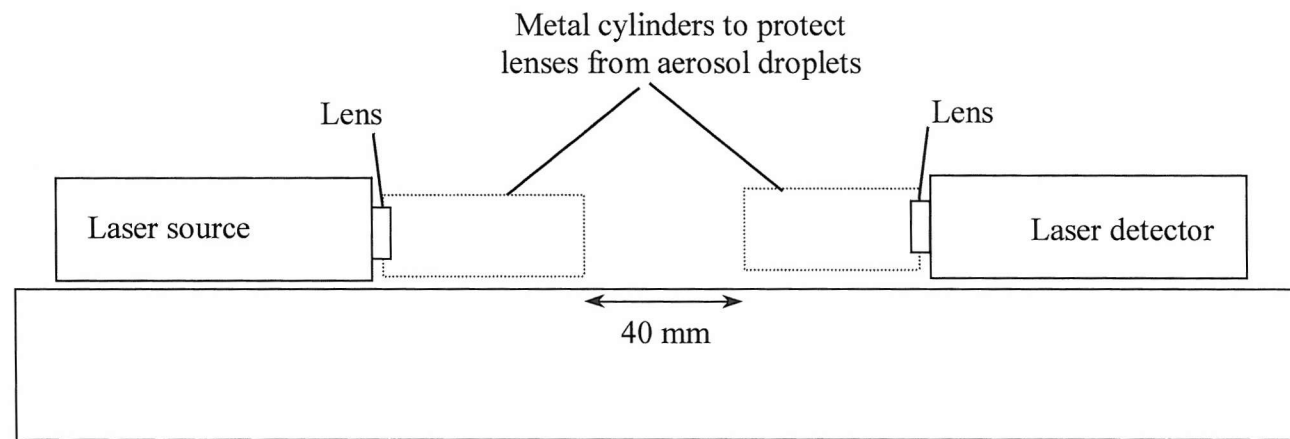


**Figure 3.6** Apparatus for measurement of droplet size distributions of liquid aerosols produced from pressure-pack dispensers.

### 3.2.4 Airborne Dust Precipitation by Uncharged and Artificially Charged Liquid Sprays

Formulation I, an alcohol-based liquid with no emulsification, was used in this investigation. The formulation ingredients are given in Table 2.1 of Chapter 2. The valve components used were those described as 'standard' in Table 2.2. The actuator was the button-style (Figure 2.3) with a 0.51 mm orifice and *Aqua* style swirl chamber. The charge-to-mass ratio normally generated was  $+2.4 \times 10^{-5}$  C.kg<sup>-1</sup>, which was measured using the method described in Section 2.2.6. This will be referred to as the 'uncharged liquid aerosol', although the droplets carried a low net electrostatic charge. An artificially charged spray, with a charge-to-mass ratio of  $+4.3 \times 10^{-4}$  C.kg<sup>-1</sup> was generated by applying 3kV (positive) to the dispenser during spraying. This was achieved by fixing the dispenser in an insulating plastic support, shown in Figure 3.7, which allowed for safe actuation of the dispenser during high voltage application. High voltage was applied to the pressure-pack dispensers via a brass screw contacting an area on the dispenser from which any decorative lacquer or paint had been removed, ensuring good electrical contact. To this screw the required voltage was applied from a power supply (Brandenburg Alpha III, model number 3807), and the dispenser was safely actuated by depressing the insulating lever. The charge on the resultant aerosol was measured by collecting the droplets on an aluminium plate, approximately 300 mm square. This was seated on a piece of polytetrafluoroethene (PTFE) to maintain electrical insulation, and was connected to an electrometer (Keithley Instruments, model number 610C solid state electrometer). The collecting plate was 250 mm from the actuator of the dispenser. The mass of liquid dispensed was calculated from the mass of the dispenser before and after spraying. Five replicates were completed for each variant, and the mean and standard error calculated. The charge-to-mass ratio calculated in this way will be an underestimation, due to the discrepancy between the mass of formulation collected on the aluminium plate, and that dispensed. Some droplets will travel past or rebound off the collecting plate, and thus the charge on those droplets would not be collected, although their mass was included in calculating charge-to-mass ratio.

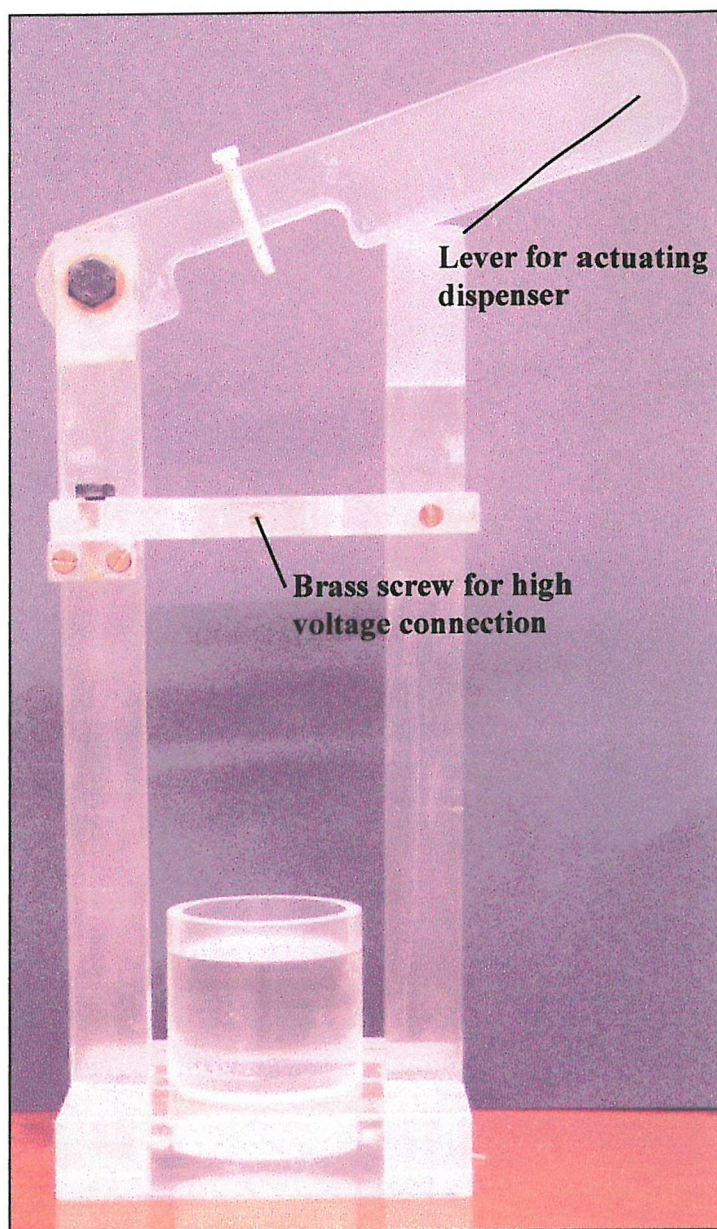


**Figure 3.7** Pressure-pack dispenser support for high voltage application

The effect on airborne dust precipitation of formulation I was compared using the method described in 3.2.2. The natural rate of precipitation of the generated dust cloud, the rate of precipitation following treatment with uncharged liquid aerosol and artificially charged formulation I were compared.

### 3.2.5 Airborne Dust Precipitation by Three Formulation Types, when Artificially Charged

Formulations I, II and III were compared in this investigation, all with their charge-to-mass ratio raised artificially by the application of high voltage. The formulations are described in Table 2.1 of the previous Chapter and the valve components used were those listed as 'standard' in Tables 2.2 (Formulations I and II) and 2.3 (Formulation III). The actuator used was the same for all formulations, and was the button-style (Figure 2.3) with a 0.51 mm orifice and *Aqua* style swirl chamber. For each formulation, the voltage required to generate an aerosol with a charge-to-mass ratio of about  $2.5 \times 10^{-4}$  C.kg<sup>-1</sup> was found, using the technique described in Section 3.2.4. For formulation I, 3kV (positive) was applied to achieve a q/m of  $+2.7 \times 10^{-4}$  C.kg<sup>-1</sup>; for formulation II, 7kV (negative) was applied, achieving a q/m of  $-2.7 \times 10^{-4}$  C.kg<sup>-1</sup>, and for formulation III, a q/m of  $-2.3 \times 10^{-4}$  C.kg<sup>-1</sup> was achieved by applying 6 kV (negative). Precipitation of airborne dust particles by the three formulations was measured according to the method of Section 3.2.2, and compared with the natural rate of precipitation of the generated dust cloud.

The droplet size distribution of these three formulations was also measured, as this factor could be important in determining differences observed in the results. This was performed according to the method of Section 3.2.3.

### 3.2.6 Airborne Dust Precipitation by Uncharged and Naturally Charged Liquid Droplets

For this investigation, formulation II (an emulsion with a continuous water-phase) was used because the experiment of Section 3.2.5 showed it precipitated more particles than formulations I or III. The formulation was described in Table 2.1 and the valve components of the uncharged aerosol in Table 2.2. The actuator used was a button-style actuator with a 0.51 mm diameter orifice and *Aqua*-type swirl chamber. The naturally charged combination consisted of an identical formulation, with the valve and actuator components modified as follows: 3.00 mm diameter dip tube, 0.64 mm diameter tailpiece orifice, 4 × 0.61 mm diameter stem holes, 1.17 mm diameter vapour phase tap, button-style

actuator with a 0.46 mm diameter round orifice and MBU-type swirl chamber. The charge-to-mass ratio achieved with these dispensers was measured using the method described in Section 2.2.6. The uncharged dispenser gave a charge-to-mass ratio of  $1.4 \times 10^{-5}$  C.kg<sup>-1</sup> (negative), and the naturally charged dispenser generated a q/m of  $1.4 \times 10^{-4}$  C.kg<sup>-1</sup> (negative). Precipitation of airborne dust particles by these two liquid aerosols was measured according to the method described in Section 3.2.2, and compared with the natural rate of precipitation of the generated dust aerosol.

Droplet size distributions were measured for the uncharged and naturally charged liquid aerosols, according to the method in Section 3.2.3.

### 3.3 Results

#### 3.3.1 Airborne Dust Precipitation by Artificially Charged Liquid Sprays of Formulation I

Figures 3.8a to 3.8e compare the rate of precipitation of 0.5-0.7, 0.7-1.0, 1.0-2.0, 2.0-5.0 and 5.0-10.0  $\mu\text{m}$  diameter particles during the natural settling of the dust cloud, and after treatment with uncharged and artificially charged liquid aerosol of formulation I. The charge-to-mass ratio of these aerosols were  $2.4 \times 10^{-5} \text{ C.kg}^{-1}$  (positive) and  $4.3 \times 10^{-4} \text{ C.kg}^{-1}$  (positive) respectively. Statistical analysis was performed, comparing the mean particle concentrations at 1.5 minutes into the experiment for each size band. This time point was chosen because it was the first result, and showed the greatest depletion in concentration, and the greatest difference between treatments. Due to high variability of some data, ANOVA could not always be applied. Therefore, t-tests were used to compare particle concentrations during natural settling and after treatment with either the uncharged or the artificially charged liquid aerosol. Unequal variance t-tests (Appendix A) were applied where variances were not homogeneous following transformation, due to the order of magnitude difference between particle counts.

The effect of the uncharged liquid aerosol on particle concentration was erratic. An initial decrease (at 1.5 minutes into the experiment) was observed for all size bands studied, compared to the dust concentration during natural settling. This was followed by an increase in concentration for 0.5-0.7  $\mu\text{m}$  and 0.7-1.0  $\mu\text{m}$  diameter particles. The initial decrease was just statistically significant for particles of 1.0-2.0  $\mu\text{m}$  diameter ( $p < 0.05$ ) and highly significant for particles of 2.0-5.0  $\mu\text{m}$  and 5.0-10.0  $\mu\text{m}$  diameter ( $p < 0.01$ ). The initial decrease in particle concentration achieved by the charged liquid aerosol, compared to the natural concentration, was not statistically significant for particles of 0.5-0.7  $\mu\text{m}$  diameter. The concentration decrease achieved for particles of 0.7-1.0  $\mu\text{m}$  diameter was found to be significant ( $p < 0.05$ ), while for particles of 1.0-2.0  $\mu\text{m}$ , 2.0-5.0  $\mu\text{m}$  and 5.0-10.0  $\mu\text{m}$  diameter the reduction was highly significant ( $p < 0.01$ ). Comparing particle concentration after treatment with the uncharged and charged liquid aerosols, the lower concentration achieved by the charged aerosol for particles of 1.0-2.0  $\mu\text{m}$  and 2.0-5.0  $\mu\text{m}$  diameter was just significant ( $p < 0.05$ ).

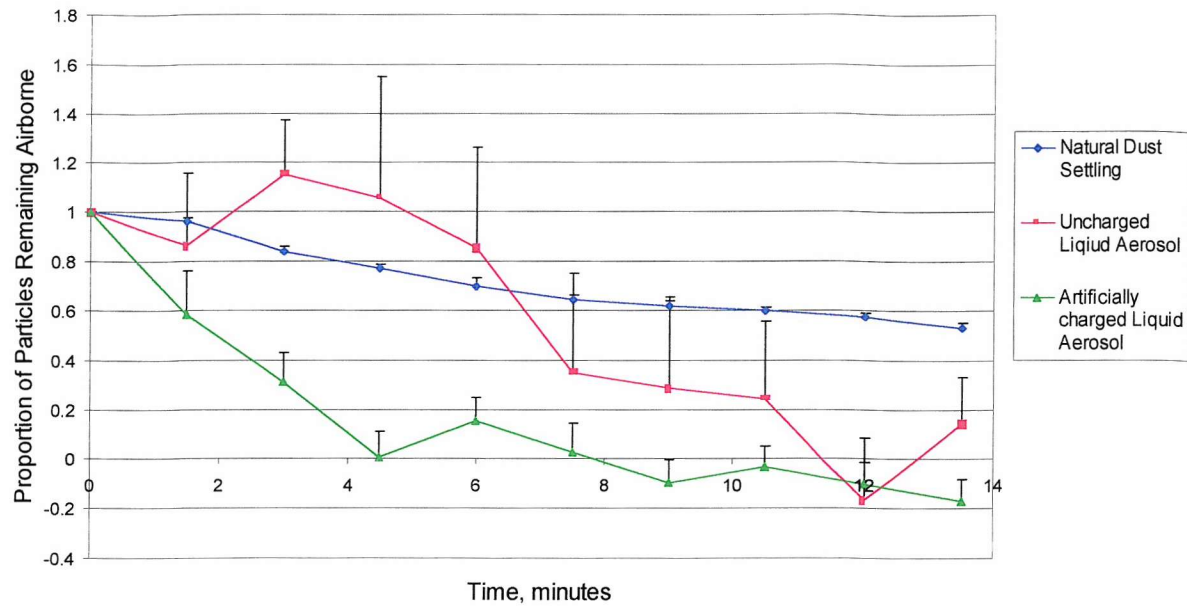


**Figure 3.8a** Depletion rates for airborne particles of 0.5 to 0.7  $\mu\text{m}$  diameter during natural settling of dust and after treatment with uncharged and artificially charged liquid aerosols of an alcohol-based formulation. Standard error bars shown.

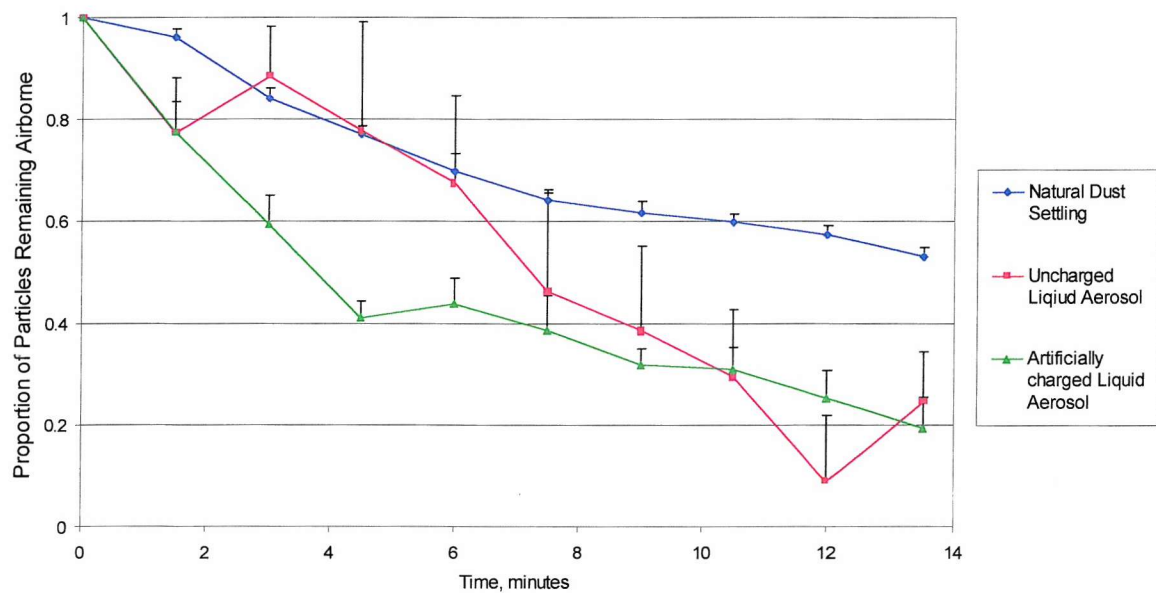


**Figure 3.8b** Depletion rates for airborne particles of 0.7 to 1.0  $\mu\text{m}$  diameter during natural settling of dust and after treatment with uncharged and artificially charged liquid aerosols of an alcohol-based formulation. Standard error bars shown.

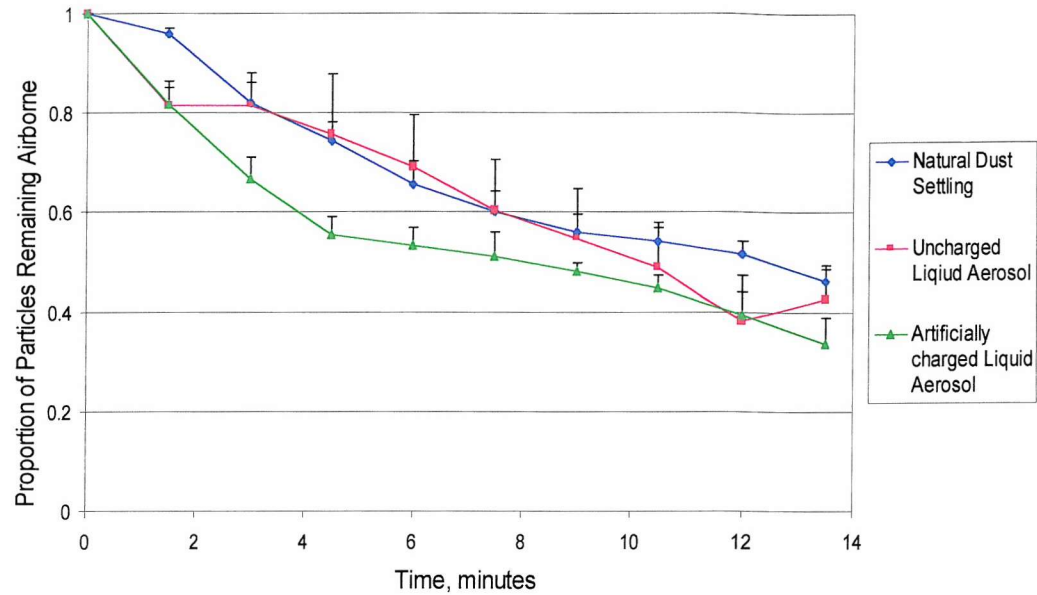


**Figure 3.8c** Depletion rates for airborne particles of 1.0 to 2.0  $\mu\text{m}$  diameter during natural settling of dust and after treatment with uncharged and artificially charged liquid aerosols of an alcohol-based formulation. Standard error bars shown.

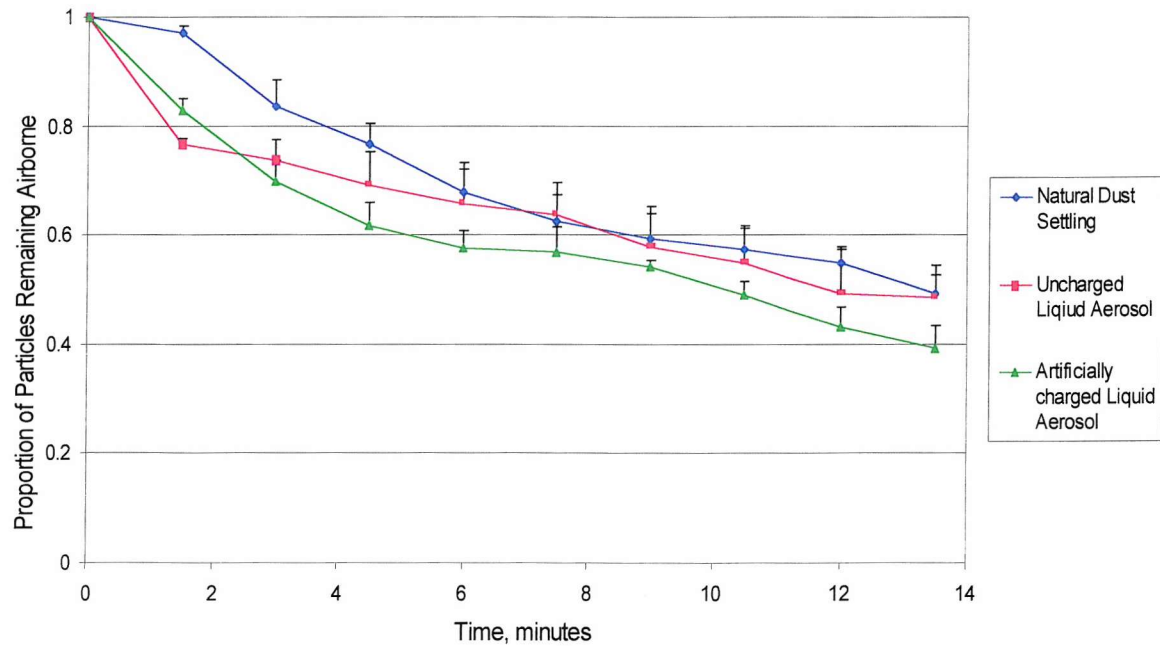


**Figure 3.8d** Depletion rates for airborne particles of 2.0 to 5.0  $\mu\text{m}$  diameter during natural settling of dust and after treatment with uncharged and artificially charged liquid aerosols of an alcohol-based formulation. Standard error bars shown.

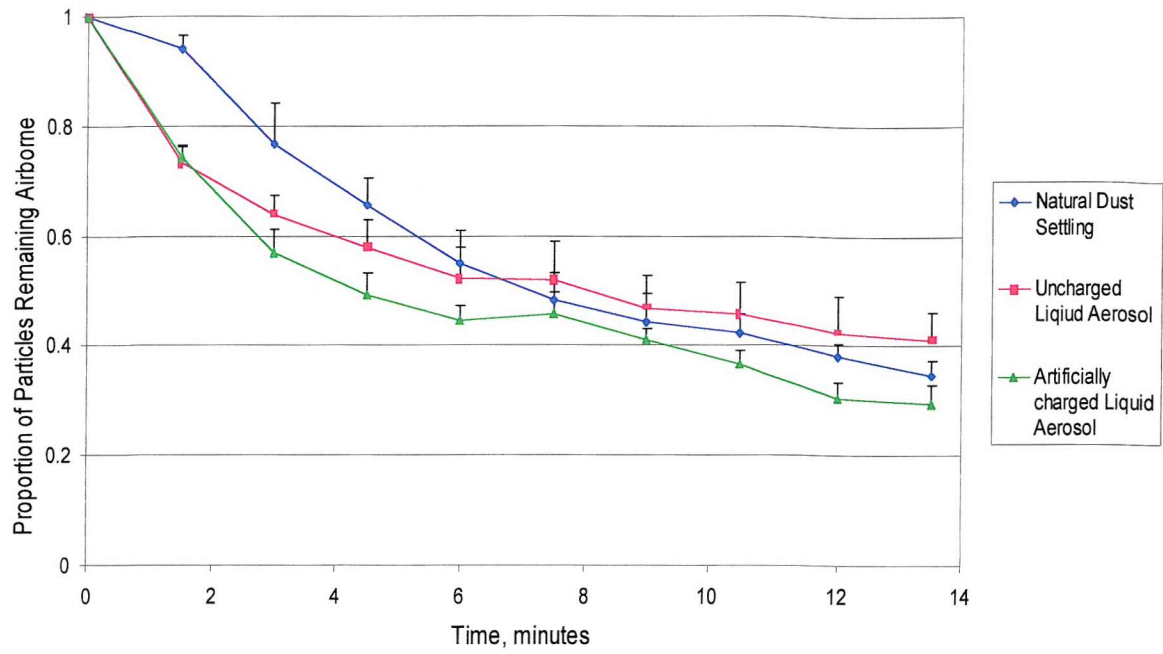


**Figure 3.8e** Depletion rates for airborne particles of 5.0 to 10.0  $\mu\text{m}$  diameter during natural settling of dust and after treatment with uncharged and artificially charged liquid aerosols of an alcohol-based formulation. Standard error bars shown.

Concentrations were also measured for particles of 0.3-0.5  $\mu\text{m}$  diameter, but these data were erratic and variable. This probably occurred because these particles were moving in air currents and their concentration had not stabilised in the test chamber. Larger particles had stabilised in their concentration, as they were less mobile. Particle concentrations were also measured for 10.0-25  $\mu\text{m}$  in diameter, but these data are not presented due to the poor counting statistics associated with the relatively low numbers of particles. The 100-fold dilution required to achieve particle concentrations within the working range of the particle counter for smaller particles meant that these counts generated large sampling errors.

### 3.3.2 Airborne Dust Precipitation by Artificially Charged Aerosols of Three Formulation Types

The rate of precipitation of airborne dust particles is shown in Figures 3.9a to 3.9e for particles of 0.5-0.7  $\mu\text{m}$ , 0.7-1.0  $\mu\text{m}$ , 1.0-2.0  $\mu\text{m}$ , 2.0-5.0  $\mu\text{m}$  and 5.0-10.0  $\mu\text{m}$  diameter respectively. These show a general trend for all three formulations to increase the rate of precipitation above that occurring naturally. Formulation II, an emulsion with a continuous water phase, appeared to achieve a larger depletion of particles than formulations I and III, which appear similar to each other for most particle sizes. Statistical analysis was performed (ANOVA followed by Tukey test as described in Appendix A), comparing the particle concentrations at 3 minutes into the experiment for each size band. The second measurement, rather than the first at 1.5 minutes, was selected for analysis in this comparison, as this showed the greatest difference between treatments.

For particles of between 0.5 and 0.7  $\mu\text{m}$  diameter, the data for formulation III was too variable for analysis. Only formulation II significantly reduced the concentration of airborne particles ( $p < 0.05$ ) compared to the natural settling rate. All data were analysed for particles of between 0.7-1.0  $\mu\text{m}$ , 1.0-2.0  $\mu\text{m}$  and 2.0-5.0  $\mu\text{m}$  in diameter. The reduction in concentration achieved by the three formulations was significantly different ( $p < 0.05$ ) from the natural concentration, but the treatments did not differ significantly from each other. For particles of 5.0-10.0  $\mu\text{m}$  diameter only formulation II significantly reduced particle concentration, compared with the natural settling rate.

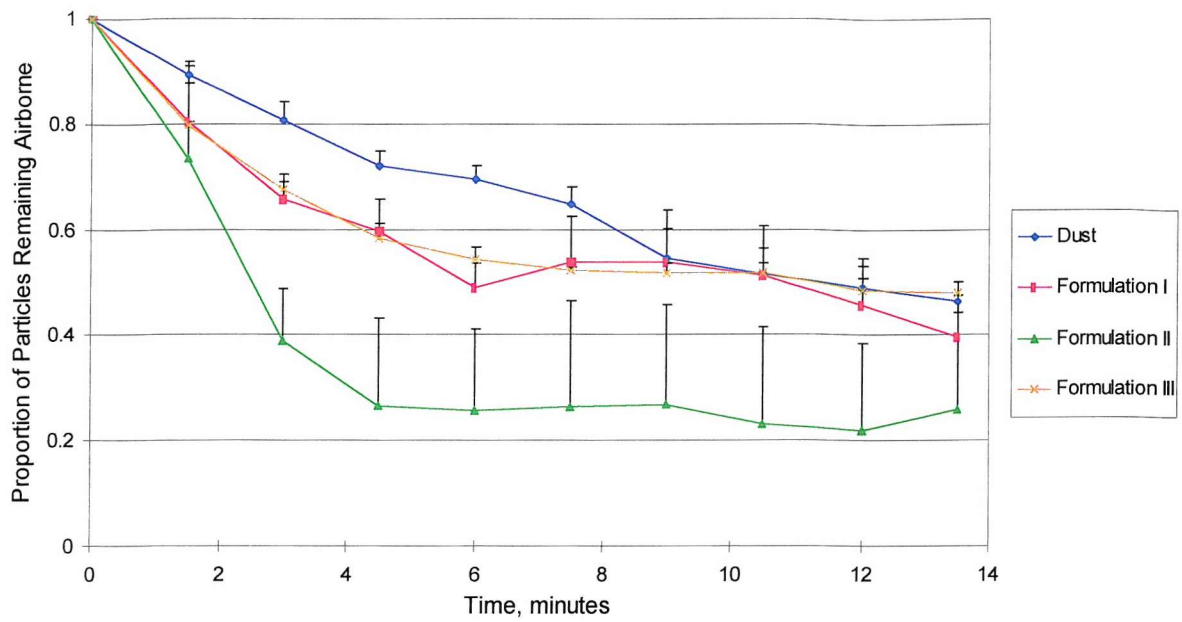


**Figure 3.9a** Depletion rates for airborne particles of 0.5 to 0.7  $\mu\text{m}$  diameter during natural settling of dust and after treatment with charged liquid aerosols of formulations I, II and III. Standard error bars shown.

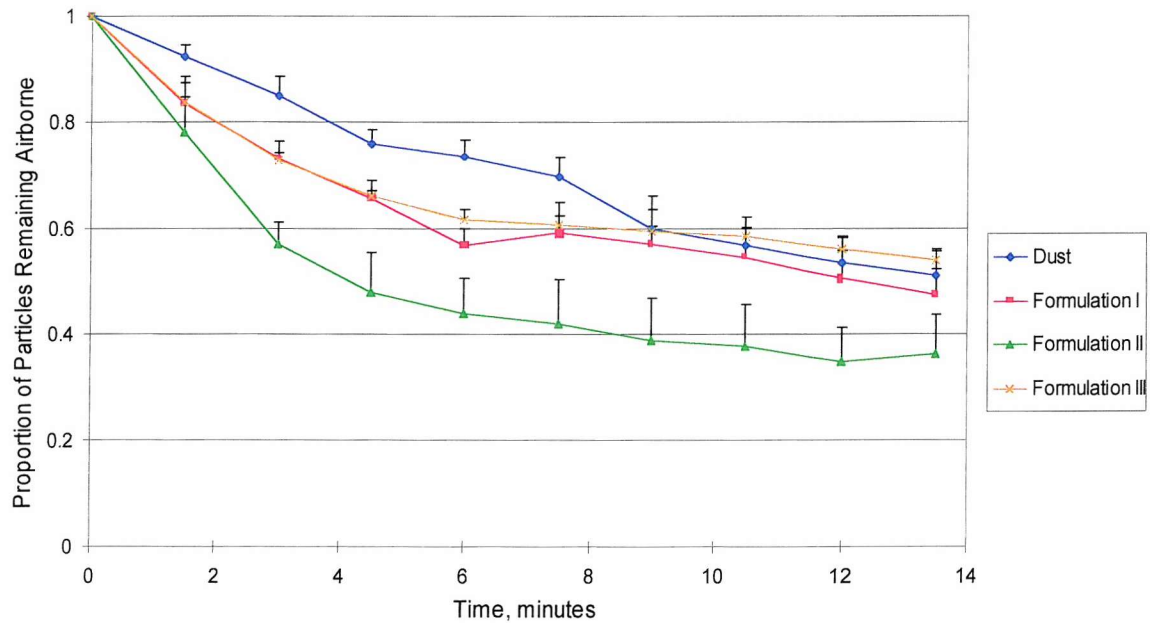


**Figure 3.9b** Depletion rates for airborne particles of 0.7 to 1.0  $\mu\text{m}$  diameter during natural settling of dust and after treatment with charged liquid aerosols of formulations I, II and III. Standard error bars shown.

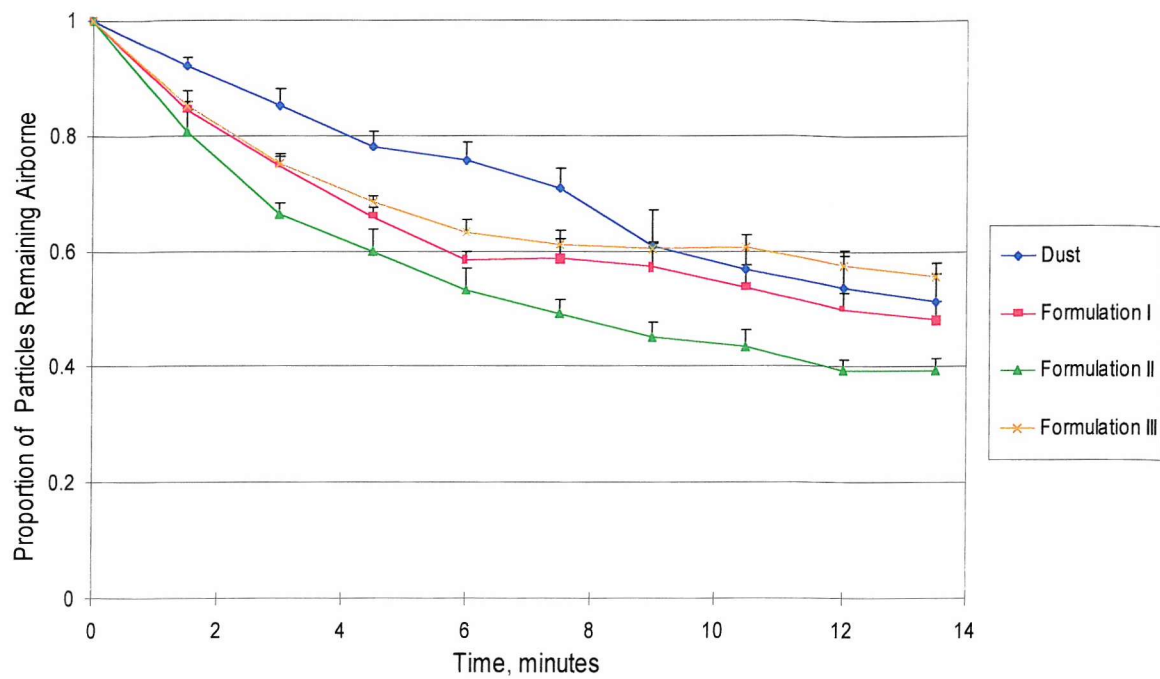


**Figure 3.9c** Depletion rates for airborne particles of 1.0 to 2.0  $\mu\text{m}$  diameter during natural settling of dust and after treatment with charged liquid aerosols of formulations I, II and III. Standard error bars shown.

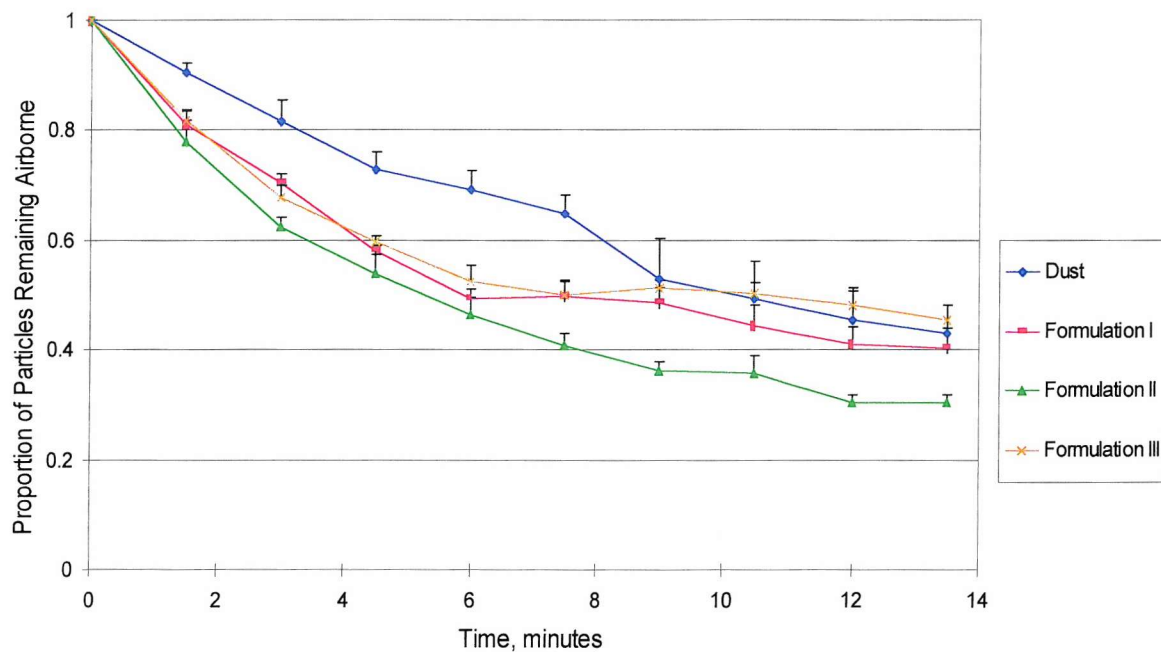


**Figure 3.9d** Depletion rates for airborne particles of 2.0 to 5.0  $\mu\text{m}$  diameter during natural settling of dust, and after treatment with charged liquid aerosols of formulations I, II and III. Standard error bars shown.

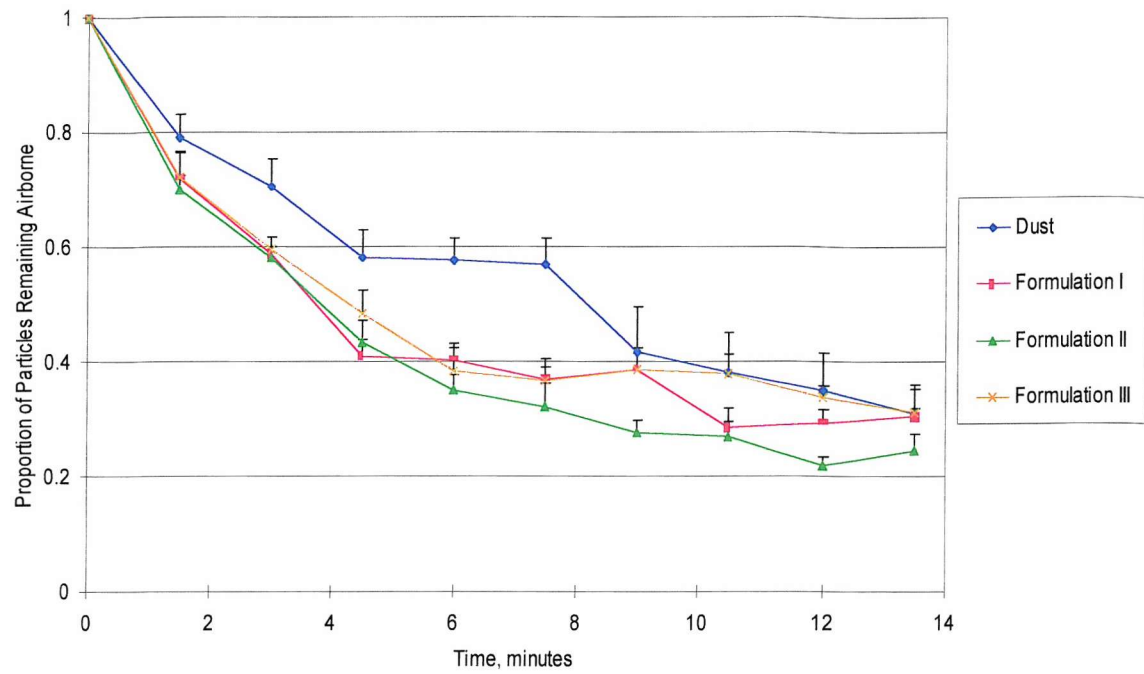


**Figure 3.9e** Depletion rates for airborne particles of 5.0 to 10.0  $\mu\text{m}$  diameter during natural settling of dust and after treatment with charged liquid aerosols of formulations I, II and III. Standard error bars shown.

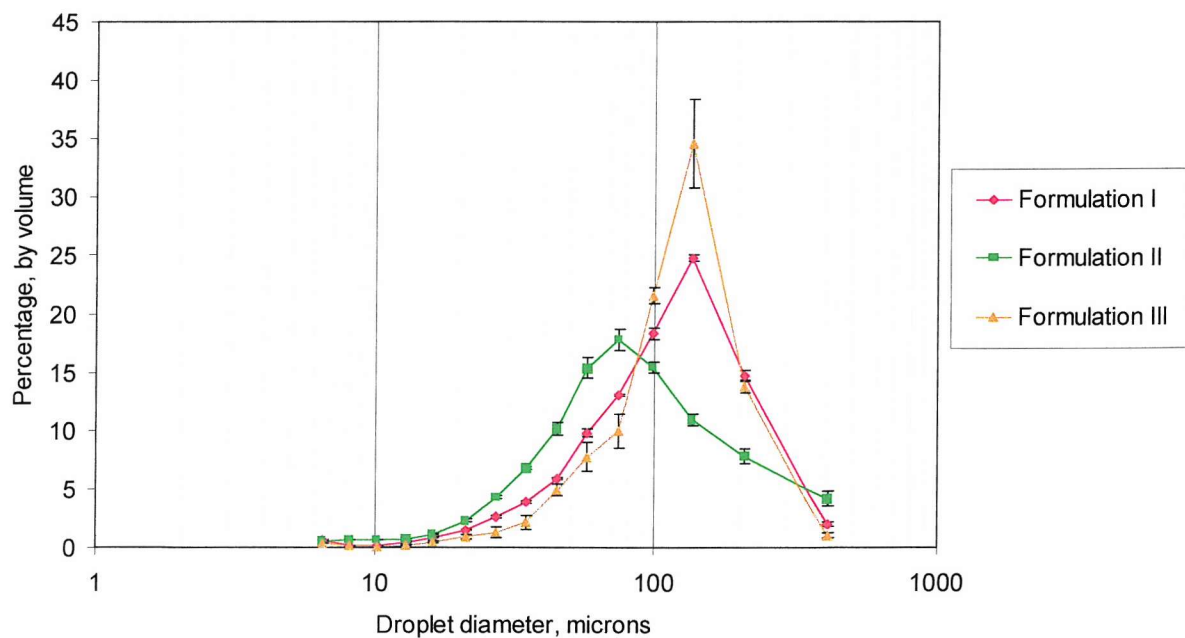


**Figure 3.10** Droplet size distribution of formulations I, II and III, showing standard error bars

The droplet size distribution of Figure 3.10 shows that formulation II generates an aerosol with a greater percentage of small droplets than the other two formulations.

Concentrations for particles of 0.3-0.5  $\mu\text{m}$  and 10.0-25.0  $\mu\text{m}$  diameter are not presented for the reasons discussed in Section 3.3.1.

### 3.3.3 Airborne Dust Precipitation by Naturally Charged Liquid Sprays of Formulation II

Figures 3.11a to 3.11e show the rate of precipitation of 0.5-0.7  $\mu\text{m}$ , 0.7-1.0  $\mu\text{m}$ , 1.0-2.0  $\mu\text{m}$ , 2.0-5.0  $\mu\text{m}$  and 5.0-10.0  $\mu\text{m}$  diameter dust particles settling naturally and after treatment with an uncharged and a naturally charged liquid aerosol. Statistical analysis was performed (ANOVA followed by Tukey test) comparing the particle concentrations at 1.5 minutes into the experiment, for each size band. For particles of 0.7-1.0  $\mu\text{m}$  and 5.0-10.0  $\mu\text{m}$  diameter, only the reduction in particle concentration achieved with the charged liquid aerosol compared with the natural settling rate of the dust was statistically significant ( $p < 0.05$ ). There was no significant difference with the uncharged aerosol. For dust particles of between 1.0-2.0  $\mu\text{m}$  and 2.0-5.0  $\mu\text{m}$  diameter the uncharged aerosol reduced particle concentration significantly ( $p < 0.01$ ) compared to the natural rate of dust settling. The further reduction achieved by the charged liquid aerosol was also significant compared to the natural rate of dust settling ( $p < 0.01$ ) and depletion by the uncharged aerosol ( $p < 0.05$ ). The droplet size distribution of the two sprays is shown in Figure 3.12, with standard error bars. This shows that the uncharged aerosol is composed of smaller droplets than the naturally charged spray.

Concentrations for particles of 0.3-0.5  $\mu\text{m}$  and 10.0-25.0  $\mu\text{m}$  diameter are not presented for the reasons discussed in Section 3.3.1.

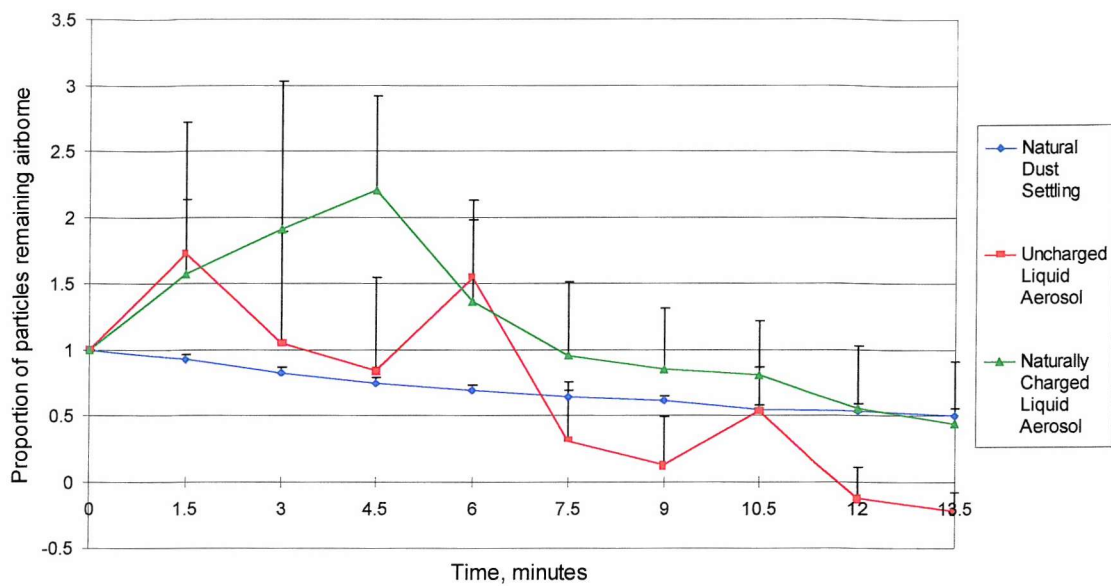


**Figure 3.11a** Depletion rates for airborne particles of 0.5 to 0.7  $\mu\text{m}$  diameter during natural settling of dust and after treatment with uncharged and naturally charged liquid aerosols of an emulsion with continuous water phase. Standard error bars shown.

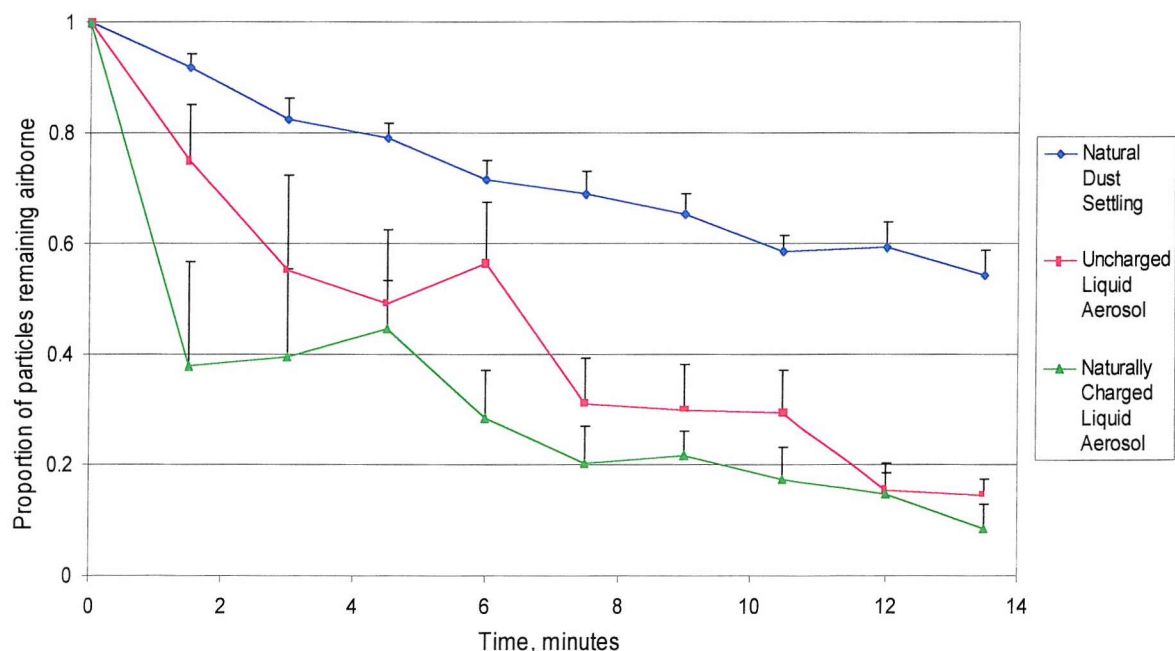


**Figure 3.11b** Depletion rates for airborne particles of 0.7 to 1.0  $\mu\text{m}$  diameter during natural settling of dust, and after treatment with uncharged and naturally charged liquid aerosols of an emulsion with continuous water phase. Standard error bars shown.

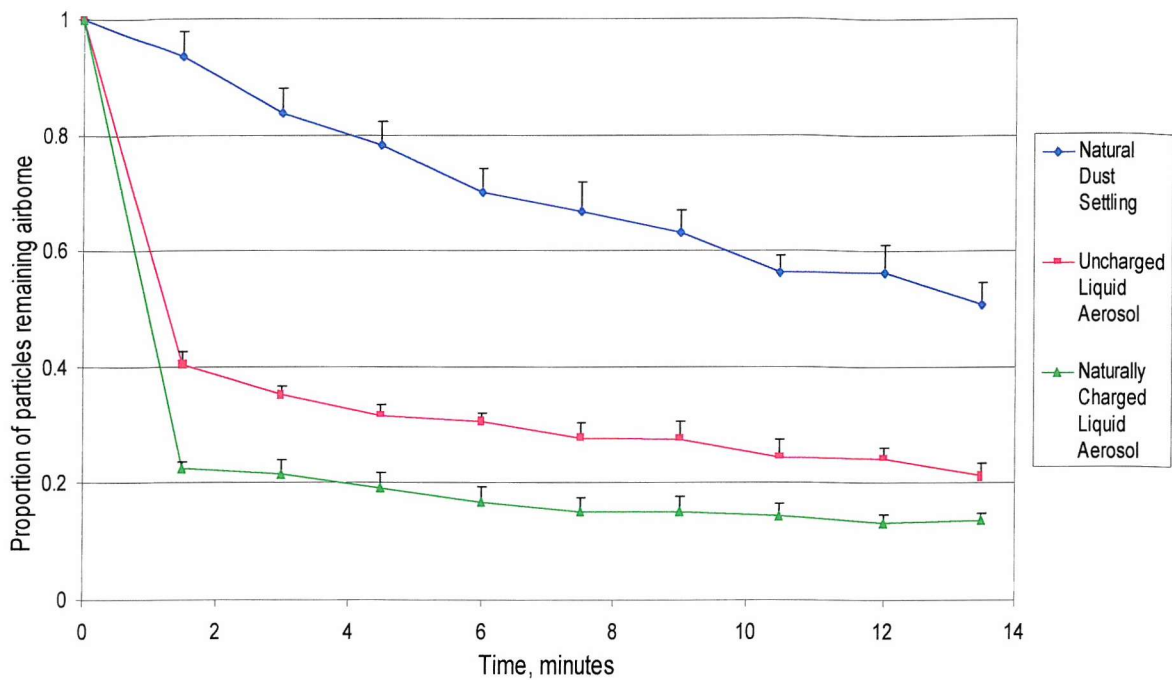


**Figure 3.11c** Depletion rates for airborne particles of 1.0 to 2.0  $\mu\text{m}$  diameter during natural settling of dust and after treatment with uncharged and naturally charged liquid aerosols of an emulsion with continuous water phase. Standard error bars shown.

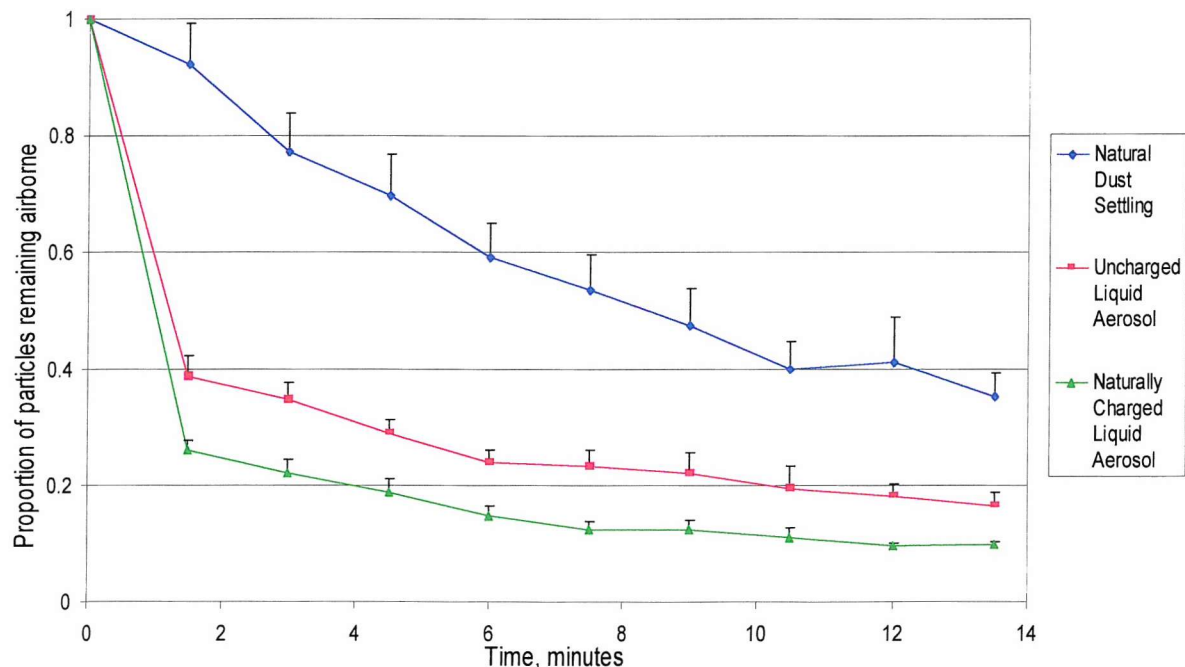


**Figure 3.11d** Depletion rates for airborne particles of 2.0 to 5.0  $\mu\text{m}$  diameter during natural settling of dust, and after treatment with uncharged and naturally charged liquid aerosols of an emulsion with continuous water phase. Standard error bars shown.

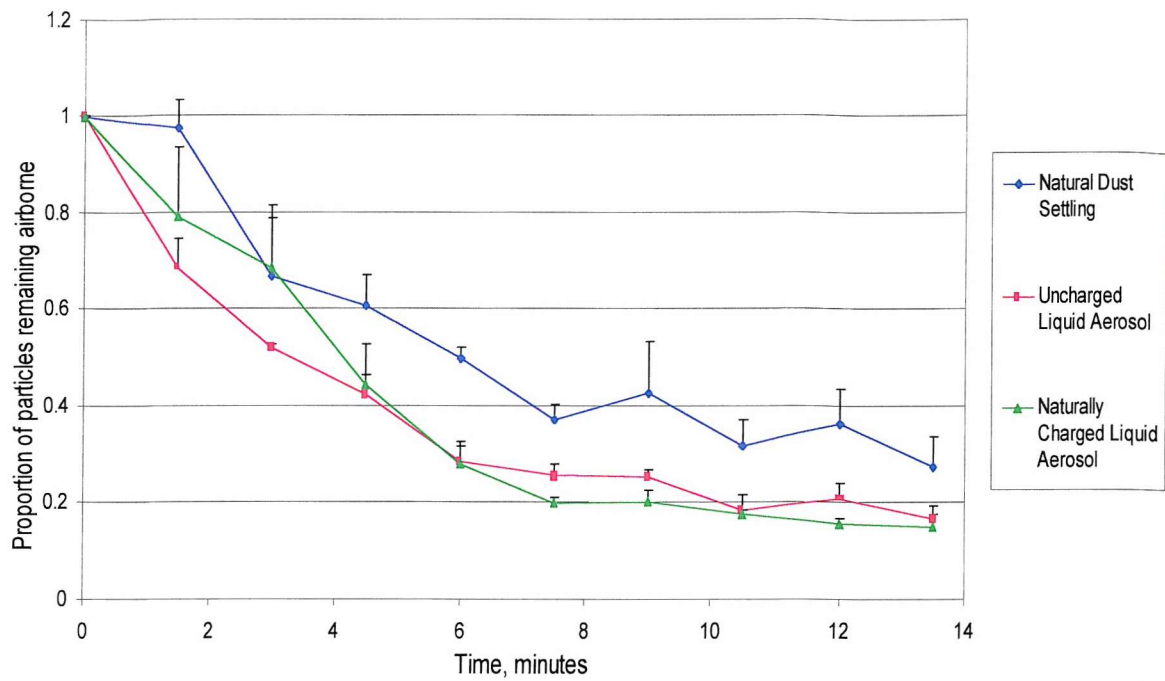


**Figure 3.11e** Depletion rates for airborne particles of 5.0 to 10.0  $\mu\text{m}$  diameter during natural settling of dust and after treatment with uncharged and naturally charged liquid aerosols of an emulsion with continuous water phase. Standard error bars shown.

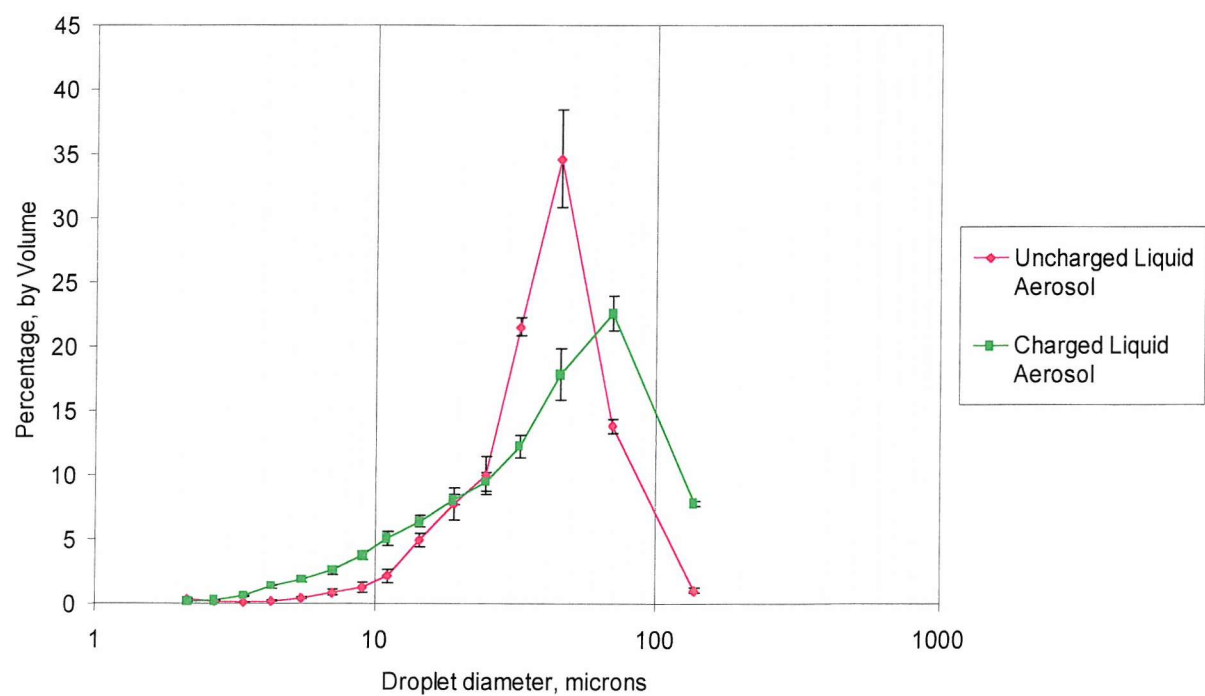


**Figure 3.12** Droplet size distribution for uncharged and naturally charged liquid aerosols, with standard error bars

## 3.4 Discussion

### 3.4.1 Precipitation of Airborne Particles

The results show that liquid aerosols have the effect of removing airborne particles, and that if the aerosol droplets carry an enhanced electrostatic charge then particle removal is increased. This effect was most pronounced for smaller particles of between 0.7  $\mu\text{m}$  and 2.0  $\mu\text{m}$  diameter. Following treatment with a charged liquid aerosol, the concentration of particles typically reduced rapidly, followed by a rate of depletion similar to that occurring naturally. Oil-in-water formulations appeared slightly more efficacious in particle precipitation than water-in-oil or alcohol-based formulation types. It is proposed that uncharged liquid aerosols remove airborne particles by contacting them through inertial impaction and interception, and removing them by sedimentation. Enhanced particle removal by charged droplets could arise by three processes: 1) improved dispersal of the aerosol within the test chamber, 2) increased contact between droplets and particles as a result of electrostatic attraction forces or 3) through reduced rebounding of particles off droplets as a result of attractive forces.

It is suggested that the uncharged liquid aerosols precipitated particles from the air mechanically, collecting them by inertial impaction and interception, and carrying them to a surface. Theory relevant to this phenomena can be found with respect to industrial pollutant scrubbers, used to remove airborne pollutant particles before air is returned to the environment. Conventional scrubbers use uncharged water droplets, which collect particles by inertial impaction. These have low efficiency for micron and sub-micron particles, because particles of this size follow the gas stream around collecting droplets, avoiding impaction (Cross, 1987, pp169; Jaworek *et al.*, 1998). If the gas stream carrying the small particles is in very close proximity to the droplet then direct interception can occur. Particle precipitation by uncharged droplets in the experiments presented was only statistically significant for particles of 1  $\mu\text{m}$  and greater in diameter, and was probably through inertial impaction.

When the liquid aerosol was highly charged, it is suggested that particle depletion was enhanced as a result of electrostatic attraction forces increasing the number of particles

collected by the droplets. Some industrial water scrubbers increase particle removal efficiency by the use of charged water droplets, often charging the pollutant particles to the opposite polarity (Cross, 1987, pp170; Jaworek *et al.*, 1998). Where the water droplets are charged, electrostatic forces can overcome inertial forces, to increase the incidence of collisions (Bertinat, 1980). Where only the liquid droplets are charged, enhanced particle collection is believed to be due to a dipole being induced on the pollutant particle in the electric field surrounding the charged droplet, resulting in Coulombic attraction (Jaworek *et al.*, 1998; Bertinat, 1980). It is also possible that particle depletion was more efficient when the liquid aerosols were charged because the electrostatic attraction reduced the incidence of particles rebounding off the droplets. This rebounding phenomenon has been observed with water droplets, and occurs as a result of high surface tension (Sumiyoshitani *et al.*, 1984). Once the dust particles are associated with the charged droplets, sedimentation of the agglomeration occurs. Electrostatic collection of particles by charged droplets in industrial scrubbers is most efficient for small particles (Jaworek *et al.*, 1998). The electrostatic attraction force increases the probability of the small particles deviating from the gas flow, resulting in interception with the droplet. As the charged liquid aerosols were found to enhance depletion of smaller particles, for example 0.7  $\mu\text{m}$  to 2.0  $\mu\text{m}$ , to a greater extent than larger ones, the proposed mechanism fits with the observed trends. Removal of larger particles in the 2.0  $\mu\text{m}$  to 10.0  $\mu\text{m}$  size range was also enhanced by charged liquid aerosol, but to a lesser extent. As particle size increased, the effect of both uncharged and charged liquid aerosols was less acute compared with the natural concentration, probably because the natural settling was faster.

Space charge effects could also contribute to the observed increase in particle removal by charged droplets, through improved dispersal of the liquid aerosol in the test chamber. Thus, the charged droplets could clean a larger volume of the air. Space charge forces would also cause particles collected by the droplets to be carried to surfaces faster, reducing concentration more rapidly.

Both uncharged and charged liquid aerosols depleted particle concentration within 3 minutes. This rate can be attributed to the naturally rapid sedimentation rate of the droplets, due to their size. The droplet size distribution was between 20  $\mu\text{m}$  to 100  $\mu\text{m}$  in diameter following atomisation (Figure 3.12), so these droplets would settle from the air more rapidly than dust aerosol 0.5 to 10.0  $\mu\text{m}$  in diameter. It is during the sedimentation of

the droplets that particle capture and removal through impaction and interception for uncharged droplets and impaction, interception and electrostatic attraction for charged droplets occurred.

There was not a large difference in particle depletion achieved by the three different formulation types, when artificially charged (Figures 3.9a to e). All reduced particle concentration below the natural level, but there was no statistically significant difference between the formulations for particles of 0.7  $\mu\text{m}$  to 5.0  $\mu\text{m}$  and 5.0  $\mu\text{m}$  to 10.0  $\mu\text{m}$  in diameter. There was a trend for the oil-in-water emulsion to achieve greater depletion than the alcohol-based and water-in-oil emulsion, and reduction of particles of between 0.5  $\mu\text{m}$  to 0.7  $\mu\text{m}$  was significantly enhanced. This difference could be accounted for by droplet-particle interaction or by droplet size effects. It has been observed that charged droplets can collect particles that are both wettable and non-wettable (Sumiyoshitani *et al.*, 1984). If the particles are wettable by the formulation they are absorbed into the droplets, while if they are not wettable, then they are held on the surface, occasionally forming dendrites if many particles are collected. This suggests that the type of formulation would not greatly influence whether particles are collected by the droplets or not. Droplet size is more likely to influence this, as observed in industrial scrubbers where smaller droplets show greater efficiency than larger ones (Jaworek, *et al.*, 1998). As the droplet size distribution of the oil-in-water formulation was smaller than that of the other two formulations (Fig. 3.10), this could account for the difference in particle removal. In addition to the initial droplet size, the rate of evaporation will determine the size distribution over time, and this could be different for the three formulations.

Enhanced particle depletion was observed when the liquid aerosols were charged artificially (using a voltage source), and subsequently when charged naturally during the atomisation process. The mechanisms involved in particle depletion by naturally charged droplets are expected to be the same as for artificially charged aerosols. The level of depletion by the naturally charged droplets (Figures 3.11a to e) appeared to be higher than that achieved by artificially charged droplets of the same formulation (Figure 3.9a to e). For example, the concentration of 1.0 to 2.0  $\mu\text{m}$  diameter particles was reduced to about 80% of the original concentration by artificially charged formulation II (Figure 3.9c), while the naturally charged formulation II reduced concentration to about 23% (Figure 3.11c). The charge-to-mass ratio of the former was  $-2.7 \times 10^4 \text{ C.Kg}^{-1}$ , while for the latter it was a

lower at  $-1.4 \times 10^{-4}$  C.Kg $^{-1}$ . Therefore, the greater particle depletion achieved by the naturally charged aerosol can not be due to a higher q/m because it was lower than that achieved by the use of a voltage supply. All conditions except the source of dust were the same in the two experiments. The naturally charged liquid aerosol had a greater percentage of larger droplets than the artificially charged aerosol, and this factor could also not account for the better performance of the naturally charged liquid aerosol.

Removal of airborne dust particles by charged liquid aerosol, in the manner shown here could be of particular benefit in the domestic environment. Local depletion of particles (including bioaerosols) could be achieved immediately following the domestic activities that re-entrain settled dust. As particle removal is most efficient for micron and submicron particles, this technique would be particularly useful for the immediate reduction of cat allergen (Fel d1), which is largely associated with particles of  $<2.5$   $\mu\text{m}$  diameter (Luczunska *et al.*, 1990). The larger particles disturbed during domestic activities, such as Der pI, could also be depleted using this technique.

### 3.4.2 Assessment of Investigation

This protocol gave an objective comparison of particle settling rates achieved by liquid aerosols, although there was often considerable variation in the data. This level of variation made statistical analysis and interpretation of the results complicated. Several sources of error can be identified in these experiments. Differences in dust aerosol composition may have arisen through variation between aliquots, different cohesion or agglomeration characteristics due to the effects of relative humidity, differences in aerosol generation and differences in air movement and replacement during sampling. The liquid aerosol is also a source of variation. There could have been some particle loss during sampling, due to particles adhering to the inner surface of the tubing leading into the particle counter. This would be especially true for the charged particles, which would experience electrostatic attraction forces towards the tubing.

As the APC counted both solid and liquid aerosols, it was impossible to assess the number of airborne dust particles alone. Correction of the data to account for this probably introduced more variation into the data and is another source of error. The correction is

based on the assumption that the number of droplets in a spray of liquid aerosol can be accurately estimated, and is proportional to the mass of the liquid dispensed. It also assumes that the presence of a high concentration of dust particles during the experiments does not influence the number of liquid droplets counted.

A comparison, using the same methodology, with portable air cleaners would have been useful. This would have allowed comparison of the rates of particle depletion and overall efficacy, by which to rate the usefulness of charged liquid aerosols for this application.

### 3.4.3 Areas for Further Investigation

This research could be extended to study the effect of liquid aerosols generated by pressure-pack dispensers on the concentration of airborne allergens in particular. This could produce more accurate data than the particle count method used in this investigation, because the complications caused by the liquid aerosol would not influence the results. The effect on tobacco smoke particles could also be measured, as it can be expected that these also can be removed by charged droplets.

## Chapter 4

---

### Bioefficacy of Electrically Charged Insecticide Aerosols Generated by Pressure-pack Dispensers

#### 4.1 Introduction

Hand-held pressure-pack sprays, of the type used against flying insects in the domestic environment, were first developed in the 1940's for use during the Second World War (Goodhue and Sullivan, 1943). Since that time significant improvements have been made, making them smaller, lighter and cheaper, with optimised spray characteristics (Sanders, 1970). An increasing knowledge of the influence on insecticide efficiency of droplet size, use of synergists and the effect of different solvents (White *et al.*, 1992; Tsuda *et al.*, 1988) has been used to increase the efficiency of insecticide sprays. One factor which has the potential to produce further improvements in efficacy however, and which has not yet been considered in the context of domestic applications, is the effect of electrostatic charge.

The characteristics of charged aerosols would be expected to confer improvements in the deposition efficiency of domestic insecticide sprays onto insects. Charged aerosols would exhibit an attractive force between the droplet of insecticide and the insect in flight,

and demonstrate wider spatial distribution. These effects have been observed during experiments with artificially charged agricultural pesticide sprays in enclosed spaces (Inculet *et al.*, 1984). In this study, deposition was significantly enhanced by the charged sprays in the upper portions of the enclosure, resulting in significantly improved immediate and residual efficacy of the insecticide against insects. In agricultural applications of charged sprays, charge-to-mass ratios of between 1 and  $5 \times 10^{-4}$  C.kg<sup>-1</sup> have been observed to enhance the deposition under laboratory and field conditions (Splinter, 1968). Higher charge-to-mass ratios between 1 and  $5 \times 10^{-3}$  C.kg<sup>-1</sup> have also been used (Giles *et al.*, 1992).

This chapter describes investigations into the effect of highly charged domestic pressure-pack insecticides on the rate of knock down and mortality. Bioassays were selected to investigate the effect on efficacy in the two most common applications of hand-held pressure-pack dispensers, namely for direct spraying of flying insects, and for space-spray treatments. Tests were conducted using the two most frequently targeted insects: houseflies and mosquitoes.

#### 4.1.1 Domestic Pressure-Pack Insecticide Sprays

The active ingredients employed in domestic insecticide sprays are almost exclusively pyrethroids. The bulk of these are synthetic pyrethroids such as allethrin, resmethrin and phenothrin, but occasionally natural pyrethrins are incorporated into the formulation. The natural pyrethrins have been extracted for their insecticidal properties from the flower heads of *Chrysanthemum cinerariaefolium*, for centuries. Pyrethrum powders were introduced to Europe during the early 19th century, and subsequently to the United States in 1860 (Gnadinger, 1936). The first successful synthetic Pyrethrum analogues were developed during the 1970's (Elliott *et al.*, 1973); the advantage of these over their natural counterparts is significantly improved photostability, with higher levels of insect mortality and low mammalian toxicity.

Pyrethroid insecticides are particularly well suited to domestic usage for a number of reasons. As broad spectrum residual contact insecticides they affect a large number of insect species, yet demonstrate very low mammalian toxicity. In addition, the mode of

action causes rapid knockdown with little recovery, using low concentrations of active ingredient. These characteristics enable a quick and effective result to be achieved from a product that is relatively safe to use.

Within the insect, pyrethroids target the central and peripheral nervous systems. The symptoms of pyrethroid poisoning are always characterised by rapid paralysis, a condition termed 'knockdown' (Sawicki, 1962). For some pyrethroid compounds knockdown may be reversible due to metabolic degradation (Burt and Goodchild, 1974), although in modern synthetic compounds this problem has been overcome, and recovery is rare (Elliott *et al.*, 1978).

Synergistic compounds, such as piperonyl butoxide or sulfoxide, are often combined with pyrethroid insecticide products to augment performance. Pesticide synergists are compounds that are non-toxic at the concentration employed, but which significantly enhance the toxicity of the pesticide. They are believed to function primarily by interfering with the process of *in vivo* detoxification (reviewed by Yamamoto, 1973). The appropriate addition of synergists can significantly reduce knockdown times, and allow pyrethroid concentrations to be reduced. Many other factors associated with formulation of the insecticide and the method of delivery also influence the rate of knockdown. Some of these will now be discussed.

#### 4.1.2 Factors Which Influence the Rate of Knockdown

The speed of knockdown is dependent upon a number of inter-related factors, including insect type, environmental, formulation and application effects, which influence the dose of insecticide collected by the insects (White *et al.*, 1992). The size and shape of the insect can be important in determining the dosage received. For example, the large surface area to volume ratio of flies and mosquitoes explains the rapid knockdown observed for these insects, when compared to knockdown of cockroaches (Miller and Adams, 1982). Temperature is another important factor, especially when considering pyrethroid insecticides that demonstrate a negative temperature coefficient (Blum and Kearns, 1956; Miller and Adams, 1982). Environmental temperature and humidity also influence the rate of droplet evaporation, and thus the availability of the insecticide over time.

The nature of the solvent is influential in determining the rate of knockdown and kill of flying insects. The solvent can affect the penetration of active ingredients through the insect cuticle to the target site, the initial size of droplets and their evaporation rate. Certain solvents have been demonstrated to penetrate the insect cuticle more efficiently than others do. For example, Wickham *et al.* (1974) demonstrated with cockroaches that water based formulations give a depressed rate of knockdown when compared to formulations containing hydrocarbon solvents. Specifically studying hydrocarbon solvents, Hadaway *et al.* (1976) found that volatile, short chain molecules penetrate the insect cuticle more effectively than less volatile long chain molecules.

White *et al.* (1992) showed that knockdown and mortality responses to insecticides are directly related to the dose collected, and that this is a function of the aerial concentration and the droplet size at exposure. Larger droplets impact with insects in flight more efficiently than smaller droplets, due to their greater inertia, but cannot maintain a high aerial concentration, and do not distribute evenly within a room or test chamber (Tsuda *et al.*, 1988). In a bioassay, this translates into a fast rate of knockdown but low mortality response, because some insects initially collect a high dose and become knocked down, but a proportion of the insects will not receive a lethal dose before the insecticide has settled from the air. Conversely, small insecticide droplets demonstrate a slower knockdown response, as the initial doses received are lower, but mortality is high as insects acquire an increasing dose through constant exposure (Tsuda *et al.*, 1987). White *et al.* (1992) found that during a standard bioassay, 95% of the dose collected by the test insect population was a result of flight through the spray cloud, rather than by passive contact with surfaces. It was also shown that insecticide collected during the initial flight (from the release point to the wall) could account for up to 47% of the final mortality. Therefore, the initial flight through the spray cloud at its most concentrated contributes significantly to exposure, but continued flights during the course of a bioassay are necessary for high mortality, and contact with residual insecticide is not likely to contribute significantly to the collected dose (White *et al.*, 1992).

The optimum droplet diameter of an oil-based spray was found by Tsuda *et al.* (1987) to be in the region of 30 $\mu\text{m}$  for the knockdown and kill of houseflies, and slightly smaller for mosquitoes. In this study the diameter of droplets was measured 300 mm from the actuator. Subsequent evaporation of solvent from the droplets would cause a reduction

in diameter, and it is the size of the droplet when it reaches the insect that is of critical importance, not its size when generated.

Aerial concentration as a function of droplet size is complicated due to the evaporation of the spray droplets, according to the characteristics of their solvent. Tsuda *et al.* (1988) found that the rate of settling for airborne spray droplets could not be predicted accurately according to Stokes law, because droplet size decreased rapidly as a result of solvent loss. The settling period of droplets was prolonged, and insecticidal actives remained airborne and available for collection.

#### 4.1.3 Considerations for the Assessment of Electrostatically Charged Insecticides

When comparing the bioefficacy of charged and uncharged insecticide droplets, by quantifying the knockdown response of flying insects, it is clearly very important to also consider other characteristics of the spray cloud. Droplet size, spray rate, cone angle and the throw of the aerosol may be altered during the process of enhancing the charge, by the changes made to the valve and actuator components of the pressure-packs (Sanders, 1970). Differences in these factors could affect the rate at which the droplets disperse into the chamber, the interaction between the droplets and the insects and the time the droplets remain airborne.

Droplet size distribution could be affected when droplets are charged, if the charge-to-mass ratio approaches the Rayleigh limiting charge. This is the maximum charge that a droplet can attain before the outward mutual repulsion force caused by the charge overcomes the stabilising surface tension force. When the Rayleigh limit is exceeded the droplet disrupts to form smaller droplets. Although a droplet may not be close to the Rayleigh limit when formed, the process of solvent loss through evaporation may cause this to be attained during flight. This may cause the production of fine aerosol droplets.

When analysing the effects of charge on the deposition and resulting knockdown rates and mortality achieved by uncharged and charged insecticide sprays, these factors must be considered. Unless spray characteristics are similar, observed differences may not be wholly attributed to the influence of charge.

#### 4.1.4 Application of Electrostatic Spraying in Agriculture

The potential application of electrostatic charge for spraying pesticides has been considered with respect to agriculture since the 1960's (Splinter, 1968), and of the devices investigated to date all use high voltage to generate the charged spray cloud (Reviewed by Matthews, 1989). The use of this concept for domestic pressure-pack insecticides has not previously been considered, and generating the required level of charge by natural processes is apparently unexplored.

Research and development into electrostatic spraying of agricultural pesticides did not begin seriously until the late 1960's (Splinter, 1968). Traditionally, agricultural pesticides are applied to the crop through hydraulic nozzles, which is extremely inefficient. Pimentel and Levitan (1986) estimated that less than 1% of the active ingredient sprayed impinges onto target insects in the foliage. Deposition studies comparing conventional spray systems with equivalent electrostatic sprayers commonly demonstrate more even distribution of pesticide (Inculet *et al.*, 1981), enhanced foliar deposition and reduced contamination of non-target surfaces (Giles *et al.*, 1992) with the latter. These characteristics of charged insecticides have been shown to increase mortality of pest insects in some glasshouse and field crops, although other field trials have not demonstrated improved pest control (Matthews, 1989).

Hydraulic application systems rely upon inertial forces, diffusion and gravity to impact droplets onto vertical surfaces in the crop, while air movements and thermal convection can carry small droplets onto horizontal surfaces (McCartney and Woodhead, 1983). When employing high-voltage electrostatic spraying techniques, deposition of the droplets is also influenced by image forces, space charge forces and the electric field between the crop and the nozzle (McCartney and Woodhead, 1983).

Image-force attraction is believed to increase deposition onto the foliage of an idealised crop by a factor of at least two (McCartney and Woodhead, 1983). Space charge forces are predicted to significantly enhance deposition in the upper canopy of an orchard crop, as a result of the expansion of the charged insecticide cloud (Castle and Inculet, 1983). An electric field also exists between the charged nozzle of the spray machinery, and the grounded crop. Charged droplets can migrate under the influence of this field, but as the nozzle is adjacent to the crop for only a short period of time, this mechanism is not believed to be significant in enhancing deposition (Castle and Inculet, 1983).

Like conventional applicators of agricultural pesticides, hand-held pressure-pack insecticide dispensers for domestic use rely upon inertial, diffusion and gravitational forces to bring droplets into contact with target flying insects. Electrostatic charge is predicted to increase the probability of droplets impinging on target insects by space charge forces and polarisation effects. Image charge forces cannot be involved, as the insects are electrically isolated in flight.

#### 4.1.5 Problems Associated With Domestic Flying Insects

In the domestic environment flying insects can be considered as a nuisance, as a sign of poor hygiene and can also be of medical importance, acting as vectors of disease and contaminating human food with pathogens. For these reasons, control of insects in the home is desirable, and pressure-pack insecticides are a convenient and common method of doing so. Common insects and arachnids found in the domestic environment include houseflies, mosquitoes, cockroaches, bees, wasps, ants, spiders, mites and fleas. Considering the immense diversity and number of insect species, however, comparatively few frequent the domestic environment and fewer still cause any annoyance or harm (Crosskey and Lane, 1993). Houseflies and mosquitoes are among the most frequent and annoying.

Mosquitoes are ubiquitous. In addition to their status as one of the most irritating biting insects, they are also responsible for transmitting a variety of diseases to man, including Malaria, Dengue and Yellow Fever (Service, 1993). For personal protection against bites, nets and chemical repellents are available, while insecticide sprays can be effectively used to reduce insect numbers temporarily. Since mosquitoes can breed profusely in almost any area of static or stagnant water, there is usually a source for constant invasion, which cannot be avoided without the implementation of large-scale control procedures.

Synanthropic flies (those associated with human habitations) can be annoying in the home, but also have the potential to mechanically transmit pathogens as a result of the habit of feeding on rubbish, excrement, carrion and sewage, as well as on human food. Although many human pathogens have been isolated from the house-fly, *Musca domestica*, including hepatitis, *Salmonella*, *Shigella* and pathogenic *Escherichia coli*, there is little evidence that

*M. domestica* plays any role in disease transmission (Crosskey and Lane, 1993). Breeding sites remote from houses act as sources from which insects will continuously invade, so most domestic control measures are short term.

#### 4.1.6 Objectives

The research presented in this chapter explores the possibility that if the droplets produced by pressure-pack insecticide dispensers are electrostatically charged, increased deposition onto flying insects would occur, resulting in improved bioefficacy. This was investigated initially by quantifying the deposition of charged and uncharged aerosols onto electrically isolated targets, using a fluorometric assay. The term ‘uncharged’ is used to describe sprays that have a low charge-to-mass ratio, which is not expected to influence the behaviour of the droplets, and to distinguish them from those with an elevated charge-to-mass ratio (referred to as ‘charged’). The hypothesis being tested was that highly charged insecticide aerosols deposit an enhanced volume onto insects, compared to uncharged aerosols. This being so, standard bioassays with houseflies (*Musca domestica*) and mosquitoes (*Culex quinquefasciatus*) were used to investigate whether the enhanced deposition translated into increased rates of knockdown and kill. When interpreting the results from these experiments it is important to consider other characteristics of the insecticide droplets that could be altered when generating charged droplets. Droplet size distribution and spatial distribution would also affect efficacy.

## 4.2 Materials and Methods

### 4.2.1 Culture of Houseflies, *Musca domestica*

Houseflies, *Musca domestica*, were maintained in laboratory cultures in the insectaries of CERIT (Centre for Entomological Research and Insecticide Technology), University of New South Wales, Sydney, Australia. The cultures originated from field collections made within the previous 12 months. Insectory cages measured 600 × 600 × 600 mm, and were constructed from metal frames over which cotton gauze was stretched. Adult flies were provided with water and a solid diet composed of sucrose, milk powder and yeast powder. Water and food was checked daily, and replenished when depleted or spoilt. A small container with dampened cotton wool was provided daily for oviposition, when the adults were more than 7 days old. Eggs were transferred to larval medium, which consisted of 2500 ml of bran, 250 ml of milk powder and 30 ml of yeast powder, mixed with 450 ml of water. All life stages were maintained at a temperature of 23 ± 2°C.

### 4.2.2 Culture of Blow Flies, *Calliphora* species

Blow flies, *Calliphora* species, were reared from larvae as required in the insectaries of the University of Southampton, UK. Larvae were obtained from a fishing bait retailer ('Homestores', Swaythling, Southampton, Hampshire), so were of an indefinite strain and had been refrigerated. *Calliphora* species were only used in experiments that would not be sensitive to variation in the behaviour of the insects or their susceptibility to insecticides, because these factors were not standardised.

The larvae were placed in a substrate of moist peat, and pupated after 3 to 5 days. The larval and pupal stages were misted daily with distilled water until the adult flies emerged. Insectory cages measuring 600 × 600 × 600 mm, constructed from metal frames over which cotton gauze was stretched, were used to house the adult flies. These were provided with water and a solid diet of 3 parts sucrose to 1 part yeast powder. Food and water was checked daily and replenished or replaced when depleted or spoilt. All life stages were maintained at a temperature of 23 ± 2°C.

#### 4.2.3 Culture of Mosquitoes, *Culex quinquefasciatus*

Mosquitoes, *Culex quinquefasciatus*, were raised in the insectaries of CERIT (Centre for Entomological Research and Insecticide Technology), University of New South Wales, Sydney, Australia. Insectory cages measured 600 × 600 × 600 mm, and were constructed from metal frames over which fine cotton mesh was stretched. Temperature was maintained at 26 ±1 °C and humidity at 75%. To stimulate egg-laying, female mosquitoes were blood-fed from an anaesthetised mouse. This was conducted in the laboratories of CERIT, under permit issued by the Animal Care and Ethics Committee (ACEC) of Australia. Small dishes 3/4 filled with water were then placed into the mosquito cages, and eggs were laid 2 to 4 days later. Eggs were laid in raft-shaped masses approximately 2 to 3 mm long, which floated on the surface. These egg rafts, which contain between 20 and 100 viable eggs, were then placed into large clean tanks, filled to a depth of around 25 mm with de-ionised water. 3 to 4 pond sticks (TetraPond Floating Pond Sticks) were added to the water to provide food for the larvae when they hatched. When the larvae had hatched the surface of the water was de-scummed and more pond sticks added occasionally. Mosquitoes were sexed at the pupal stage, to provide test cages consisting of females only. Female pupae are obviously larger than male pupae, and often pupate later than the males. The female pupae were removed from the larval container and released into a small container of deionized water. These containers were then placed into insectory cages until the adult mosquitoes emerged. The adults were fed on 10 % sugar solution, which was presented in small plastic cups with lids, through which dental wicks were pushed so the bottoms were in the sugar water. All-female cages were used for testing, but it was also necessary to make up some breeding cages containing males as well as females.

#### 4.2.4 Specifications of Pressure-pack Insecticide Sprays

The water-in-oil emulsion (formulation III) described in Table 2.1 was used for the experiments in this chapter. Synthetic pyrethroid insecticides were added to this

formulation at a concentration of less than 1% (0.241% Bioallethrin and 0.046% Bioresmethrin). The pressure-packs were prepared and supplied by Reckitt and Colman Products Pty Ltd, Australia in three-piece tinplate, welded side-seam cans. The valve comprised a 3.00 mm polypropylene dip tube, 1.27 mm housing orifice, 0.64 mm vapour phase tap and 2 × 0.61 mm stem holes. The uncharged spray had a one-piece overcap actuator with a 0.85 mm diameter orifice, shown in Figure 2.3. A naturally highly charged equivalent was generated using a two-piece button-style actuator (Figure 2.3) with the novel actuator orifice, design B described in Figure 2.5.

#### 4.2.5 Measurement of Charge-to-Mass Ratio

The charge-to-mass ratio of liquid aerosols was measured according to the method in Section 2.2.6. For the experiment described in Section 4.2.6 high voltage was used to artificially increase the charge-to-mass ratio of the insecticide. This was achieved according to the method described in Section 3.2.4

#### 4.2.6 Deposition of Highly Charged Insecticide Sprays onto Tethered Flies

Blow Flies, *Calliphora* species, of between 3 and 7 days post emergence were killed by freezing at -20 °C for at least 30 minutes, then allowed to reach room temperature again. Individual flies were attached using a fine entomological pin to an electrically insulating plastic support, positioned 1.8 m from the can holder (Figure 3.7). Fluorescein (Sigma F7505) was added to the standard formulation described, at a concentration of 0.05% w/w. The dispenser was located in the can holder, such that the tethered insect was central in the plume. This apparatus is illustrated in Figure 4.1. The pressure-pack was actuated for approximately 2 seconds, delivering  $4.4 \pm 1.0$  grams of insecticide formulation. The tethered fly was immediately removed from the support, and placed in 5 ml of cold phosphate buffer solution, pH 6.8 (0.1M  $\text{Na}_2\text{HPO}_4 + \text{NaH}_2\text{PO}_4 \bullet \text{H}_2\text{O}$ ). The buffer was stored in the dark at 4 °C for 24 hours, for the fluorescein to elute, after which time the fly was removed with clean forceps. This solution was stored in the dark at 4 °C until analysis

could be performed. The procedure was performed with no voltage applied (uncharged spray) to the can during actuation, and with +10kV (positively charged spray) and -10kV applied (negatively charged spray), according to the method described in Section 3.2.4. At least 10 replicates were performed for each treatment.

A control solution for the fluorometric assay was prepared by repeating the procedure described, without dispensing any insecticide. The fly and solution were treated in the same manner as for the test solutions.

Calibration of the fluorometric assay was achieved by applying 10 $\mu$ l of the insecticide formulation to a prepared fly, and placing this in 5 ml of cold phosphate buffer solution. As before, this solution was stored in the dark at 4 °C for 24 hours, before removing the fly. From this, four dilutions were prepared: 1/2, 1/5, 1/10 and 1/50. Ideally a range of volumes between 0.1 and 5.0  $\mu$ l, of formulation would have been applied to, and eluted from flies, but these volumes could not be accurately measured using the equipment available. The minimum volume that could be accurately measured was 10 $\mu$ l.

The fluorescein test solutions were analysed using a luminescence spectrophotometer (Perkin-Elmer LS3-R), operating at 473 nm excitation and 562 nm emission wavelengths. The control solution was used to set the zero, against which the absorbency of the test solutions were measured.

A calibration graph was generated using the fluorescence values for the solutions containing known volumes of the formulation. By extrapolation, the volume of insecticide formulation deposited on each fly was then calculated. The volume derived for each fly was divided by the mass of insecticide product dispensed for that fly, to give the volume of insecticide deposited for each gram dispensed. The mean volume of formulation deposited per gram dispensed was calculated for the uncharged, negatively charged and positively charged sprays.



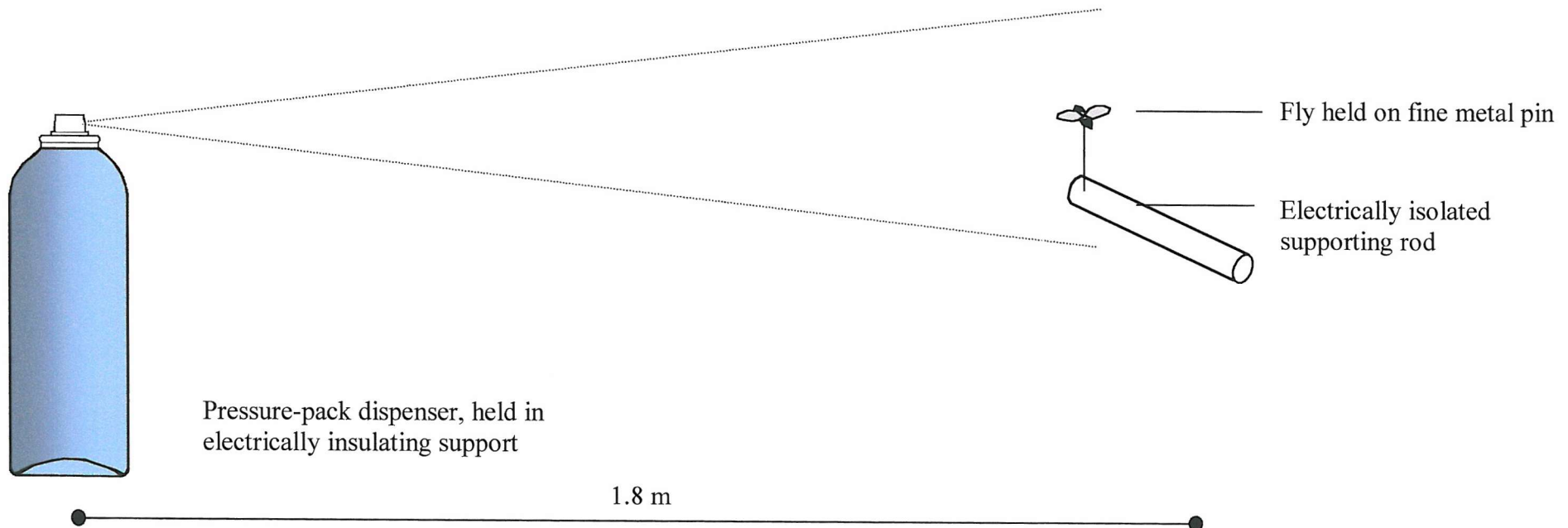


**Figure 4.1** Schematic illustration of apparatus used to quantify liquid aerosol deposition onto electrically isolated flies.

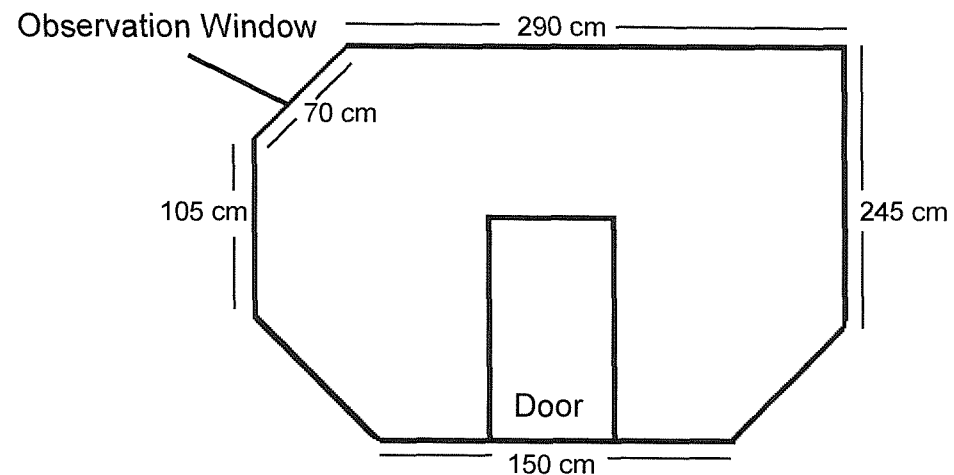
#### 4.2.7 Assessment of Knockdown and Mortality - Direct Spray Protocol for Houseflies

Knockdown and mortality of houseflies, *Musca domestica*, was assessed for the uncharged and charged sprays described in Section 4.2.4, according to the CERIT direct spray protocol CE/HF-HM/FIK 2.0 01/08/96. Experiments were conducted under direction at CERIT, University of New South Wales, Sydney, Australia. The direct spray protocol was designed to simulate domestic use, in which insecticides are aimed at flying insects. This protocol was used as the automated procedure provides consistent, reproducible measurements. A microcomputer controlled the key functions of the procedure, by automatically actuating the dispenser during calibration and during the assay, automatically triggering the release of insects, prompting the operator to make counts of knockdown at appropriate intervals, and by timing and switching on the exhaustion system.

The test chamber was 3.82 m long, 3.33 m wide and 2.47 m high, and the lower third of the walls sloped inwards to reduce the floor area on which the insects fell. The test chamber is shown in Figure 4.2. Each replicate used at least 50 healthy houseflies (*Musca domestica*) at 3-7 days post emergence and of a mixed sex ratio (approximately 1:1). The flies were collected from the rearing cages, using a low powered suction device, directly into the plastic containers from which they would be released during the experiment.

The delivery rate of each dispenser was calibrated by actuating for approximately 2 seconds, and dividing the mass sprayed during this period by the precise duration of the spray. The computer automatically controlled actuation and timing of this operation. The dispenser was positioned in the test chamber, adjacent to the door, and centrally in the width of the room. The actuator of the dispenser was 0.22 m from the wall and 0.70 m from the ceiling. The insects were released from a position 1.80 m in front of the can, and 0.22 m above the level of the actuator (position A).  $2.0 \pm 0.2$  grams of insecticide formulation were sprayed into the room, and the flies released  $2.0 \pm 0.1$  seconds after completion of the spray. These operations were controlled and timed by the microcomputer. Knockdown was evaluated visually from outside the test chamber via a viewing window, at 0.5, 1.0, 1.5, 2.0, 2.5, 3.0, 4.0, 6.0, 8.0 and 12.0 minutes. The operator did not enter the chamber during the experiment. A minimum of 5 replicates were performed for each dispenser combination. The order of testing of the dispensers was randomised.

Transverse View of Bioassay Chamber  
(Not to scale)



Aerial View of Bioassay Chamber  
(Not to scale)

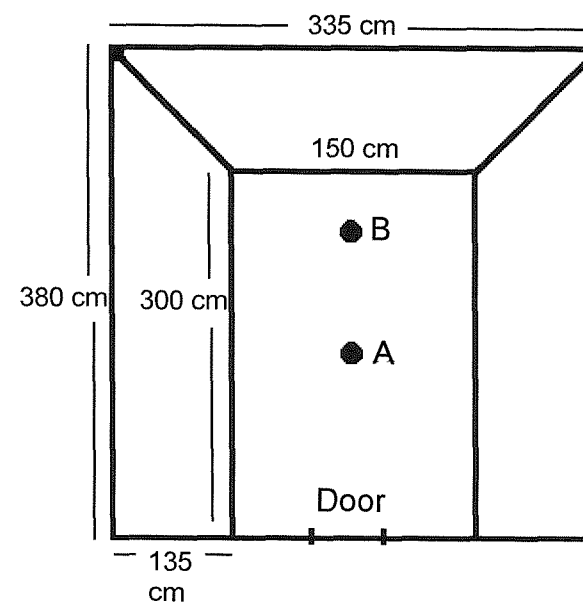


**Figure 4.2** Schematic diagrams of the chamber used for the direct and space spray bioassays, showing dimensions and fly release positions A and B in aerial view

Following each test the insects were carefully collected into recovery chambers. Insects that had been knocked down were gently swept using a soft brush, while any still in flight were caught using a butterfly net. The flies were held at  $25.0 \pm 2.0$  °C for 24 hours, and supplied with food and water. After this time mortality was recorded.

The test chamber was evacuated after each test for at least 15 minutes by a ceiling vent pumping air at approximately 10 cubic metres per minute. To check for contamination of the test chamber a control test was performed following the final test of each day. This was conducted by repeating the above procedure without spraying any insecticide into the chamber. The room was considered contaminated if more than 10 % of the insects were knocked down at the end of the test, and in this case all results performed during the day were discarded. The chamber was subsequently cleaned by washing the walls with a solution of detergent ('Pyroneg', Diversey) and re-tested for contamination. The results of any individual test were also discarded if the specified quantity of formulation delivered was exceeded.

#### 4.2.8 Assessment of Knockdown and Mortality - Space Spray Protocol for Houseflies

Knockdown and mortality of houseflies, *Musca domestica*, was assessed for the uncharged and charged sprays described in Section 4.2.4, according to the CERIT space spray protocol CE/HF-HM/FIK 1.0 01/08/96. These experiments were conducted, under direction, at CERIT, University of New South Wales, Sydney, Australia. The space spray protocol was designed to simulate the use of domestic pressure-pack insecticides in which the room is sprayed in general, rather than insects being targeted.

The space spray protocol was conducted in the same chamber, and the pressure-packs calibrated in the same manner as for the direct spray protocol (Section 4.2.7). At least 50 healthy houseflies of 3 to 7 days post emergence, and of mixed sex ratio (approximately 1:1) were used for each replicate. These were prepared as in the direct spray protocol.

The dispenser was positioned in the test chamber as previously described. The release position of the flies was altered to a location central in the width of the room, 0.7 m above the floor and 3.0 m in front of the actuator of the dispenser (position B in Figure

4.2). 2.0 ± 0.2 grams of insecticide formulation were sprayed, and the flies released 10.0 ± 0.1 seconds after the end of this spray. Knockdown was evaluated visually from the viewing window of the test chamber at 1, 2, 3, 4, 5, 6, 8, 12, 16 and 20 minutes after the release of the flies. The operator did not enter the chamber during the test. A minimum of 5 replicates were performed for each dispenser. The order of testing for the formulations was randomised.

At the end of the test the insects were carefully collected and placed in a recovery chamber as in the direct spray protocol (Section 4.2.7). Mortality was assessed after 24 hours. Following the final test of the day a contamination test was performed, as described in Section 4.2.7.

#### 4.2.9 Assessment of Knockdown and Mortality - Space Spray Protocol for Mosquitoes

Knockdown and mortality of mosquitoes, *Culex quinquefasciatus*, was assessed for the uncharged and charged sprays described in Section 4.2.4, according to the CERIT space spray protocol CE/HF-HM/FIK 1.0 01/08/96, as described in Section 4.2.8. The mosquitoes were raised as described in Section 4.2.3, and each test used at least 50 insects. At least 5 replicates were performed for each dispenser.

#### 4.2.10 Quantification of Spray Characteristics

As characteristics of the aerosol can alter the effect of an insecticide on insects in a bioassay, it is important to consider any differences between the spray patterns of pressure-packs when comparing them. The characteristics measured were the spray rate, cone angle, throw and droplet size distribution, as illustrated schematically in Figure 4.3. The spray characteristics were measured for the uncharged and naturally charged liquid aerosols used in experiments 4.2.7, 4.2.8 and 4.2.9. The following methods give approximate values for these parameters.

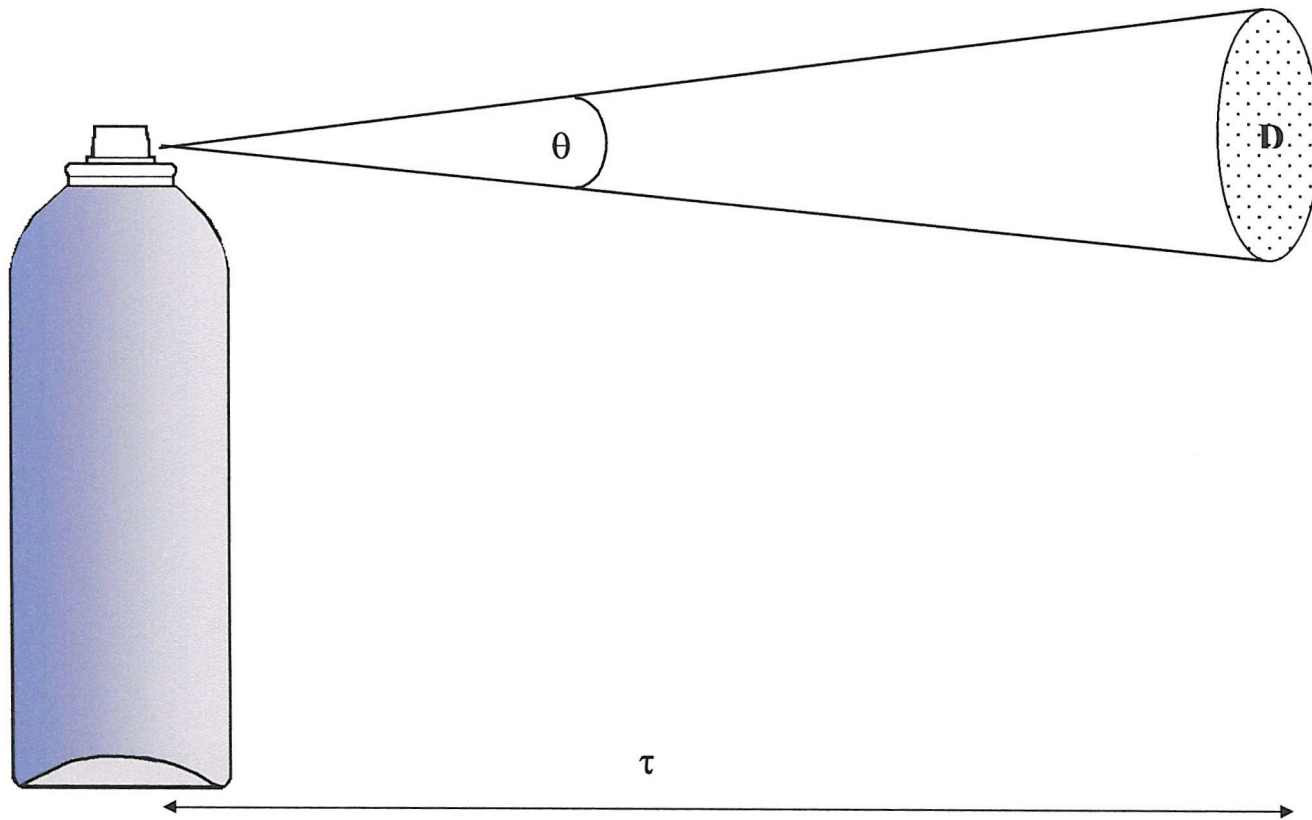


**Figure 4.3** Schematic drawing of a pressure-pack dispenser and the spray characteristics, cone angle ( $\theta$ ), droplet size distribution ( $D$ ) and plume throw ( $\tau$ ).

## Spray Rate (R)

The spray rate was measured according to the method described in Section 2.2.7. The average of at least three replicates was calculated.

## Cone Angle ( $\theta$ )

The cone angle ( $\theta$ ) is defined as the angle, in degrees, which is formed by the plume of liquid droplets as they emerge from the actuator of the dispenser. It is a measure of the spread of the droplets as they emerge and assumes the spray distribution to be conical with a circular cross section. Cone angle was measured by positioning the dispenser 300 mm from a vertical surface covered with a sheet of absorbent paper, measuring approximately 250 × 450 mm. The dispenser was then actuated for 2.0 ± 0.2 seconds, and the radius ( $r$ ) of the circle of moisture created subsequently measured (mm). The cone angle was then calculated trigonometrically, using the equation:

$$\theta = 2 \operatorname{Tan}^{-1} (r/300)$$

This equation is derived from the following equation:

$$\operatorname{Tan} \theta = \alpha/\beta$$

Where  $\alpha$  is the side opposite and  $\beta$  is the adjacent side to the angle  $\theta$ . The average of at least three replicates was calculated.

## Throw (T)

The throw (T) is defined as the distance that droplets travel from the actuator during spraying. This was measured by placing a length of absorbent paper along a bench, and standing the dispenser at one end. This was actuated for 2.0 ± 0.2 seconds, and the distance from the dispenser to the farthest detectable droplet on the paper taken to be the throw. The accuracy of this measurement depends upon the size of the droplets produced, as very small droplets would not have been detectable on the absorbent paper. This means that only the throw of droplets with a sufficiently large volume was recorded. Thus,

pressure-pack dispensers with very different droplet size distributions would give different throw measurements. The average of at least three replicates was calculated.

### Droplet Size Distribution

Droplet size distribution was measured according to method 3.2.3. In this instance a 300 mm lens was used, which measured droplets between 5.8 and 564  $\mu\text{m}$  in diameter. The dispenser was placed 600 mm from the beam, in order to achieve the optimum concentration of aerosol for measurement. The mean of 8 measurements was calculated for the charged and uncharged aerosols.

## 4.3 Results

### 4.3.1 Deposition of Charged Insecticide Droplets onto Tethered Flies

The deposition of uncharged and artificially charged liquid aerosols onto electrically isolated flies is shown in Figure 4.4, with standard error bars. The q/m of the insecticide sprays is given in Table 4.1 with the standard error in brackets.

**Table 4.1** Charge-to-mass ratio of insecticide sprays, standard error shown in brackets

Without voltage applied	With - 10 kV applied	With + 10 kV applied
$+1.86 \times 10^{-5} \text{ C}.\text{kg}^{-1}$ ( $4.93 \times 10^{-7}$ )	$-1.96 \times 10^{-4} \text{ C}.\text{kg}^{-1}$ ( $6.31 \times 10^{-6}$ )	$+3.05 \times 10^{-4} \text{ C}.\text{kg}^{-1}$ ( $2.3 \times 10^{-5}$ )

The effect of enhanced electrostatic charge on the droplets was to increase the volume of formulation deposited onto the insects. When the charge-to-mass ratio was increased from  $+1.86 \times 10^{-5} \text{ C}.\text{kg}^{-1}$  to  $+3.05 \times 10^{-4} \text{ C}.\text{kg}^{-1}$  by applying +10 kV, there was a 22 % increase in the volume of formulation deposited. When -10 kV was applied, and the q/m increased to  $-1.96 \times 10^{-4} \text{ C}.\text{kg}^{-1}$ , the volume of formulation deposited was increased by 43 %. Statistical analysis (ANOVA) indicated a significant difference in deposition ( $p < 0.05$ ). A subsequent Tukey test revealed that only the increase in deposition between uncharged and negatively charged aerosols was statistically significant.

These results show that negatively charged insecticide aerosols have greater deposition efficiency than uncharged aerosols onto electrically isolated flies. In a realistic scenario this may not translate into a faster knockdown rate or higher mortality of insects, however. An increase in dosage may not increase insecticide efficacy if the uncharged aerosol already deposits sufficient active ingredient for optimum performance.

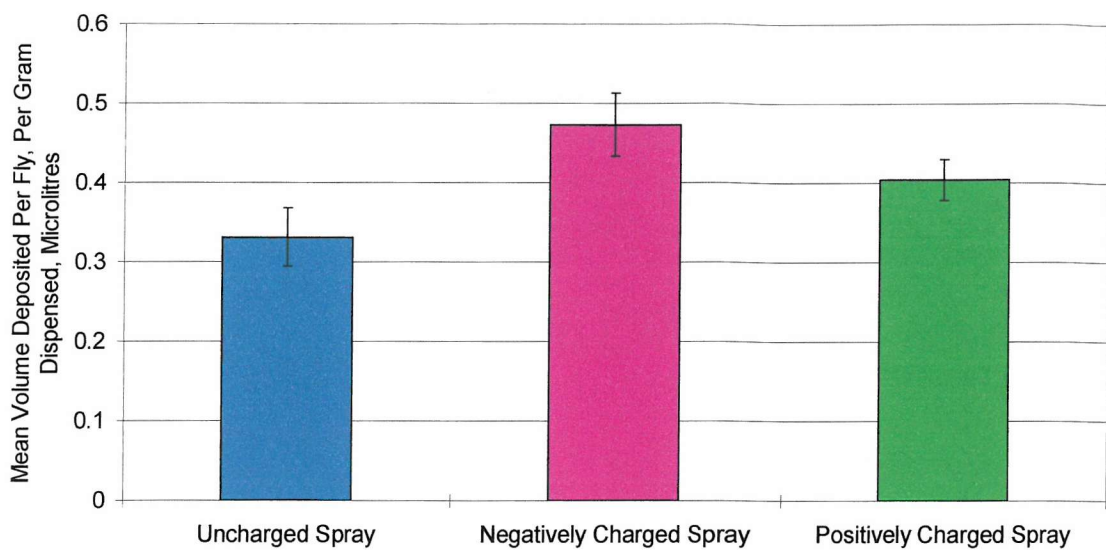


**Figure 4.4** Deposition of uncharged, negatively charged and positively charged liquid aerosols onto electrically isolated flies. Standard error bars shown

#### 4.3.2 Effect of Charge on Insecticide Aerosol Bioefficacy

Figures 4.5, 4.6 and 4.7 compare the mean rates of knockdown for uncharged and charged insecticide aerosols in the direct spray protocol for *Musca domestica*, the space spray protocol for *M. domestica* and *Culex quinquefasciatus* respectively. The charge-to-mass ratio of the uncharged aerosol was  $-2.21 \times 10^{-5}$  (standard error of  $1.71 \times 10^{-5}$ ), and of the charged spray was  $-1.06 \times 10^{-4}$  (standard error of  $8.37 \times 10^{-6}$ ).  $KD_{50}$ , the estimated time to achieve knockdown of 50% of the test insects was calculated for each replicate by linear interpolation of the two points either side of the 50% ordinate. For two replicates of the space spray of mosquitoes with the uncharged aerosol, 50% KD was not achieved during the test. In these instances,  $KD_{50}$  was estimated by extrapolation of the two final points measured.  $KD_{95}$  (time to knockdown 95% of the insects) was also calculated for the houseflies in the direct spray protocol. This was not done for the other assays as this level of knockdown was not achieved in the duration of the experiments, so could not be accurately estimated. The calculated values for  $KD_{50}$  and  $KD_{95}$  are shown in Table 4.2.

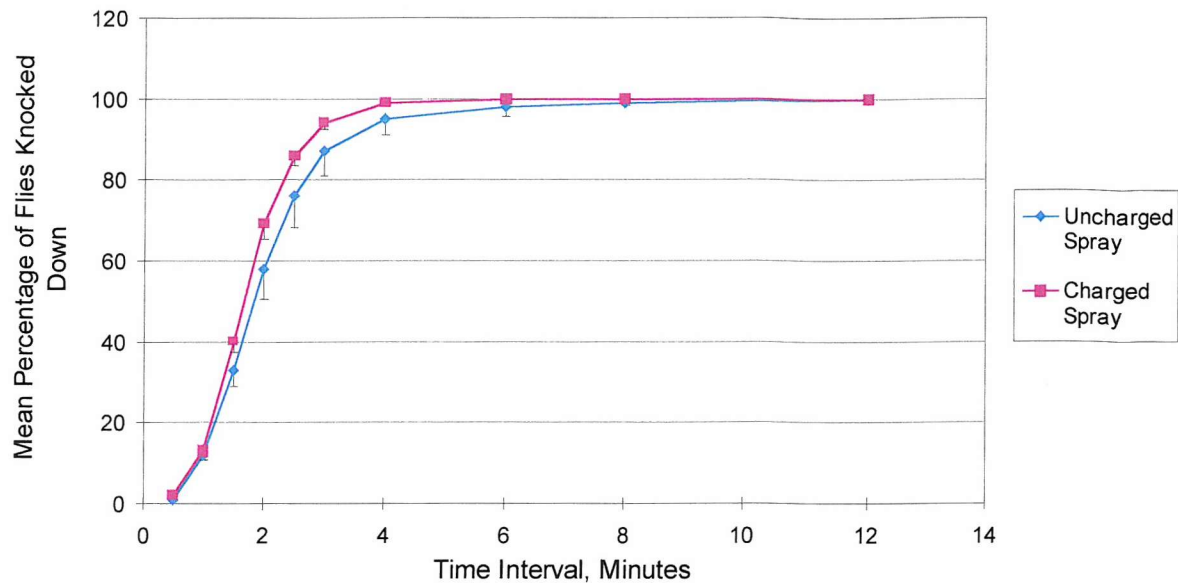


**Figure 4.5** Knock down of houseflies, *Musca domestica*, by uncharged and naturally charged insecticide aerosol, using the CERIT direct spray protocol. Standard error bars shown

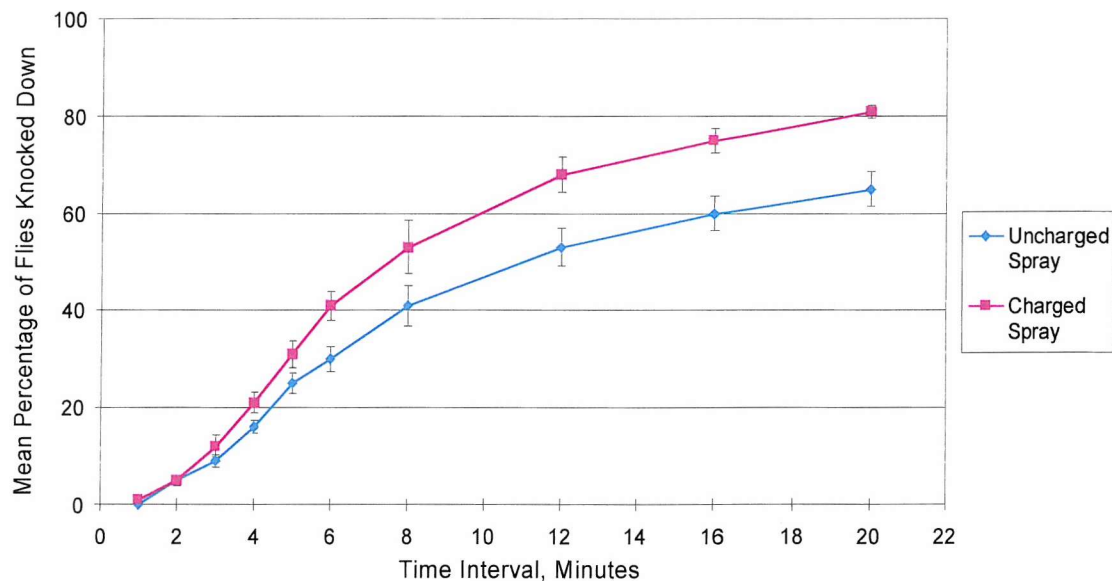


**Figure 4.6** Knock down of houseflies, *Musca domestica*, by uncharged and naturally charged insecticide aerosol, using the CERIT space spray protocol. Standard error bars shown

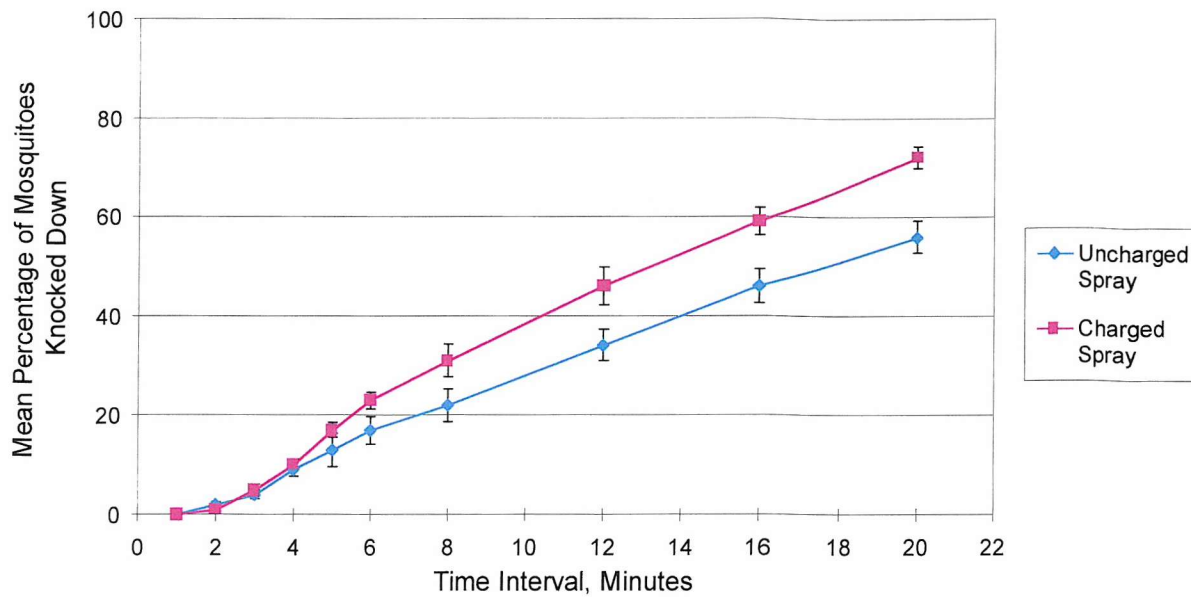


**Figure 4.7** Knock down of mosquitoes, *Culex quinquefasciatus*, by uncharged and naturally charged insecticide aerosol, using the CERIT space spray protocol. Standard error bars shown

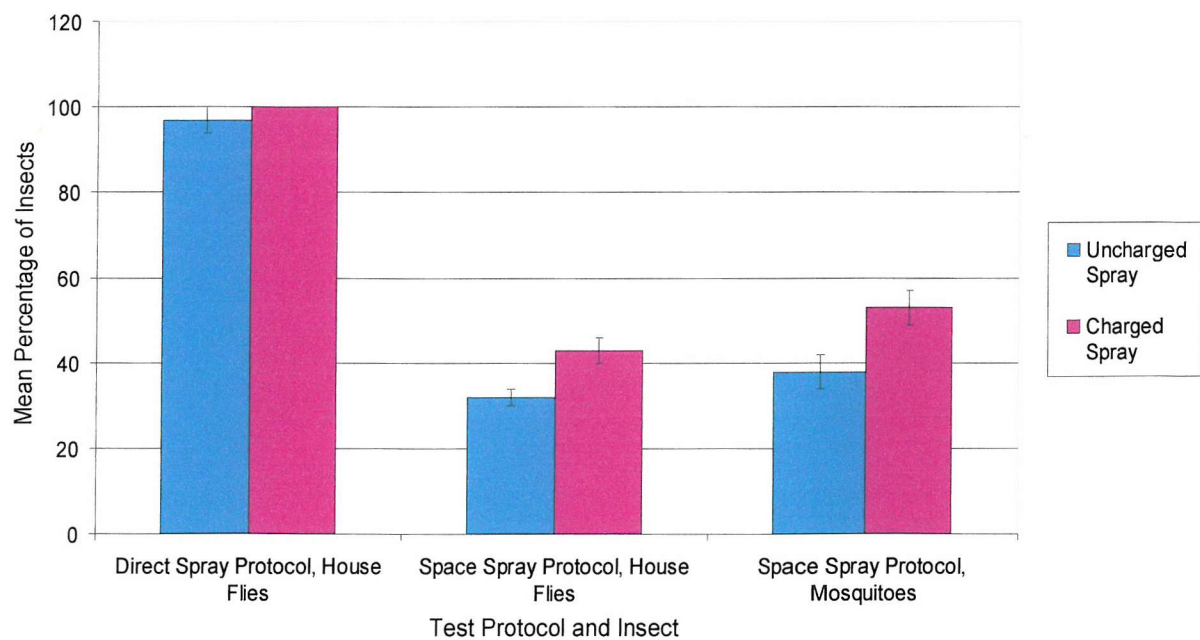


**Figure 4.8** Mortality of houseflies, *Musca domestica*, and mosquitoes, *Culex quinquefasciatus*, by uncharged and naturally charged insecticide aerosol, using the CERIT direct spray and space spray protocol. Standard error bars shown

**Table 4.2** Calculated values for  $KD_{50}$  and  $KD_{95}$  for the three bioassays

	Uncharged Spray	Charged Spray
<b>Direct spray protocol, houseflies</b>	$KD_{50} = 1 \text{ min, 56 secs}$ $KD_{95} = 4 \text{ mins, 9 secs}$	$KD_{50} = 1 \text{ min, 40 secs}$ $KD_{95} = 3 \text{ min, 13 secs}$
<b>Space spray protocol, houseflies</b>	$KD_{50} = 11 \text{ mins, 41 secs}$	$KD_{50} = 7 \text{ mins, 45 secs}$
<b>Space spray protocol, mosquitoes</b>	$KD_{50} = 17 \text{ mins, 53 secs}$	$KD_{50} = 13 \text{ mins, 11 secs.}$

Comparing the mean  $KD_{50}$ , the charged aerosol achieved faster knockdown than the uncharged in all three bioassays. Statistical analysis (t-test) showed that neither the faster  $KD_{50}$  nor  $KD_{95}$  achieved with charged aerosol was significant in the direct spray of *M. domestica*. For the space spray of both *M. domestica* and *C. quinquefasciatus* the charged insecticide achieved a significantly faster mean  $KD_{50}$  than the uncharged aerosol ( $p < 0.05$ ).

In all three bioassays conducted, higher percentage mortality was recorded using charged insecticide, than uncharged aerosol, as shown in Figure 4.8. Statistical analysis showed that the slightly higher mortality of *M. domestica* using charged insecticide was not significant during the direct spray, but was significant during the space spray assay ( $p < 0.05$ ). Enhanced mortality with charged insecticide in the space spray of *C. quinquefasciatus* was highly statistically significant ( $p < 0.01$ ).

#### 4.3.3 Spray Characteristics of Insecticide Aerosols

The mean spray rate, cone angle and throw of the aerosol plumes, are shown in Table 4.3 for the uncharged and charged sprays, with standard errors in brackets. The mean droplet size distribution, based on eight replicates, is shown in Figure 4.9, with standard error bars.

**Table 4.3** Spray Characteristics of Uncharged and Charged Insecticide Aerosols Standard Error in Brackets

Spray Characteristic	Uncharged		Charged	
Spray Rate, g.sec <sup>-1</sup>	2.10	(0.04)	1.90	(0.08)
Throw, m	1.85	(0.07)	1.56	(0.10)
Cone Angle, degrees	25°	(1.2)	21°	(0.9)

The analysis of spray characteristics shows that the uncharged and charged aerosol plumes were not identical. The uncharged aerosol ( $q/m$  of  $-2.21 \times 10^{-5} \text{ C}.\text{kg}^{-1}$ ) had a flow rate of about 0.2 grams per second greater than the charged ( $q/m$  of  $-1.06 \times 10^{-4} \text{ C}.\text{kg}^{-1}$ ), a throw 0.29 m longer and a cone angle 4° wider. The droplet size distribution of the uncharged aerosol tended towards a higher percentage volume of smaller droplets than the charged. These spray characteristics are quite closely matched, but these small differences must be taken into consideration when discussing the results of the bioassays.

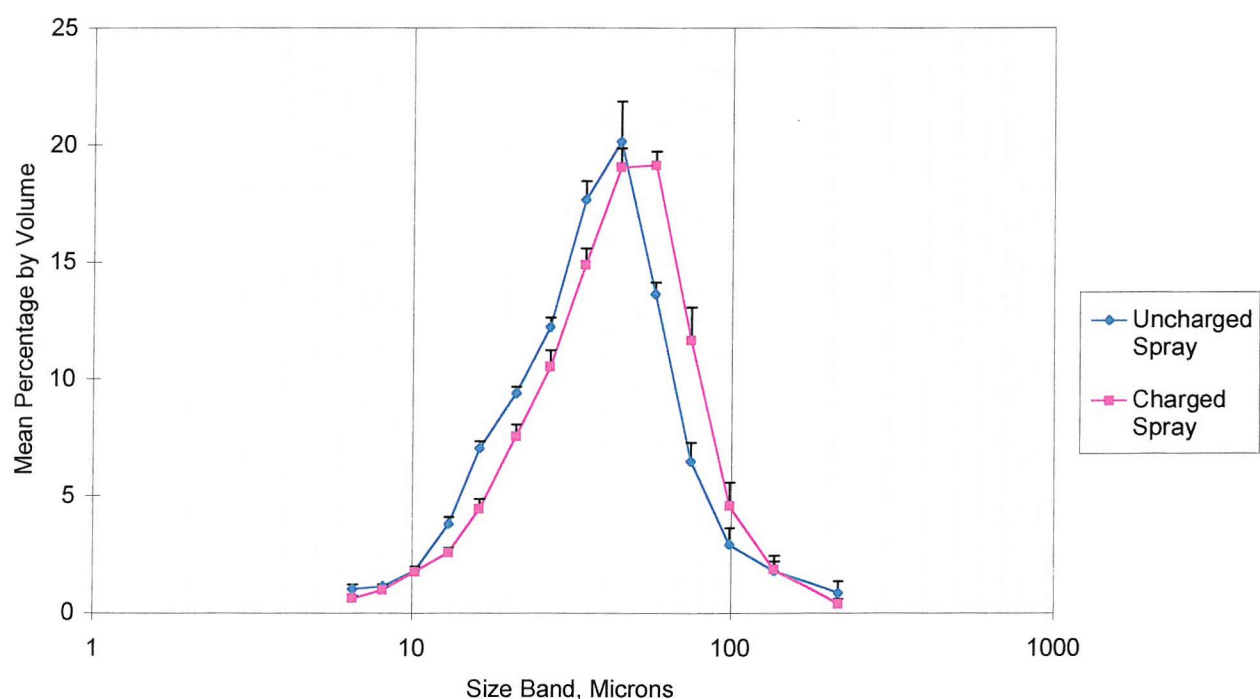


**Figure 4.9** Droplet size distribution of uncharged and naturally charged insecticide aerosol sprays, showing standard error bars

## 4.4 Discussion

### 4.4.1 Deposition of Charged Insecticide Aerosol onto Tethered Flies

The fluorometric assay demonstrated that the deposition of insecticide formulation was significantly increased when the charge-to-mass ratio of the droplets was raised to  $-1.96 \times 10^{-4}$  (negative) C.kg<sup>-1</sup>. Raising the charge-to-mass ratio of the liquid aerosol from  $+1.86 \times 10^{-5}$  (positive) had the effect of increasing deposition from 0.331 µl per fly, per gram of formulation sprayed to 0.473 µl, an increase of 43%. The increase was only 22% when the charge-to-mass ratio was increased to  $+3.05 \times 10^{-4}$  (positive) C.kg<sup>-1</sup>, which was not statistically significant.

Deposition of aerosol droplets onto insects conventionally relies upon inertial forces, and insects only collect droplets whose trajectory they directly intercept (McCartney and Woodhead, 1983). The uncharged liquid aerosol was likely to have been collected in this way. Highly charged droplets are believed to have had a higher probability of deposition due to electrostatic attraction forces. As the charged droplets approached the tethered insect, Coulombic attraction would have increased deposition.

A gradient of electrical potential between the charged aerosol and the insect would have driven the droplets towards the target. The charge status of the insect would influence this interaction, as the insects could have been electrically neutral or could have carried a net charge of the same or the opposite polarity as the charged aerosol. If the insect had no net electrostatic charge, then the potential gradient and polarisation would have caused an attractive force, increasing the probability of droplet deposition. A net electrostatic charge on the insect opposite in polarity to the charged aerosol would have resulted in a greater potential difference and Coulombic attraction forces. If there were a net charge of the same polarity as the aerosol, then Coulombic repulsion forces would prevent close approach and deposition of droplets. If the potential of the fly was different to the space potential of the charged aerosol, however, droplets could still move towards the insect due to the potential difference. Polarisation of the insect in the electric field of the charged aerosol could have created an area of opposite charge to which droplets could approach and deposit on. Considering these scenarios, deposition would be most greatly increased if the insect and the liquid aerosol possessed opposite charges. Deposition would

have been increased to a lesser extent if the insect were electrostatically neutral. If the insect and aerosol had net electrostatic charges of the same polarity some enhanced deposition could have occurred if the electric field created by the charged aerosol was sufficient to induce polarisation within the insect.

The presence of a net electrostatic charge on the test insects could have arisen due to handling techniques. During capture and handling, the flies could have acquired a charge on the cuticle by tribo-electric charging against the surfaces of retaining receptacles (for example beakers and petri dishes). It has been found that a variety of insects (including certain species of fly, moth and beetle) acquire a net positive charge when gently rubbed against glass, mica, wood and metals (Edwards, 1962). These insects also charged negatively against asbestos (with the exception of some moth species), suggesting the cuticle of many insects to fall between glass and asbestos in the tribo-electric series, an example of which is included in Appendix B. Most flies, including *Calliphora* species, would therefore be likely to become positively charged when in contact with plastic surfaces. It is likely then that the insects used in this fluorometric assay became charge by contact charging against the containers. For the insects in the later bioassays, there are other mechanisms by which charge can be accumulated, which will be discussed later.

If the insects used in the fluorimetric assays acquired a net positive charge through contact charging, then deposition of negatively charged aerosol would be expected to be higher than that of positively charged aerosol. This was the observed trend, with a 43% increase with the negatively charged aerosol compared to 22% with the positively charged.

During deposition experiments, the insects were supported on an insulating plastic rod. This was a large object in comparison to the flies (as indicated by Figure 4.1) and its geometry and any charge on its surface could consequently have altered the trajectories of approaching droplets. The rod was made of nylon; a dielectric material with a strong tendency to acquire a net positive charge through contact charging (Appendix B). If charge acquired by the rod were positive in polarity, positively charged aerosol would be repelled from this area, in which the fly was located. Charge on the supporting rod was not quantified. It is difficult to assess the rods effect, although it is probable that deposition was influenced.

The charge-to-mass ratio was raised artificially in these experiments by the use of a high voltage power supply. As the pressure-pack dispensers were at high electrical potential, an electric field was established that would have provided an additional force to

aid deposition of droplets. In the following bioassays, this factor was absent, as the charge was generated naturally during atomisation.

#### 4.4.2 Effect of Charged Insecticide Droplets on Bioefficacy

The knockdown bioassay experiments demonstrated that the highly charged insecticide aerosol had greater knockdown and mortality efficiencies than the conventional equivalent. The rate of knockdown of house flies, *Musca domestica*, and mosquitoes, *Culex quinquefasciatus*, was faster when the charge-to-mass ratio of the insecticide aerosol was increased from  $-2.52 \times 10^{-5}$  C.kg<sup>-1</sup> to  $-1.06 \times 10^{-4}$  C.kg<sup>-1</sup>. However, the improvement was only statistically significant for space spray protocols, with a delay of 10 seconds between spraying the insecticide and releasing the insects, and not in the direct spray protocol, which had a 2 second delay. The direct spray protocol did not demonstrate a statistically significant improved rate of knockdown. This was most likely because the insects collected a sufficiently high dose of conventional insecticide that any increase in deposition had no significant effect on the rate of knockdown. With the space spray protocol however, the insecticide aerosol was more dispersed when the insects were released, so the effect of the charged droplets has a greater opportunity to manifest itself.

An increase in mortality after 24 hours was also recorded when the insecticide aerosol was charged. Therefore, a greater proportion of the test insects received a lethal dose of insecticide during the bioassay. The increased mortality of *M. domestica* and *C. quinquefasciatus* in the space spray protocol was statistically significant, although mortality of *M. domestica* in the direct spray protocol was not. As the mortality of houseflies in the direct spray protocol was 97 % with the uncharged aerosol, a significant improvement by the charged insecticide would be difficult to measure without a large number of replicates.

Enhanced deposition of charged aerosols onto electrically isolated insects in these assays probably occurred due to space charge forces and polarisation. Polarisation in the insects as charged droplets approached is postulated to operate as discussed in Section 4.4.1. Attraction of droplets to the flies could have increased the aerosol concentration around the insects, increasing the probability of deposition as the insects move through the

aerosol. Any net electrical charge associated with the insect would influence the degree of attraction, as discussed in Section 4.4.1.

There are additional mechanisms to those discussed in Section 4.4.1 by which insects could acquire a net electrical charge. Since the insects were released from plastic containers, charge could have developed on the insect cuticles prior to release into the test chamber. Evidence suggests that this charge is likely to be positive (Edwards, 1962). In addition, flying insects can acquire a net charge by two further methods. First, tribo-electric charging can occur during flight, when the insects contact airborne particles. Although the work of Edwards (1962) suggests that insect cuticle is likely to attain positive charge, it is not possible to determine the frequency or nature of any contact events, and therefore the polarity and magnitude of charge. As a second mechanism, insects can collect free ions from the air while in flight, which could accumulate to produce a net charge. Natural space charge seldom exceeds  $10^6$  elementary charges per cubic metre, which occur in approximately equal numbers of positive and negative ions (Hinds, 1982). As the composition of airborne particulates and ions is variable, any charge accumulated on the test insects due to this mechanism is unpredictable and variable.

Space charge forces would have been influential during these assays, as the resulting improved dispersion of the aerosol would have increased insect exposure. It has been shown that deposition onto the upper portions of test chambers, where flies tend to congregate, is significantly greater with charged than uncharged aerosols (Inculet *et al.*, 1984). The effect of this was not relevant to the fluorimetric assay. Uncharged droplets rely largely upon inertial, gravitational and diffusion forces to disperse through the room. This results in most droplets lingering in the area in front of the dispenser into which they were propelled, and moving downwards due to gravity and forwards due to diffusion and inertia. The space charge effects within the charged aerosol will enhance dispersion through the test chamber. Space charge forces result from the mutual repulsion of the like-charged droplets, and work in addition to inertia, gravity and diffusion to cause droplet migration in directions not in the initial area of delivery. This enhanced dispersal could improve bioefficacy through increased exposure of the insects in flight, especially in the upper portions of the chamber, around the ceiling and upper walls where flies are observed to linger.

Charged aerosols could demonstrate enhance deposition onto the walls, floors, ceilings and other surfaces because of enhanced dispersion and attractive forces. As the

collection of insecticides by contact with residues is minimal (White *et al.*, 1992), this could reduce insect exposure. However, this could be beneficial to the user of domestic insecticide products, as exposure and inhalation of the droplets would be reduced by faster clearing of the droplets from the air.

#### 4.4.3 Effects of Spray Characteristics on Bioefficacy

Analysis of the spray characteristics of the uncharged and naturally charged insecticide aerosols showed some difference in spray rate, throw, cone angle and droplet size distribution. The uncharged aerosol had a flow rate of about 0.2 grams per second more than the charged spray, while the throw was about 0.29 m further, the cone angle 4° wider, with the droplets generated generally tending to be smaller. Differences in flow rate were accounted for during the experiments, as the mass of aerosol dispensed was standardised. The wider cone angle and longer throw of the uncharged aerosol would be expected to translate into faster knockdown than the charged spray, due to better availability to flying insects. As this was not observed, these differences in spray characteristics can be ignored.

The droplet size distribution of an insecticide aerosol is of great importance in determining efficacy in bioassays. Droplet size determines the time the insecticide remains available in the air, and the volume reaching the insect on collection (Wickham, *et al.*, 1974). Aerosols comprised of larger droplets characteristically demonstrate faster knockdown than smaller droplets, but typically achieve a lower mortality (White *et al.*, 1992). Therefore, the faster KD achieved by the charged aerosol could be attributed partially to droplet size effects, but the higher mortality could not. The charged aerosol is only a little larger than the uncharged, and this difference is probably not sufficient to account for the observed improvement in KD. As the mortality was significantly increased with charged aerosols, this aspect of the improved insecticide performance can be attributed to electrostatically enhanced deposition, and not differences in spray characteristics.

## Chapter 5

---

### Conclusions and Further Work

This work has shown that, through modifications to the formulation and packaging of commercially available pressure-pack sprays, it is possible to generate a charge-to-mass ratio in excess of  $\pm 1 \times 10^{-4}$  C.kg<sup>-1</sup> during the atomisation of the liquid formulation. Through the invention of a novel terminal orifice design, it also became possible to maintain required spray characteristics. Although many factors influenced the spray characteristics and the level of charge separation achieved, the nature of the liquid formulation and the actuator orifice transpired to be most significant. The methods by which the charge-to-mass ratio naturally generated by pressure-pack dispensers are enhanced to levels in excess of  $\pm 1 \times 10^{-4}$  C.kg<sup>-1</sup> are disclosed in patent WO 97/28883 (Fox *et al.*, 1997). It has been postulated that charged aerosols were produced as a result of shearing of the electrical double layer that occurs at solid-liquid interfaces. In keeping with this hypothesis, modifications to dispenser components that were believed to increase turbulence, velocity and the area of contact between the liquid and solid invariably increased the charge-to-mass ratio measured. The optimum formulation type for charge separation was an emulsion with external oil phase, which also fitted with published observations (Krämer, 1981). Although a positive correlation was measured between liquid-solid contact area at the terminal orifice and charge-to-mass ratio, the design giving the highest level of charge performed better than could be predicted by this relationship

alone. The narrow channels of this design, in comparison to other designs tested, allowed the electrical double layer to extend a greater proportion across the width of the channel. This factor could account for a more highly developed double layer shearing process.

Further research would be required to describe the charge separation process in pressure-pack dispensers. Through identification of the zone or zones in which charge separation primarily occurs, a deeper understanding of the processes involved could be gained, which could enable further enhancement of charge separation to be achieved. It would also be useful to investigate whether the charged aerosol generated by the modified pressure-pack dispensers is unipolar or bipolar, and whether charge is evenly distributed across the droplet size ranges. This would help identify whether double layer shearing is the only charge separation mechanism occurring or whether disruption of the double layer at the liquid-gas interface (as during spray electrification) or statistical charging are also involved. These mechanisms were described in Chapter 2. If disruption of the double layer at the liquid-gas interface was occurring during liquid fragmentation, then the aerosol would be expected to be bipolar with small and large droplets carrying charges of opposite polarity. If statistical charging were making a considerable contribution to charge separation, the aerosol cloud would probably be bipolar. These mechanisms seem unlikely to be important, because of the considerable net electrostatic charge of one polarity measured on the liquid aerosols.

The application of this novel technology to commercial products proved to be beneficial. Chapter 3 documented the ability of liquid aerosols sprayed from pressure-pack dispensers to sweep particles from the air. If the liquid aerosol carried a charge-to-mass ratio in excess of  $\pm 1 \times 10^{-4} \text{ C.kg}^{-1}$ , then the depletion rate of these particles was significantly enhanced. This concept is disclosed in patent WO 97/28883 (Fox *et al.*, 1997). The depletion of particles by uncharged droplets was believed to occur as a result of impaction and interception of the dust particles by the droplets, leading to sedimentation of the agglomerations on to surfaces. When the aerosol was charged, space charge effects and attractive forces between the dust and the liquid droplets were believed to enhance the number of particles contacted and removed from the air. The three formulations tested all demonstrated enhanced particle precipitation, but the water-in-oil emulsion was more efficient than either the oil-in-water emulsion or the alcohol-based formulation. This was most likely a droplet size effect, as the water-in-oil emulsion had

slightly smaller droplets which is known to enhance particle precipitation in industrial scrubbers (Jaworek *et al.*, 1998).

Immediate, short-term reductions in airborne particle concentrations can be achieved on a local scale by naturally, highly charged liquid aerosols. Although the long-term benefits of portable air cleaning devices are probably not achieved, charged liquid aerosols can provide an immediate particle reduction that these devices do not. Charged liquid aerosols could be used for the immediate reduction of the airborne dust generated during domestic activities such as bed making, vacuuming and dusting. The immediate reduction of allergens associated with larger particles such as Der p1 (major house dust mite allergen), and the concentration of persistent aeroallergens associated with small particles, like Fel d1 (major cat allergen), could be reduced in this way.

A second successful application was discussed in Chapter 4: the improved bioefficacy of highly charged insecticide sprays produced by pressure-pack dispensers. This concept is disclosed in patent WO 99/01227 (Fox *et al.*, 1999). When the liquid aerosol is generated with a charge-to-mass ratio in excess of  $\pm 1 \times 10^{-4}$  C.kg<sup>-1</sup>, the insecticide droplets are deposited onto electrically isolated flies with significantly higher frequency than equivalent, uncharged droplets. This enhanced deposition is translated into faster rates of knockdown and higher levels of mortality in houseflies, *Musca domestica* and mosquitoes, *Culex quinquefasciatus*. Increased bioefficacy was statistically significant in space spray bioassays, in which there is a delay of 10 seconds between spraying the insecticide and insect release, but not in direct spray bioassays, in which the delay is only 2 seconds. Efficacy was probably significantly enhanced in the space spray protocols because droplets of the charged aerosol are electrostatically attracted to the insects in flight, and because space charge effects cause improved distribution of aerosol in the air.

These efficiency improvements are commercially beneficial, allowing products to be manufactured which are either more efficient than current products, or which maintain the current level of efficiency using lower concentrations of insecticide ingredients. Rational design of insecticide formulations can produce highly efficient sprays (White *et al.*, 1992; Tsuda, 1991), but the advantages available by the application of highly charged droplets have not been considered with respect to pressure-pack sprays, to date. Although agricultural applications of charged sprays have been researched and implemented, these

exclusively employ high voltage power supplies (Matthews, 1989), and the generation of sufficiently high charge-to-mass ratio through natural processes is unique.

This work has shown that, through modifications to components of commercially available pressure-pack dispensers (particularly the formulation and actuator), a charge-to-mass ratio in excess of  $1 \times 10^{-4}$  C.kg<sup>-1</sup> can be generated. Two viable applications of this emerging technology have been demonstrated which show considerable improvements in the performance of these products. This work resulted in the following publication: Whitmore *et al.*, 1999. Application of charged aerosol technology to pressure-pack products with various functions could offer a range of benefits. Improved deposition onto surfaces and furniture items by cleaners, disinfectants and polishes could be envisaged due to electrostatic attraction. ‘Wrap-around’ by the charged droplets onto surfaces facing away from the direction of the spray, a familiar effect in electrostatic coating applications (Hughes, 1984), would be highly beneficial to these products. Dispersion of Room fragrance products could be achieved more rapidly and evenly as a result of space charge effects.

Quantification of these hypothesised effects would be a matter of appropriate experimental design. As the formulation of many domestic products is determined by the function, achieving the required charge-to-mass ratio would be more difficult. This work has successfully generated a charge-to-mass ratio in excess of  $1 \times 10^{-4}$  C.kg<sup>-1</sup> only with water-in-oil formulations, while maintaining spray characteristics similar to the equivalent products. As this formulation would not be suitable for all pressure-pack spray products, methods would have to be sought whereby oil-in-water emulsions and homogeneous alcohol-based formulations could also be charged during atomisation, without abrogating spray characteristics.

In addition to these further domestic applications of this technology, natural charge separation in agricultural and horticultural spray systems is also feasible. It is well known that charged droplets achieve higher deposition rates in agricultural spraying (McCartney and Woodhead, 1983), and appliances are available which utilise this phenomenon (Matthews, 1989). Production of charged spray droplets without the requirement of an external power supply would be advantageous in reducing the size, initial cost and running expenses of such equipment. Portable backpack units are currently available, which carry a battery for a supply of power (Matthews, 1989). These could be made lighter and more convenient if the charge was generated naturally during atomisation. This work

demonstrates techniques that could be applied in achieving natural charge separation in devices suitable for spraying agricultural or horticultural crops, although considerable research would be required. The formulation types (emulsion or homogenous liquid) used in these sprayers would be important in determining how readily the required charge was achieved, as only a water-in-oil emulsion was successfully charged in this work. Another problem may arise from the duration of spraying, as formation and shearing of the electrical double-layer can only continue if surface charge is replenished (Gavis and Koszman, 1961). This must occur for constant generation of charged droplets during spraying.

In conclusion, it has been shown that, through modifications to components of commercially available pressure-pack dispensers, a charge-to-mass ratio in excess of  $1 \times 10^{-4}$  C.kg<sup>-1</sup> can be generated by natural processes. Through the invention of a novel terminal orifice design this level of charge has been achieved while maintaining spray characteristics suitable for commercial spray products. The proposed mechanism by which charge was imparted to the liquid during atomisation was formation and shearing of the electrical double layer at liquid-solid interfaces. In support of this hypothesis, the charge-to-mass ratio was increased by modifications to dispenser components that were believed to increase turbulence, velocity and the area of contact between the liquid and solid. Two commercially beneficial applications for this technology have been demonstrated. Charged liquid aerosols have been shown to significantly reduce the concentration of airborne dust particles within three minutes of spraying. This technology would be extremely beneficial for the immediate reduction of the airborne dust generated during domestic activities such as bed making, vacuuming and dusting. In particular, the concentration of aeroallergens such as Der p1 and Fel d1 could be beneficially reduced in this way. The second application demonstrated enhanced bioefficacy by charged insecticide aerosols. The rate of knockdown and mortality of houseflies (*Musca domestica*) and mosquitoes (*culex quinquefasciatus*) was significantly increase without additional insecticide actives. This represents a considerable advance in domestic insecticide technology, reflecting the advantages that charged spraying has brought to agricultural applications.

## APPENDIX A - Statistical Analysis

---

### Comparison of Means

The null hypothesis used to test for a statistical difference between the means of two test groups is:

$H_0$ : the two samples are drawn from populations with identical means and variances.

It therefore follows that to show a significant difference between the means of two test groups it is first necessary to check that there is no difference in variance. If there is a difference in variance then a test for the difference between means cannot be applied validly. If the variances of the treatment groups have been shown to be homologous, and the null hypothesis has been rejected, then it can be concluded that the samples are drawn from populations with different means (there is a statistically significant difference between the means).

### The F-Test

The F-test is used to determine whether the difference between two sample variances is so small that it may be ignored, when comparing the difference between two means. This test is applied routinely before comparing means by statistical analysis, to show the variances are homologous. An F-test is performed as follows:

$$F = \frac{\text{greater variance (sample 1)}}{\text{lesser variance (sample 2)}}$$

where the degrees of freedom are  $(n_1-1)$  and  $(n_2-1)$  for samples 1 and 2 respectively.

The calculated value of F is compared to tabulated critical values of F, for the relevant degrees of freedom. Tabulated values of F are published in the relevant statistical texts (Fowler and Cohen, 1990).

If the F-test suggests that the variances of the sample groups to be compared are not homologous, then  $\log_{10}$  transformation of each observation is performed, which stabilises the variance and removes the dependence of the variance upon the mean. The F-test can then be repeated to confirm homogeneity of variance, and further analysis performed using the transformed data.

## The T-Test

A t-test is a parametric test used to compare the means of small samples, with less than 30 observations. The formula for t is given below:

$$t = \frac{(\bar{x}_1 - \bar{x}_2)}{\sqrt{\left[ \frac{(n_1 - 1)s_1^2 + (n_2 - 1)s_2^2}{(n_1 + n_2 - 2)} \right] \left( \frac{n_1 + n_2}{n_1 n_2} \right)}}$$

where the degrees of freedom are  $(n_1 + n_2) - 2$ . The calculated value of t is compared to tabulated critical values of t, for the relevant degrees of freedom, and can be compared for different levels of significance.

An event is considered to be statistically significant if there is a less than 5% probability ( $p < 0.05$ ) of it occurring, and highly significant if there is a less than 1% probability ( $p < 0.01$ ) of it occurring. Therefore, if the calculated value of t exceeds the tabulated value, for the appropriate degrees of freedom, at  $P=0.05$ , then the probability that the two means being compared are the same is less than 5%, and the difference is significant at the  $P<0.05$  level. Similarly, if the calculated value of t exceeds the tabulated value at  $P=0.01$ , then the difference between the means is highly significant. If the calculated value for t does not

exceed the tabulated value, for the appropriated degrees of freedom, at  $P=0.05$  then the difference between the means being compared is deemed to be not statistically significant.

An unequal variances t-test can also be performed in which observations are independent, random observations from normal distributions. This can be used where the variances of the two samples being compared are not homogeneous, even after appropriate transformation. This can be performed using the statistical analysis facility of 'Microsoft' 'Excel' or using specialist software, such as 'SPSS'.

## One-way ANOVA Analysis of Variance

ANOVA is used to compare the means of more than two samples, and as with t-test it is assumed that the samples are drawn from normally distributed populations, and that the variances are equal. Therefore, the F-test must always be performed before an ANOVA, using the smallest and the largest variances from the samples being compared. One-way ANOVA is used where the effect of one independent variable on a dependent variable is under investigation. Where the effect of two independent variables is required, two-way ANOVA is applied, which is described later.

ANOVA works upon the principle that the total variability within an aggregated set of observations is made up of the variability around each mean within a sample and the variability between means of the sample groups. Or:

$$\text{Variability}_{\text{total}} = \text{Variability}_{\text{within}} + \text{Variability}_{\text{between}}$$

If the samples are all drawn from the same population, then the within variance is the same as the between variance. If this is not the case however, then the samples have been drawn from populations with different means and/or variances. Since variances are assumed equal, then the samples must be drawn from populations with different means.

One-way ANOVA was performed according to either procedures documented in statistical texts (Fowler and Cohen, 1990) or using the data analysis facility of 'Microsoft' 'Excel' or 'SPSS'. Where ANOVA indicates that there is a significant difference between the means of the samples, a Tukey test is used to distinguish which sample means differ significantly from each other.

## Tukey Test

This procedure assumes that there are the same number of observations in each sample group. The test is conducted by firstly calculating the difference between each pair of samples, ignoring any negative signs. A test statistic is then calculated, with which these values are compared. The test statistic is calculated according to the equation:

$$T = (q) \times \sqrt{(\text{within variance} / n)}$$

where  $n$  = the number of observations in each sample group and the *within variance* is the value calculated during the ANOVA procedure. The value of  $q$  is found by consulting a published table of the distribution of  $q$ , using the number of sample groups being compared and the degrees of freedom of the *within variance* (calculated during ANOVA). Where the mean differences between pairs of sample groups exceed the calculated value of  $T$ , the difference is considered to be significant at  $p = 0.05$ .

## Two-way ANOVA

Two-way ANOVA allows the effects of two independent variables on a dependent variable to be estimated. Either independent variable may have an effect, and the two variables may interact in producing an effect. Like one-way ANOVA, it is assumed that all samples are drawn from normally distributed populations, and that the variances are equal. Thus, the F-test must be performed before two-way ANOVA, using the smallest and the largest variances from the samples being compared.

As in one-way ANOVA, two-way ANOVA also partitions the total variability, but now the variation between samples can be further partitioned;

Variation between samples due to variable A

Denoted by  $(SS_A)$

Variation between samples due to variable B

Denoted by  $(SS_B)$

Variability between samples due to the interaction of variable A and variable B

Denoted by (SS<sub>i</sub>)

The equation for two-way ANOVA is;

$$\text{Variability}_{\text{total}} = \text{Variability}_{\text{within}} + (\text{SS}_A + \text{SS}_B + \text{SS}_i)$$

Two-way ANOVA was performed either according to procedures documented in statistical texts (Fowler and Cohen, 1990) or using the data analysis facility of 'Microsoft' 'Excel'. A Tukey test is also used to distinguish which sample means differ significantly from each other where ANOVA indicates that there is a significant difference between the means of the samples.

## Standard Error

The standard error of a mean (S.E.) is a figure for the spread of data around the mean, and is calculated by:

$$\text{S.E.} = \frac{s}{\sqrt{n}}$$

where  $s$  is the sample standard deviation and  $n$  is the number of observations.

The standard error of the mean is an indication of the quality of an estimate of the sample mean, equating to a 68 % confidence that the mean falls within 1 S.E of the mean.

## The Product Moment Correlation Coefficient

This parametric statistic indicates the degree to which two variables are related. The correlation coefficient ( $r$ ) is given by the formula;

$$r = \frac{n \sum xy - \sum x \sum y}{\sqrt{\left[ n \sum x^2 - (\sum x)^2 \right] \left[ n \sum y^2 - (\sum y)^2 \right]}}$$

This is then compared to a probability distribution of  $r$ , provided in statistical texts. If the calculated value of  $r$  exceeds the tabulated value at the appropriate degrees of freedom, then the null hypothesis is rejected, and the correlation considered statistically significant.

## APPENDIX B      Triboelectric Series

---

The following triboelectric series is taken from Unger (1981). The materials at the top of the table were generally found to charge positively when rubbed against those lower in the series. Triboelectric series compiled by different authors often present materials in slightly different orders, probably due to different experimental conditions and differences in the source and impurities of the materials.

- +    Asbestos
- Glass
- Mica
- Human Hair
- Nylon
- Wool
- Fur
- Lead
- Silk
- Aluminium
- Paper
- Cotton
- Steel
- Wood
- Hard Rubber
- Nickel, Copper
- Brass, Silver
- Gold, Platinum
- Sulphur
- Acetate Rayon
- Polyester
- Celluloid
- Orlon
- Saran
- Polyurethane
- Polyethylene
- Polypropylene
- PVC
- Silicon
- Teflon

## Publications arising from this work

Fox RT, Hughes JF, Harrison NM and Whitmore LF. 1997 'Method of precipitating airborne particles' Patent WO 98/28883

Fox FT, Harrison NM, Hughes JF and Whitmore LF. 1998 'Compressed gas propelled aerosol devices' Patent WO 99/21659

Fox FT, Harrison NM, Hughes JF and Whitmore LF. 1999 'Improved targeting of flying insects with insecticides and apparatus for charging liquids' Patent WO 99/01227

Whitmore LF, Hughes JF, Fox RT and Harrison NM. 1999 'Novel applications of natural charge exchange phenomena in domestic aerosol products' Conference record of the 1999 IEEE Industry Applications Conference 34<sup>th</sup> Annual Meeting 1:3-7

Fox FT, Harper D, Harrison NM, Hughes JF, Jerrim KL and Whitmore LF. 1999 'Treatment of airborne microorganisms' WO 00/01423

Fox FT, Harper D, Harrison NM, Hughes JF, Jerrim KL and Whitmore LF. 1999 'Inhalation of aerosol actives' WO 00/01494

Fox FT, Harper D, Harrison NM, Hughes JF and Whitmore LF. 1999 'Treatment of airborne allergens' WO 00/01429

Fox FT, Harper D, Harrison NM, Hughes JF and Whitmore LF. 1999 'Fragrance dispersion' WO 00/01422

Fox FT, Harper D, Harrison NM, Hughes JF and Whitmore LF. 1999 'Aerosol spraying' WO 00/01493

Fox FT, Harper D, Harrison NM, Hughes JF and Whitmore LF. 1999 'Malodour treatment' WO 00/01421

## GLOSSARY

---

**Aerosol** is defined as a solid or liquid suspended in gas, such as a dispersed cloud of particles or a mist of droplets. It is not used to describe hand-held pressurised dispensers.

**Actuator** The pressure-pack components which allows the user to depress the valve, and is responsible for atomisation of the liquid in to an aerosol.

**Anion** negatively charged ion.

**Bioassay** experimental assessment of a biological process

**Cation** positively charged ion.

**Coulombs Law** states that like charges repel (Coulombic repulsion) and opposite attract (Coulombic attraction)

**Domestic** pertaining to the home or house

**Electric field** is a region of space around a charged object in which electrical forces act. This can be visualised in terms of field lines, which originate on a positive charge and terminate on a negative charge, all lines terminating at right angles at the electrode surface.

**Electrical Double Layer** two layers of charge in the liquid arising from the electrochemical reaction at the liquid/solid interface.

**Electrostatics** the study of the causes and effects of charge accumulation in solids and liquids.

**Emulsion** a dispersion of one liquid in another. A water-in-oil emulsion consists of droplets of water in a continuous oil phase, while an oil-in-water emulsion consists of droplets of oil in a continuous water phase.

**Flashing** is the rapid conversion of a liquid to a gas during a drop in pressure

**Flow electrification** separation of charge during flow of liquids (insulating or conducting) either in pipes or other situations, leading to accumulation of a net electrical charge in the bulk of the liquid.

**Formulation** the liquid inside pressure-pack dispensers.

**Image charge** arises when a charged object approaches a grounded object, and in which charge of the same magnitude and opposite polarity is induced in the latter.

**Isokinetic sampling** ensures a representative sample of an aerosol enters the inlet of a sampling tube when sampling from a moving aerosol stream. This is usually achieved by aligning a thin-walled sampling tube or probe with the gas stream. Particle loss at the inlet is ensured in this way, although losses between the inlet and the collector can occur.

**Knockdown** defines a state in insects following exposure to insecticides whereby they are incapable of co-ordinated movement.

**Mortality** in bioassays, an insect was defined as dead if no body appendages moved during three seconds of observation

**Polarisation** is the alignment of permanent dipoles or the reorganisation of free charge carriers, due to the presence of a charged object.

**Pressure-pack dispenser** -a hand-held, self contained, sprayable product in which a propellant force is applied by liquefied gas. Such spray devices are commonly used to dispense surface polishes, insecticides, personal hygiene products and room fragrances. These are casually referred to as 'aerosols' or 'aerosol products, but for clarity these terms have not been used in this respect.

**Propellant** liquefied gas in pressure-pack dispensers providing the pressure that forces the product out of the container when the valve is opened.

**Space Charge Force** is the net outward force arising from the mutual repulsion of a cloud of like-charged objects.

**Spray Characteristics** are properties of the liquid aerosol sprayed from pressure-pack dispensers, such as droplet size distribution, length of produce throw, cone angle and spray rate.

**Spray Rate** is the mass of liquid formulation dispensed per second ( $\text{g.sec}^{-1}$ ) from pressure-pack dispensers.

**Triboelectric charging** is the reorganisation of charge when two materials are brought into contact with each other, or rubbed against each other, usually resulting in the surfaces attaining net electrical charge.

**Valve** is the component of a pressure-pack dispenser that allows the liquid formulation that is under pressure, to flow into the actuator.

## REFERENCES

---

- Adams AJ, Lindquist, RK, Adams, IHH and Hall FR 1991 'Efficiency of bifenthrin against pyrethroid-resistant and -susceptible populations of glasshouse whitefly in bioassays and using three spray application methods' *Crop Protection* **10**:106-110
- Ahmad CN and Balachandran W. 1991 'Suppression of smoke particles using electrostatic spraying' *NIST Special Publication* **813**: 797-804
- Bailey AG. 1988 'Electrostatic Spraying of Liquids' John Wiley & Sons inc.
- Bertinat MP 1980 'Charged droplet scrubbing for controlling submicron particle emissions' *Journal of Electrostatics* **9** 137-158
- Blum MS and Kearns CW. 1956 'Temperature and the action of pyrethrum in the American cockroach' *Journal of Economic Entomology* **49**: 862-865
- Blumenthal M, Blumenthal M, Bousquet J et al. 1993 'Evidence for an increase in atopic disease and possible causes' *Clinical and Experimental Allergy* **23**: 484-492
- Boleij JSM and Brunekreef B 1982 'Indoor air pollution' *Public Health Reviews* Vol. X (2): 169-198
- Boulet LP, Turcotte H, Laprise C, Lavertu C, Bédard PM, Lavoie A and Hébert J. 1997 'Comparative degree and type of sensitisation to common indoor and outdoor allergens in subjects with allergic rhinitis and/or asthma' *Clinical and Experimental Allergy*, **27**: 52-59
- Burge H. 1990 'Bioaerosols: Prevalence and health effects in the indoor environment [CME article]' *Journal of Allergy and Clinical Immunology* **86**: 687
- Burt PE and Goodchild RE. 1974 'Knockdown by pyrethroids: Its role in the intoxication process' *Pesticide Science* **5**: 625-633
- Castle PGS and Inculet II. 1983 'Space charge effects in orchard spraying' *IEEE Transactions on Industry Applications* **1A-19**: 476-480
- Chapman DL. 1913 'Theory of electrocapillarity' *Phil. Mag.* **25**: 475-485
- Cross JA, Haig IG, Cetronio A. 1977 'Electrostatic hazards from pumping insulating liquids in glass pipes' *Proceedings of the third international congress on static electricity (Grenoble)* 1977 (Paris: Société de chimie industrielle Paris)
- Cross JA. 1987 'Electrostatics: principles, problems and applications' Adam Hilger, Bristol
- Crosskey RW and Lane RP. 1993 'House-flies, blow-flies and their allies (calyptrate

Diptera)' pp 403-428 In 'Medical insects and arachnids' Ed Lane RP and Crosskey RW. Chapman & Hall.

- Currie BW and Alty T. 1929 'Adsorption at a water surface' Proceedings of the Royal Society of London A **106**: 622-633
- deBlay F, Spirlet F, Gries P, Casel S, Ott M, Pauli G. 1998 'Effects of various vacuum cleaners on the airborne content of major cat allergen (Fel d 1)' Allergy **53**: 411-414
- Edwards DK. 1962 'Electrostatic charges on insects due to contact with different substrates' Canadian Journal of Zoology **40**: 579-584
- Elliott M, Janes NF and Potter C. 1978 'The future of pyrethroids in insect control' Annual Review of Entomology **23**: 443-469
- Elliott M, Farnham AW, Janes NF, Needham PH, Pulman DA and Stevenson JH. 1973 'A photostable Pyrethroid' Nature **246**: 169-170
- Elster J and Geitel H. 1890 Wein. Ber. 94
- Fernández-Caldas E and Fox RW. 1992 'Environmental control of indoor air pollution' Clinical Allergy. Medical Clinics of North America **76**: 935-952
- Fowler J and Cohen L. 1990 'Practical statistics for field biology' John Wiley and Sons
- Fox RW. 1994 'Air cleaners: a review' Journal of Allergy and Clinical Immunology **94**: 413-416
- Fox RT, Hughes JF, Harrison NM and Whitmore LF. 1997 'Method of precipitating airborne particles' Patent WO 98/28883
- Fox FT, Harrison NM, Hughes JF and Whitmore LF. 1999 'Improved targeting of flying insects with insecticides and apparatus for charging liquids' Patent WO 99/01227
- Gavis J and Koszman I. 1961 'Development of charge in low conductivity liquids flowing past surfaces: a theory of the phenomenon in tubes' Journal of Colloid Science **16**: 375-391
- Gergen PJ and Weiss KB. 1992 'The increasing problem of asthma in the United States' American review of Respiratory Disease **146**: 823-824
- Gibson N and Lloyd FC. 1970 'Effect of contamination of the electrification of toluene flowing in metal pipes' Chemical Engineering Science **25**: 87-95
- Giles DK, Blewett TC, Saiz SG, Welsh AM and Krieger RI. 1992 'Foliar and non-target deposition from conventional and reduced-volume pesticide application in greenhouses'

Journal of Agricultural Food Chemistry **40**: 2510-2516

- Gnadinger CB. 1936 'Pyrethrum flowers' 2nd Edition. McLaughlin Gormley King, Minnesota
- Goodfellow HD and Graydon WF. 1968 'Dependence of electrostatic charging currents on fluid properties' Canadian Journal of Chemical Engineering **46**: 342-
- Goodhue LD and Sullivan WN. 1943 U.S. Patent 2321023.
- Gouy G. 1910 'Constitution of electrical charge at surface of an electrolyte' Journal Physique **9**: 457
- Hadaway AB, Barlow F and Flower LS. 1976 'Penetration of insecticides from solutions into tsetse flies and other insects' Centre for Overseas Pest Research Misc. Rep. 1-14
- Haydon DA. 1974 'The electrical double layer and electrokinetic phenomena' In 'Recent progress in surface science. vol 1' Ed Danielle, JF, Pankhurst KGA and Riddiford AC. Academic Press, New York. pp 94-153
- Helmholtz H. 1879 'Studiern über electrische grenzschichten' Weid. Ann. Phys **7**: 337-382
- Hinds WC. 1982 'Aerosol Technology' Wiley, New York
- Hughes JF. 1984 'Electrostatic powder coating' Research Studies Press, UK.
- Hughes JF, Bright AW, Makin B and Parker IF. 1973 'A study of electrical discharges in a charged water aerosol' Journal of Physics D: Applied Physics **6**: 966-975
- Inculet II, Castle GSP, Menzies DR and Frank R 1981 'Deposition studies with a novel form of electrostatic crop sprayer' Journal of Electrostatics **10**: 65-72
- Inculet II, Surgeoner GA, Haufe WO, Hodgson KJ and Almeida LT. 1984 'Spraying of electrically charged insecticide aerosols in enclosed spaces (Part I)' IEEE Transactions on Industry Applications **20**: 677-681
- Iribarne JV and Mason BJ. 1967 'Electrification accompanying the bursting of bubbles in water and aqueous solutions' Transactions of the Faraday Society **63**: 2234-2245
- Jaworek A, Krupa A, Adamiak K. 1998 'Submicron charged dust particle interception by charged drops' IEEE Transactions on Industry Applications **34**: 985-991
- Klinkenberg A and van der Minne L.J. 1958 'Electrostatics in the petroleum industry' Elsevier
- Koszman I and Gavis J. 1962a 'Development of charge in low conductivity liquids flowing past surfaces. Experimental verification and application of the theory developed for tube

flow' Chemical Engineering Science **17**: 1023-1040

- Koszman I and Gavis J. 1962b 'Development of charge in low conductivity liquids flowing past surfaces. Engineering predictions from the theory developed for tube flow' Chemical Engineering Science **17**: 1013-1022
- Krämer H and Fröchtenigt H. 1993 'Electrostatic charging of spray cans' Journal of Electrostatics **30**: 159-164
- Krämer H. 1981 'Electrostatic charging of poorly conductive liquid systems-suspensions, emulsions and solutions- by agitation' Journal of Electrostatics **10**:89-97
- Lenard P. 1915 Ann. d. phys. **47**: 463
- Lenard P. 1892 Annals of Physics **46**: 584
- Loeb 1958 'Static Electrification' Springer-Verlag pp59-124
- Luczunsk CM, Martin YL, Chapman MD and Platts-Mills TAE. 1990 'Airborne concentrations and particle size distribution of allergen derived from domestic cats (*Felis domesticus*)' American Review of Respiratory Disease **141**: 361-367
- Makin B. 1975 'Static electrification in supertankers' Physics in Technology **6**: 109-116
- Matthews GA. 1989 'Electrostatic spraying of pesticides: a review' Crop protection **8**: 3-15
- Miller TA and Adams ME. 1982 'Mode of Action of Pyrethroids' In 'Insecticide mode of Action' Ed Coats, JR. Academic Press
- McCartney AH and Woodhead T. 1983 'Electric charge, image-charge forces, and the deposition of pesticide drops' Pesticide Science **14**: 49-56
- Nelson HS, Hirsh SR, Ohman JL et al. 1988 'Recommendations for the use of residential air-cleaning devices in the treatment of allergic respiratory diseases' Journal of Allergy and Clinical Immunology **82**: 661
- Offermann FJ, Sextro RG, Fisk WJ, Grimsrud DT, Nazaroff WW, Nero AV, Refzan KL and Yater J. 1988 'Control of respirable particles in indoor air with portable air cleaners' Atmospheric Environment **19**: 1761-1771
- Ottewill RH. 1975 'Electrostatics in colloid science' Institute of Physics Conference Series No. 27 pp 56-73
- Owen MK, Ensor DS, and Sparks LE. 1992 'Airborne Particle Sizes and Sources Found in Indoor Air' Atmospheric Environment **26A**: 2149-2162

- Palumbo JC and Coates WE 1996 'Air-assisted electrostatic application of pyrethroid and endosulphan mixtures for sweetpotato whitefly (Homoptera: aleyrodidae) control and spray deposition in cauliflower' *Journal of Economic Entomology* 89: 970-980
- Parsons R. 1971 'The electrical double layer, electrode reactions and static' *Static Electrification* (London) 1971 (Institute of Physics Conference Series 11) pp 124-138
- Pimentel D, and Levitan L. 1986 'Pesticides: Amount applied and amounts reaching pests' *BioScience* 36: 86-91
- Platts-Mills TAE, Tovey ER, Mitchell EB, Mozorro H, Nock P and Wilkins SR. 1982 'Reduction of bronchial hyperreactivity during prolonged allergen avoidance' *Lancet* 2: 675-678
- Platts-Mills TAE, Heymann MD, Longbottom JL and Wilkins SR. 1986 'Airborne allergens associated with asthma: Particle sizes carrying dust mite and rat allergens measured with a cascade impactor' *Journal of Allergy and Clinical Immunology* 77:850-857
- Raabe OG. 1982 'Comparison of the criteria for sampling 'inhalable' and 'respirable' aerosols' *Annals of Occupational Hygiene* 26: 33-45
- Roberts JMC and Hughes JF. 1979 'Elimination of electrostatic charging in punctured aerosol cans' *IEEE Transactions on Industry Applications* vol. 1A 1: 104-109
- Rutgers AJ, de Smet M and de Myer G. 1956 'Influence of turbulence upon electrokinetic phenomena' *Transactions of the Faraday Society* 83:393-396
- Sanders PA. 1970 'Principles of aerosol technology' Van Nostrand Reinhold Company. pp 1-72
- Sawicki RM. 1962 'Insecticidal activity of pyrethrum extract and its four insecticidal constituents against houseflies. III. Knockdown and recovery of flies treated with pyrethrum extract with and without pipernyl butoxide' *Journal of the Science of Food and Agriculture* 13: 283-292
- Service MW. 1993 'Mosquitoes (Culicidae)' pp 120-240 In 'Medical Insects and Arachnids' Ed Lane RP and Crosskey RW. Chapman & Hall
- Singh S, O'Neil BC and Bright AN. 1978 'A parametric study of electrostatic powder coating' *Journal of Electrostatics* 4: 325-334
- Splinter WE. 1968 'Electrostatic charging of agricultural sprays' *Transactions of the*

American Society of Agricultural Engineers 11: 491-495

- Stern O. 1924 'Theory of the electrolytic double layer' *Z. Electrochem.* **30**: 508
- Sumiyoshitani S, Okada T, Hara M and Akazaki M. 1984 'Direct observation of the collection process for dust particles from an air stream by a charged water droplet' *IEEE Transactions on Industry Applications* 1A-20: 274-281
- Taylor DM and Secker PE. 1994 'Industrial electrostatics: fundamentals and measurements' Research Studies Press Ltd. pp 16-128
- Touchard G. 1995 'Flow electrification of liquids' In 'Handbook of electrostatic Processes' Ed Chang JS, Kelly AJ, and Crowley JM. Marcel Dekker pp 83-87
- Touchard G and Romat H. 1981 'Electrostatic charges convected by flow of dielectric liquid through pipes of different length and different radii (theoretical model and experimental results)' *Journal of Electrostatics* 10:275-281
- Touchard G, Benyamina M, Borzeix JAG and Romat H. 1989 'Static electrification by laminar flow through artificially roughened pipes' *IEEE Transactions on Industry Applications* 25: 1067-1072
- Touchard G, Patzek TW and Radke CJ. 1996 'A physiochemical explanation for flow electrification in low-conductivity liquids in contact with a corroding wall' *IEEE Transactions on Industry Applications* 32:1051-1057
- Tsuda S. 1991 'Relationship between physical properties of aerosol formulation and its insecticidal efficacy' *Journal of Pesticide Science* 16: 533-543
- Tsuda S, Nishibe I and Shinjo G. 1987 'Effect of the diameter of spray droplets on the insecticidal efficacy of oil based aerosols' *Journal of Pesticide Science* 12: 483-489
- Tsuda S, Nishibe I and Shinjo G. 1988 'Influence of droplet sizes on the percentage of airborne spray droplets in oil based aerosols' *Journal of Pesticide Science* 13: 253-260.
- Unger BA. 1981 'Electrostatic discharge failures of semiconducting devices' *IEEE/Proc. IRPS* pp 193-199
- Verrall B, Muir DCF, Wilson WM, Milner R, Johnston M and Dolovich J. 1988 'Laminar flow air cleaner bed attachment – A controlled trial' *Annals of Allergy* 61: 117-122
- Walmsley HL and Woodford G. 1981 'The generation of electric currents by the laminar flow of dielectric liquids' *Journal of Physics D: Applied Physics* **14**: 1761-1782
- White AWC, Martin R, Stewart DC and Wickham JC. 1992 'Assessing the performance

against houseflies of indoor aerosol space sprays. Part I. Factors examined during tests with houseflies in free flight' *Pesticide Science* 34: 153-162

- Whitmore LF, Hughes JF, Fox RT and Harrison NM. 1999 'Novel applications of natural charge exchange phenomena in domestic aerosol products' Conference record of the 1999 IEEE Industry Applications Conference 34<sup>th</sup> Annual Meeting 1:3-7
- Wickham JC, Chadwick PR and Stewart DC. 1974 'Factors which influence the knockdown effect of insecticide products' *Pesticide Science* 5: 657-664
- Woodfolk JA, Luczynska CM, de Blay F, Chapman MD and Platts-Mills TAE 1993 'The effect of vacuum cleaners on the concentration and particle size distribution of airborne cat allergen' *Journal of Allergy and Clinical Immunology* 91: 829-837
- Yamamoto I. 1973 'Mode of action of synergists in enhancing the insecticidal activity of pyrethrum and pyrethroids' pp 195-208 In 'Pyrethrum the natural insecticide' Ed Casida JE. Academic Press